University of Alberta

The Free Air Space and Bulk Density of Compost and Compost Materials

by

Joy Melanie Agnew

©

A thesis submitted to the Faculty of Graduate Studies and Research in partial fulfillment of the requirements for the degree of Master of Science

in

Bioresource and Food Engineering

Department of *Agricultural, Food and Nutritional Science*

Edmonton, Alberta

Fall, 2002

National Library of Canada
Acquisitions and Bibliographic Services
395 Wellington Street
Ottawa ON K1A 0N4
Canada

Bibliothèque nationale du Canada
Acquisitions et services bibliographiques
395, rue Wellington
Ottawa ON K1A 0N4
Canada

Your file Votre référence

Our file Notre référence

The author has granted a non-exclusive licence allowing the National Library of Canada to reproduce, loan, distribute or sell copies of this thesis in microform, paper or electronic formats.

The author retains ownership of the copyright in this thesis. Neither the thesis nor substantial extracts from it may be printed or otherwise reproduced without the author's permission.

L'auteur a accordé une licence non exclusive permettant à la Bibliothèque nationale du Canada de reproduire, prêter, distribuer ou vendre des copies de cette thèse sous la forme de microfiche/film, de reproduction sur papier ou sur format électronique.

L'auteur conserve la propriété du droit d'auteur qui protège cette thèse. Ni la thèse ni des extraits substantiels de celle-ci ne doivent être imprimés ou autrement reproduits sans son autorisation.

0-612-81352-5

Canada

University of Alberta

Library Release Form

Name of Author: *Joy Melanie Agnew*

Title of Thesis: *The Free Air Space and Bulk Density of Compost and Compost Materials*

Degree: *Master of Science*

Year this Degree Granted: *2002*

Permission is hereby granted to the University of Alberta Library to reproduce single copies of this thesis and to lend or sell copies for private, scholarly or scientific research purposes only.

The author reserves all other publication and other rights in association with the copyright in the thesis, and except as herein before provided, neither the thesis nor any substantial portion thereof may be printed or otherwise reproduced in any material form whatever without the author's prior written permission.

Joy Agnew

RR 2
Prince Albert, SK
S6V 5P9

Date: June 4, 2002

University of Alberta

Faculty of Graduate Studies and Research

The undersigned certify that they have read, and recommended to the Faculty of Graduate Studies and Research for acceptance, a thesis entitled *The Free Air Space and Bulk Density of Compost and Compost Materials* submitted by *Joy Melanie Agnew* in partial fulfillment of the requirements for the degree of *Master of Science* in *Bioresource and Food Engineering*.

J.J. Leonard
Supervisor

J.J.R. Feddes
Committee Member

Y. Feng
Committee Member

Date: June 4, 2002

Abstract

A method of measuring the bulk density and free air space (FAS) of compost that is quick, accurate and simulates *in situ* conditions was required for more efficient management of the composting process. The modified air pycnometer designed and built to meet this need included two 30L PVC vessels for pressure difference determination and an air cylinder with piston to simulate the stress conditions found at all pile depths. The FAS and bulk density of manure compost, municipal solid waste compost and mixtures of biosolids and amendment material (leaves, straw and woodchips) were measured at various moisture contents and compressive loads. The particle densities of the compost materials were roughly similar (1500-1800kgm^{-3}), and linear bulk density and FAS profiles (variation with depth) were observed for all materials, and the linear relationship between bulk density and FAS had an R^2 value of 0.97.

Acknowledgements

A graduate student is only as good as their advisor, and after impulsively deciding to move to Edmonton, I stumbled upon the best advisor possible. I extend sincere thanks to Jerry Leonard for "taking me in" and providing a year and a half of support, encouragement, ideas, as well as more than a few laughs.

Thanks to Ray Holowach for his expertise and tremendous patience during the construction of the pycnometer. The original design was full of mistakes, and he brought me down to earth to build a machine that worked better than designed. And thanks to Chris Ouellette for his help with the instrumentation, and fellow U of S graduate Penny Howells for her AutoCad expertise.

Thanks also to the "composting group" and fellow graduate students who shared the office and provided support and competition. Thanks, Natasha, for sharing your love of compost (and your puppies), and for being a great roommate on the road at various conferences. Jason and Mark, thanks for keeping the group meetings interesting, and thanks to Juan Carlos and Mahendran for always being up for a game of volleyball.

Dr. Feddes and Dr. Feng, thank you for the input and ideas throughout the project. Your enthusiasm encouraged me to explore every corner of this study.

To my friends outside of the University: you may not have always known what I was up to, but your encouragement kept me motivated. Thanks, Kelly and Rob, for keeping me sane and helping me focus on the goal. Thanks to my good friend Scott, the mechanical genius, who knew what I was designing even before I knew it. Your words of encouragement and faith in me got me where I am today.

Finally, to my mom: thanks for the strength and freedom to make my own mistakes, and thanks for always being the first to say you were proud of me. Love you.

This thesis is dedicated to my father who passed away before I could complete my work. Thoughts of his hearty laugh and extreme pride in life got me through the difficult times and the long nights of grad school.

Thanks, Dad.

Table of Contents

1. Introduction **1**

1.1. The Composting Process 1
1.2. Objectives 4

2. Literature Review **5**

2.1. Bulk Density 5
2.2. Porosity and Free Air Space 7
2.3. Particle Density 10
2.4. Particle Size Distribution 10
2.5. Compressibility 11
2.6. Recent Research 11
2.7 Property Relationships 14

3. Design and Calibration of Pycnometer **16**

3.1 Rationale 16
3.2. Pycnometer Principle 16
3.3. Pycnometer Design 18
3.3.1 Sample Vessel 19
3.3.2. Load Cylinder 21
3.3.3. Pressure Measurement and Regulation 21
3.4. Pycnometer Construction 23
3.5. System Calibration 27
3.6. Simulating Compressive Loading 29
3.7. System Operation 31

4. Bulk Density and Free Air Space Measurements **33**

4.1. Materials and Methods 33
4.1.1. Materials 33
4.1.2. Experimental Methods 34
4.1.3. Statistical Methods 35
4.2. Results 36
4.2.1. Manure Compost and MSW Compost 36
4.2.2. Amendment Materials 38
4.2.3. Biosolids 40
4.3. Interpretation of Results 41
4.3.1. Pycnometer Performance 41
4.3.2. FAS and Bulk Density 42
4.3.3. Particle Density and Moisture Content 44
4.3.4. Porosity and FAS 48
4.3.5. Wet Bulk Density Profiles and Dry Bulk Density 49

4.3.6. Compressibility and the Soil Compression Equation 51
4.4. Limitations and Recommendations 54

5. Conclusions **57**

6. References **59**

7. Appendices **62**

APPENDIX A. Pycnometer Pictures and Equipment Specifications 62
APPENDIX B. Calibration of Pycnometer 66
APPENDIX C. Comparable Data 70
APPENDIX D. Raw Data 73
APPENDIX E. Profiles and BD vs FAS Graphs 85
APPENDIX F. Summary of Calculations 90
APPENDIX G. Error Analysis 97
APPENDIX H. Operator's Manual for Pycnometer 102
APPENDIX I. Detailed Drawings 120

List of Tables

Table 3.2. Variation of FAS readings at various operating pressures 20

Table 4.1. Initial properties of the materials. 34
Table 4.2. Particle densities and standard errors of materials 45
Table 4.3. Summary of bulk density and depth regression coefficients 51

Table B.1. Calibration of pycnometer with water data 69

Table C.1. Initial properties of feedstock material (prior to mixing and loading). 71
Table C.2. Initial properties of the materials used in this study. 71
Table C.3. Free air space and wet bulk density of loaded amendments 72

Table D.1. Raw data for manure compost (MC = 25%). 74
Table D.2. Raw data for MSW compost. 77
Table D.3. Raw data for biosolids material. 78
Table D.4. Raw data for straw 80
Table D.5. Raw data for woodchips. 81
Table D.6. Raw data for leaves. 83

Table E.1. Summary of slope, intercept and standard error values from regression equations 89

Table F.1. Summary of calculations for manure compost. 92
Table F.2. Summary of calculations for MSW compost. 93
Table F.3. Summary of calculations for leaves 93
Table F.4. Summary of calculations for straw. 94
Table F.5. Summary of calculations for woodchips 95
Table F.6. Summary of calculations for pure biosolids 95
Table F.7. Summary of calculations for woodchips-biosolids. 96
Table F.8. Summary of calculations for leaves-biosolids. 96
Table F.9. Summary of calculations for straw-biosolids. 96

Table G.1. Relative errors for FAS and P_2 readings for manure compost 98

List of Figures

Figure 3.1. Simple Pycnometer 17
Figure 3.2. Schematic drawing of overall system. 23
Figure 3.3. Dimensions of end caps and groove. 25
Figure 3.4. Details of sample vessel and piston assembly. 26
Figure 3.5. Calibration of pycnometer with water 28

Figure 4.1. Profiles for manure compost 36
Figure 4.2. FAS vs BD for manure compost. 37
Figure 4.3. Profiles for MSW compost. 38
Figure 4.4. FAS vs BD for MSW compost 38
Figure 4.5. Bulk density and FAS relationship for leaves, straw and woodchips. 39
Figure 4.6. Profiles for straw-biosolids, MC = 69% a) FAS and b) bulk density 40
Figure 4.7. FAS vs BD for straw-biosolids. 41
Figure 4.8. FAS vs BD for data from Baker *et al.* (1998). 42
Figure 4.9. FAS vs BD summary of all values from this study 43
Figure 4.10. Regression equation curves of bulk density at any depth 50
Figure 4.11. Comparison of FAS values of manure compost from pycnometer and soil compression equations 53

Figure A.1. Overall pycnometer setup. 63
Figure A.2. Air cylinder and piston assembly. 63
Figure A.3. Sample vessel drainage floor 64
Figure A.4. Drainage tile. 64

Figure B.1. Calibration curve for determining sample volume. 68

Figure E.1. Profiles for leaves 86
Figure E.2. Profiles for straw. 86
Figure E.3. Profiles for woodchips 86
Figure E.4. Profiles for pure biosolids 87
Figure E.5. Profiles for woodchips-biosolids 87
Figure E.6. Profiles for leaves-biosolids 87
Figure E.7. FAS vs BD for pure biosolids. 88
Figure E.8. FAS vs BD for woodchips-biosolids. 88
Figure E.9. FAS vs BD for leaves-biosolids. 88

Figure G.1. Error analysis of Equation 2.10 100

List of Symbols and Abbreviations

α	alpha value
A	Constant
B	Exponent
BD	wet bulk density (kgm^{-3})
BD_{dry}	dry bulk density (kgm^{-3})
C:N	carbon to nitrogen ratio
D	diameter of vessel (m)
FAS	free air space (%)
FAS_i	initial free air space (%)
FAS_o	free air space at given depth (%)
h	height of vessel (m)
kgm^{-3}	kilogram per cubic meter
kPa	Kilopascal
M_A	mass of amendment material (kg)
M_B	mass of biosolid material (kg)
MC	wet basis moisture content (decimal or %)
MC_A	moisture content of amendment material (decimal or %)
MC_B	moisture content of biosolid material (decimal or %)
MC_{dry}	dry basis moisture content (decimal or %)
MC_T	target wet basis moisture content (decimal or %)
MC_{vol}	volumetric moisture content (decimal or %)
M_S	mass of solid material (kg)
M_T	mass of total material (kg)
n	number of moles
P	overall pressure (kPa or psi)
P_1	pressure of compressed air vessel (kPa or psi)
P_2	equilibrium pressure (kPa or psi)
PD	particle density (kgm^{-3})
PVC	polyvinyl chloride
R	universal gas constant (L atm $mole^{-1}$ K^{-1})
R^2	coefficient of determination
ρ_w	density of water (kgm^{-3})
std dev	standard deviation
T	temperature (°C or Kelvin)
V	overall volume (L or m^3)
V_A	volume of compressed air vessel (L or m^3)
V_{air}	volume of air in sample (L or m^3)
V_B	volume of sample vessel (L or m^3)
V_i	volume of initial sample (L or m^3)

V_o	volume of sample at given depth (L or m^3)
V_S	total volume of sample (L or m^3)
V_{sol}	volume of solids (L or m^3)
V_t	total volume of sample (L or m^3)
V_T	total volume of vessel(s) (L or m^3)
V_W	volume of water in sample (L or m^3)
W	mass of water added (kg)
w.b.	wet basis
x	exposed rod length (mm or in)
z	depth in pile (m)

1. Introduction

The development of the composting process has been studied extensively over the past few decades. Properly managed, composting can effectively inactivate pathogens and weed seeds while breaking down the organic matter in wastes into a useable, soil-like product. The effects of waste volume reduction and the possible uses in soil amendment and land remediation have caught the attention of farmers and environmentalists alike.

Although the decomposition of organic materials occurs naturally, the process involves a wide variety of parameters and biological interactions. In order to optimize the process to shorten composting time and to increase the quality of the end product, the producers must manage the most important composting parameters like temperature, carbon to nitrogen ratio and moisture content. These parameters are often related to the physical properties of compost materials.

The physical properties of compost materials play an important role in every stage of compost production as well as in the handling and utilization of the end product. From the mixing of various feedstocks and process monitoring and maintenance, to the packaging and shipping of the final product, parameters such as bulk density, porosity and free air space (FAS) dictate the requirements for the optimum composting environment, and the design of machinery and aeration equipment used in the system.

1.1. The Composting Process

Before describing the research in detail, it is important to outline the entire composting process and how the physical properties of the materials affect the various stages of decomposition. Composting is "the biological decomposition and stabilization

of organic substrates, under conditions that allow development of thermophilic temperatures (between 40 and 70°C) as a result of biologically produced heat, to produce a final product that is stable, free of pathogens and plant seeds, and can be beneficially applied to land" (Haug 1995).

Temperature is an important parameter in composting both as a consequence and as a determinant of activity. Thermophilic organisms are generally accepted to be more productive, and the thermophilic temperatures kill the pathogens and weed seeds that may have been present in the initial mixture.

Before active decomposition can occur, the compost materials must have a carbon to nitrogen ratio (C:N) that permits microbial activity and should be in the range of 25:1 to 35:1 (Haug, 1995; Rynk, 1992). The organisms need approximately 25 to 35 units of carbon to digest each unit of nitrogen. The actual C:N depends on the nature of the initial materials and the availability of the carbon source. If the C:N is too high, the microbes use all the available nitrogen before the carbon material is broken down. If the C:N is too low, the excess nitrogen is lost as ammonia, resulting in odour problems.

Optimum air and moisture contents are also important in keeping microbial populations active. It is generally accepted that a moisture content of 40 to 60% wet basis (w.b.) will maintain ideal conditions (Haug 1995; Rynk 1992). If the material is too dry, the microbes will have no nutrient or transport mechanisms, and if it is too wet, the excess water will limit the oxygen supply. A constant oxygen supply is needed to maintain aerobic conditions. If anaerobic conditions exist, the composting process slows and odourous by-products are emitted.

Maintaining optimum C:N, temperature, and oxygen and water contents is key to providing the proper environment for composting. If these requirements are satisfied, microbial activity will generate heat and increase temperatures in the compost. The microbial populations then break down the starches, sugars, cellulose and lignin available in the feedstock material. The active decomposing stage generally lasts up to 6 weeks, depending on the maintained temperature and the nature of the initial mixture. The curing period which follows active composting gives the compost the added time to make nutrients available to plants (i.e. nitrogen, potassium, phosphorous) and to bring the C:N down to 20:1 (Haug 1995; Rynk 1992). The curing time required to produce a good quality compost depends on the carbon content of the initial ingredients and can be as short as a few months or as long as two years.

Reaching and maintaining these optimum composting conditions also requires management (and, therefore measurement) of key physical properties like bulk density and FAS. The bulk density of compost influences the strength, porosity and ease of compaction (Agnew and Leonard, 2002), so the knowledge of bulk density is important for aeration, handling and storage requirements. The realization that bulk density changes throughout the vertical profile of a pile is important to avoid miscalculating these requirements. Previous attempts to simulate compressive loading while measuring the bulk density of compost proved to be very time consuming and labour intensive (Schaub-Szabo and Leonard, 1999).

The air content and air movement throughout the pile is important to maintain an optimum oxygen supply, remove carbon dioxide, ammonia and excess moisture, and limit excessive heat production (Haug, 1995). Maintaining adequate FAS levels satisfies

the air content and continuity levels required to reach the desired composting conditions. Measuring the FAS of compost with the existing methods described in Section 2.2 is cumbersome, time consuming and inaccurate. Also, the FAS has been shown to change throughout the vertical profile of the pile (McCartney and Chen, 2000). Measuring the FAS of compost *in situ* is impossible using the existing methods.

1.2. Objectives

The main goal of the research described in this thesis was to develop and test a device that could measure the free air space (FAS) and bulk density of compost while simulating compressive loading in a compost pile. The device needed to be capable of providing accurate and precise measurements of FAS and bulk density of a wide range of compost and compost feedstocks and require minimal handling of the material. Ideally, the apparatus needed to be able to simulate *in situ* conditions and measure the required parameters with minimal input from the user. The secondary goal was to use the apparatus to develop empirical formulas describing bulk density and FAS of composting materials based on moisture content, material, and pile depth.

2. *Literature Review*

2.1. Bulk Density

The wet bulk density of compost is a measure of the mass of material (solids and water) within a given volume and is important in the determination of initial compost mixtures. Dry bulk density is the mass of solids within a given volume and is sometimes used when comparing materials of differing moisture contents. The wet bulk density determines how much material can be placed at a certain site or hauled in a truck of a given size. The density of compost also influences the mechanical properties such as strength, porosity, and ease of compaction (Agnew and Leonard, 2002). Therefore, knowledge of the bulk density of the material throughout the pile is important for aeration, handling and storage requirements.

Although bulk density is an important parameter, there is no standardized method for bulk density determination of a compressible material. A starting point in this regard could be existing standards for peat (ASTM, 1994) or other horticultural substrates, but large errors and inconsistencies can arise from the use of disturbed or compacted samples and the non-homogeneity of small samples. Methods of sampling and of treating samples need to be specified to overcome these problems and eliminate errors in estimating aeration and storage requirements.

A majority of compost researchers (e.g. He *et al.*, 1995; Glancey and Hoffman, 1994) used the simple mass per unit volume technique as described in the ASTM standards. The mass of material required to fill a container of known volume can be measured and the bulk density can then be calculated. However, the disturbance of the material required for

this method changes the compost matrix, which in turn alters the bulk density, giving erroneous values.

Leege and Thompson (1997) took the mass per unit volume approach one step further and recommended allowing partially filled vessels to fall from a 100mm height onto a rubber mat. This forces the material to settle and collapses large pores. While this procedure is a more standardized way to measure the bulk density of a compressible material, it still does not accurately represent the conditions within a pile.

Because of material compressibility, bulk density is dependent on the location within a pile. Bulk density values from small, disturbed samples will reflect only the properties of the material on the surface of the pile and may lead to errors if they are used to calculate aeration requirements. Therefore, it is important to recognize the relationship between bulk density and depth in the pile. Fogiel *et al.* (1999) showed that for dairy manure compost, samples from the bottom of the pile had higher bulk densities than at the top. This is in agreement with data published by Schaub-Szabo and Leonard (1999), Mu and Leonard (1999) and van Ginkle *et al.* (1999). The latter showed a linear relationship between bulk density and depth for a compost of chicken manure and wheat straw.

As mentioned, it is difficult to measure bulk density *in situ* without disturbing the sample or the load on it. Consequently, Schaub-Szabo and Leonard (1999) developed a laboratory method to simulate the variation of density with depth of material. A sample of material was compressed with weights that simulated the compaction that would be experienced at various depths in a pile. This method was used with compost, peat, moss,

wood shavings and straw, and resulted in density versus depth data that were fitted to curves of the form:

$$BD = Az^{B} \tag{2.1}$$

where BD is the wet bulk density (kgm^{-3}) at any depth (z) in meters ($z > 0$), and the exponent (B) is an indicator of the compressibility of the material. Higher values of B indicate a more compressible material. The constant A is dependent on the material. This exponential relationship is in contrast to the linear relationship found by van Ginkle *et al.* (1999). For compost with moisture content of 47% (w.b.), Schaub-Szabo and Leonard (1999) found the constant A to be approximately 495 and exponent B to be 0.104.

2.2. Porosity and Free Air Space

The composting process should be maintained in an aerobic state to increase the rate of decomposition and to reduce the amount of foul odours given off by anaerobic decomposition. The porosity, or percentage of air and water filled voids (Baker *et al.*, 1998), of the material dictates how much water and air is available to the microorganisms. For optimum microbial activity, the material must contain approximately 50% moisture (w.b.) and minimum oxygen concentration of 5% within the pore spaces (Rynk, 1992). Since air contains about 20% oxygen, the air voids must constitute 20-35% of the pile or windrow by volume for maximum oxygen consumption (Haug, 1995). Also, the continuity of these voids is an important factor, which describes how easily air and water will flow through the material. The quantification of the continuity of air voids was beyond the scope of this project and will not be discussed

further. FAS, or air-filled porosity of the unsaturated organic matrix (Haug, 1995), also influences heat and mass transport processes and, therefore, microbial kinetics (Jeris and Regan, 1973; Miller, 1991; Haug, 1995). In addition, the FAS of compost is explicitly correlated to the oxygen diffusion coefficient and friction factors (Oppenheimer *et al.*, 1996).

Air must be supplied to an aerobic composting system for three basic purposes: 1) to satisfy oxygen demands and remove carbon dioxide and ammonia, 2) to remove moisture, and 3) to remove heat (Haug, 1995). If no forced aeration is used (e.g., static piles, windrows, etc.) the physical properties of the materials must be managed to ensure oxygen does not become a limiting factor in the pile (Shell, 1955; Hamelers, 1992; Tseng *et al.*, 1995). Knowledge of the physical properties of the feedstock materials can help determine initial mixing ratios. Proper mixing and selection of bulking agents can help maintain pile structure, eliminating excessive compaction at the bottom of the pile or windrow. Measuring and monitoring the porosity or FAS of the compost during the process can help determine turning schedules and the selection of optimum bulking agents.

Methods of measuring porosity of compost are few. Most researchers have used methods adapted from the analysis of soils or other granular materials, like the water displacement method (Leege and Thompson, 1997), also known as water pycnometry. This method includes adding a known volume of water to a compost mass until all of the air voids are expelled. The volume of water added is equivalent to the volume of air voids in the sample. Typically, this method uses disturbed samples and does not account for the compressive settlement that occurs within a compost pile. This means that the

values obtained for air space will only be accurate for the top portion of the pile (McCartney and Chen, 2000). The absence of compressive settlement in existing physical models may lead to errors if the data are used to design full-scale windrow composting facilities.

Mohsenin (1986) described an air comparison pycnometer, as well as conventional pycnometer methods, that could be used in determining air volume in granular organic materials. Air and gas pycnometers use the same principle as the water displacement method with pressurized gases and the ideal gas law being used instead of water. Oppenheimer *et al.* (1996) and Baker *et al.* (1998) also found the air pycnometer to be a quick and accurate device for measuring the air-filled porosity of unsaturated organic matrices.

Other methods of determining soil porosity and FAS could be extended for use in the composting industry. The specific gravity bottle (Waller and Harrison, 1991), water retention apparatus (Raviv *et al.*, 1987; Waller and Harrison, 1991), mercury porosimetry and nitrogen adsorption (Oppenheimer *et al.*, 1996), and paraffin wax methods (Waller and Harrison, 1991) have been used in the past. However, these methods are costly, time consuming, and require the material to be completely dry. The problem is one of measuring FAS of a matrix composed of compounds in all three different phases: insoluble organics, liquid water and air (Oppenheimer *et al.*, 1996). Again, the absence of compressive settlement analysis can lead to errors in aeration predictions which would lead to anaerobic regions in the bottom or middle of a pile.

Recently, McCartney and Chen (2000) presented the potential use of "biocells" for FAS analysis. The use of "biocells" allows researchers to subject materials to loads similar

to those found *in situ* and then calculate the FAS based on the volume reduction and unloaded FAS using soil compression equations. This method eliminates the errors incurred by using disturbed samples but still assumes that compost particles behave like incompressible soil particles.

2.3. Particle Density

Particle density is defined as the mass of solids divided by the volume the solids occupy. Since the determination of particle density requires the measurement of the air voids, little work has been done to establish the relationship among particle density, moisture content, bulk density and compression. Calculation of the particle density from the data presented in Baker *et al.* (1998) showed no direct relationship between particle density and wet bulk density, dry bulk density or moisture content. However, the average particle density for the manure and cornstalks mixture was relatively constant over the range of moisture contents (56 – 68% w.b.) at 1563kgm^{-3} with a standard deviation of 189kgm^{-3} (Baker *et al.*, 1998).

2.4. Particle Size Distribution

Particle size distribution dictates the surface area available for microorganisms and can also be related to ease of compaction (Agnew and Leonard, 2002). Since the size and orientation of compost particles often dictate the size and amount of air voids present in the mass, the influence of particle size distribution on FAS was examined by Oppenheimer *et al.* (1996). Dog food and sewage sludge were mixed with three sizes of

woodchips and the air voids were measured using a custom pycnometer. There was no observed influence of particle size on FAS. The authors theorized that the size of the aggregates that formed was not governed by the size of the wood chips alone. Like many soil aggregates, the size and shape of the organic aggregates are influenced by complex mechanisms, such as adsorption, chemical bonding, physical entanglement and biological cementation (Oppenheimer *et al.*, 1996).

2.5. Compressibility

The effect of sewage sludge content on soil compressibility was examined by Stone and Ekwue (1996). Soil compressibility is defined as the ease with which soil decreases in volume when subjected to a mechanical load. Sandy loam, clay loam and clay soils were amended with sewage sludge (up to 12% by mass) and compression curves (void ratio versus log applied stress) for each soil were almost linear over the range of applied stress. The applied stress was dependent on the soil type, but sewage sludge increased soil compressibility in all cases (Stone and Ekwue, 1996). In other words, higher moisture contents increased the compressibility of the soil. This was also shown in the work of Schaub (1997) where the compressibility of peat and compost increased when the moisture content was increased from approximately 20% (w.b.) to about 50% (w.b.).

2.6. Recent Research

Schaub (1997) measured the wet and dry bulk densities of peat and compost at three moisture contents and various compressive loads. An "effective pile density" was

determined by integrating Equation 2.1 for each of the materials. This "effective pile density" gave a good estimation of the overall pile density, considering both the compressed and uncompressed material.

Both wet and dry effective densities increased with moisture content (24 to 47% w.b.) for the compost material. However, the dry effective density of the wet peat (74% w.b.) was lower than the dry effective density for the drier peat (52% w.b.). These conflicting observations may be explained by the behaviour of the material as water was added to the matrix. As the moisture in the compost increased, the water displaced air spaces and caused the particles to "settle". As well, the water may have weakened bonds within the compost matrix, collapsing some of the particles, reducing the overall volume. Since the mass of the dry matter was unchanged, this collapse of pores resulted in an increase of dry bulk density. In special cases, like the peat studied by Schaub (1997), this collapse may be resisted by the extremely fine particle sizes and the rigidity of the material. In fact, the overall matrix may swell due to the hydrophobic nature of peat, increasing the total volume and decreasing the dry bulk density.

Baker *et al.* (1998) built a custom iron pycnometer to examine the impact of moisture content and dry bulk density on the free air space of dairy manure and sawdust mixes. As expected, the FAS decreased with increasing moisture while the wet density increased with higher moisture contents. When the moisture content was 70% (w.b.), the FAS was approximately 35% and when the moisture content was 55% (w.b.), the FAS increased to about 42%. The authors concluded that if the total solids are held constant, incremental increases in moisture content cause a proportionately greater decrease in FAS.

As mentioned, McCartney and Chen (2000) used "biocells" to investigate the effect of settlement on the bulk density and FAS of biosolids, leaves, straw and woodchips. The authors used a commercial pycnometer to obtain the particle density and Equations 2.2, 2.3 and 2.4 to calculate the initial FAS.

$$Porosity = (1-\frac{BD_{dry}}{PD})*100\% \quad (2.2)$$

$$MC_{vol} = (\frac{MC_{dry}BD_{dry}}{\rho_w})*100\% \quad (2.3)$$

$$FAS = Porosity - MC_{vol} \quad (2.4)$$

where BD_{dry} is the dry bulk density (kgm^{-3}), PD is the particle density (kgm^{-3}), MC_{vol} is the volumetric moisture content (% v/v), ρ_w is the density of water (kgm^{-3}) and MC_{dry} is the moisture content expressed on a dry basis (mass fraction). The dry bulk density is the mass of solid material divided by the total volume of the wet material.

The FAS of the compacted material was calculated based on the volume reduction and the soil compaction relationship shown in Equation 2.5.

$$FAS_i = \frac{FAS_o V_o - (V_o - V_i)}{V_i} \quad (2.5)$$

where FAS_i is the compacted FAS, FAS_o is the original FAS, V_o is the original volume and V_i is the volume of the compacted material. This equation assumes a constant moisture content and particle density at all compressive loads.

The settlement behaviour of the biosolids mixtures was found to fit established soil compaction equations and new equations were developed to represent the vertical FAS and bulk density profiles in composting systems (McCartney and Chen, 2000). The FAS of all

materials decreased with depth (compression) and the bulk density increased with depth, as can be seen in their data shown in Table C.3 in Appendix C.

2.7 Property Relationships

Examining the relationships among the physical properties allows an estimation of the influence of one parameter on another. For example, FAS is obviously related to the moisture content as the FAS is equal to the total voids minus the water-filled voids (Equation 2.4). However, the direct relationship between FAS, bulk density and particle density is less intuitive. The FAS can be expressed as a function of bulk density, moisture content and particle density by noting that:

$$V_t = V_{air} + V_W + V_{sol} \tag{2.6}$$

where V_t is the total volume, V_{air} is the volume of air voids, V_W is the volume of water, and V_{sol} is the volume of solids. Rearranging, and substituting for $V_{sol} = M_s/PD$:

$$V_A = V_t - V_w - \frac{M_s}{PD} \tag{2.7}$$

where PD is particle density (kgm^{-3}). Dividing all terms by V_t and noting that FAS = V_{air}/V_t,

$$FAS = 1 - \frac{V_w}{V_t} - \frac{M_s}{PDV_t} \tag{2.8}$$

Since $V_w = (M_T MC/\rho_w)$ and $M_s = M_T(1\text{-}MC)$, Equation 2.8 becomes:

$$FAS = 1 - \frac{M_T MC}{V_t \rho_w} - \frac{M_T(1-MC)}{PDV_t} \tag{2.9}$$

Noting that $V_t = M_T/BD$ where BD is bulk density (kgm^{-3}) and rearranging further results in the following equation,

$$FAS = 100 - BD\left(\frac{MC}{\rho_w} + \frac{(100 - MC)}{PD}\right) \qquad (2.10)$$

where MC is expressed as a percentage and ρ_w is the density of water ($1000kgm^{-3}$). Conversely, if the FAS, BD and MC are known, the PD can also be calculated using the theoretical relationship in Equation 2.10.

This relationship is valid for all materials where each of the variables is known. For compost, the moisture content and uncompressed bulk density can easily be determined. However, as discussed in Section 2.3, the particle density of compost is not as readily determined since it often requires an air volume measurement. Literature values of the particle density of common compost mixtures are few and varied, but the development of an accurate, simple way of measuring the air space of compost materials would allow the development of accurate and reliable compost particle density values.

In order to determine the sensitivity of the parameters on the FAS calculation in Equation 2.10, partial differentiation and error analysis using typical values of bulk density, moisture content and particle density was carried out (equations and analysis are presented in Appendix G). The analysis suggests that in order to maintain a 5% error in FAS calculation, the moisture content and particle density parameters can have an error of up to 20% while the bulk density value must be accurate to approximately 5%. In other words, the theoretical relationship among the parameters (Equation 2.10) is most sensitive to the bulk density value and care must be taken to reduce the error associated with the bulk density measurement.

3. Design and Calibration of Pycnometer

3.1 Rationale

Of the methods available for FAS determination, the air pycnometer has been shown to be the most accurate and reliable (Baker *et al.*, 1998; Oppenheimer *et al.*, 1996). Water pycnometers are also reliable, but the addition of water makes repeated analysis difficult and may give erroneous values for material with high moisture contents due to surface tension and cohesion effects. Material with small pores filled with water may not completely drain between measurements, or small air pockets may not be expelled during the addition of water, trapping air within the sample.

On the other hand, FAS readings from an air pycnometer are not affected by the moisture content of the material. As well, air pycnometers require minimal handling of the material and, once calibrated, require very little input from the user. The vessels may be scaled up to accommodate larger samples and modified to allow compressive loading simulation. Another advantage of the pycnometer was the ability to accurately measure the sample volume while loading. Therefore, if the mass of the sample was known, the bulk density can be calculated. This would allow the determination of bulk density as well as FAS at all pile depths.

For these reasons, the decision was made to design and build an air pycnometer that could be used with composting materials and with provisions for applying compressive loads to samples.

3.2. Pycnometer Principle

To obtain air volume readings, the pycnometer uses Boyle's Ideal Gas Law,

$$PV=nRT \tag{3.1}$$

where P = pressure, V = volume, n = moles of gas, R = gas constant, T = temperature. A simple schematic diagram of a pycnometer is shown in Figure 3.1.

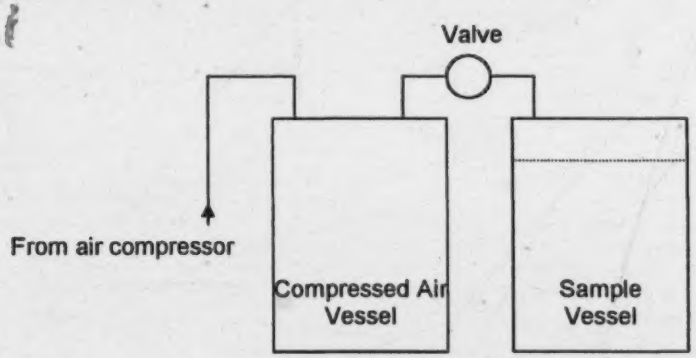

Figure 3.1. Simple Pycnometer

Two chambers are connected with a valve so the compressed air vessel can be isolated. The sample is placed in the sample vessel and the air vessel is pressurized to a set pressure. The valve is opened and the pressure is allowed to equilibrate. In a closed system, as in the pycnometer, the term nRT of the ideal gas law remains constant so, if the initial pressure and volume are known, and the final pressure is measured, the final volume can be calculated using the relationship:

$$P_1V_A = P_2V_T \tag{3.2}$$

where P_1 = initial pressure in compressed air vessel, P_2 = final pressure of equilibrated system, V_A = volume of compressed air vessel, and V_T = volume of overall system (compressed air vessel, sample vessel, pipe, and fittings). Expanding the V_T term:

$$P_1V_A = P_2(V_B + V_A - V_S(1 - FAS)) \tag{3.3}$$

where V_B = volume of sample vessel, V_S = volume of solid sample and FAS = volume of air in sample/V_S (fraction).

Solving for FAS of the sample:

$$FAS = \frac{\frac{P_1 V_A}{P_2} - V_B - V_A + V_S}{V_S} \qquad (3.4)$$

When calibrating the pycnometer using water, which has no FAS, the equation simplifies to:

$$P_2 = \frac{P_1 V_A}{V_B + V_A - V_S} \qquad (3.5)$$

Air pycnometers are commercially available. However, they are expensive, and the largest sample chamber available is only 0.15L (Geddis *et al.*, 1996), which is unsuitable for compost mixtures containing woodchips and other large particle sizes.

3.3. Pycnometer Design

McCartney and Chen (2000) and Schaub-Szabo and Leonard (1999) used a piston assembly with weights to compress the compost samples, but this method was very labour intensive and limited the maximum depth that could be simulated. The loads required to simulate depths of up to 3m would be very high, so the pycnometer design was modified to incorporate an air cylinder in the sample vessel to minimize manual labour. The three critical components of the design were the sample vessel, the loading cylinder, and the pressure measurement system. These are described below.

3.3.1 Sample Vessel

The effects of wall friction in the sample vessel needed to be minimized. Schaub-Szabo and Leonard (1999) showed that these friction effects have significant effects on bulk density measurements in smaller containers (surface area to volume ratio greater than $10m^2m^{-3}$). Since a container with a surface area to volume ratio of less than $10m^2m^{-3}$ would be impractically large, this vessel was designed to have a surface area to volume ratio of $10m^2m^{-3}$. If the surface area was taken as the cylindrical area of the sample vessel wall (πDh) and the volume was the entire vessel volume ($\pi D^2h/4$), then for a surface area to volume ratio of $10m^2m^{-3}$, the diameter of the chamber needed to be 0.4m.

The sample volume must be large enough to accommodate a representative sample of compost material and amendment. In addition, larger containers would reduce the effects of volumes of fittings and hoses and errors in volume determination. Baker *et al.* (1998) used a 22L sample vessel while Oppenheimer *et al.* (1996) used a 1L container. With an optimum diameter of 0.4m, the 1L container would have a height of less than 1cm. Therefore, a 25L chamber was designed for, with a diameter of 0.4m and a height of approximately 0.2m.

Baker *et al.* (1998) used an initial pycnometer pressure of 207kPa while Oppenheimer *et al.* (1996) used initial pressures in the range of 300-500kPa. For a 25L plastic vessel, initial pressures of 500kPa are impractical as the forces on the walls and end-caps would require thicknesses of about 10cm. A preliminary experiment was performed with the 25L vessels and a sample of manure compost. Four initial pressures were tested (70, 140, 172 and 200kPa) and four FAS values were taken at each pressure. At higher pressures, the final air volume reading was less variable, as shown in Table 3.2.

This variability may have been due to the sensitivity of the pressure transducer. The diaphragm used for this experiment was rated for the pressures used (70 – 200kPa), but the voltage output was more sensitive at full scale readings (180 – 200kPa). An initial pressure of approximately 200kPa provided a good compromise between precision and practicality.

Table 3.2. Variation of FAS readings at various operating pressures for manure compost (MC = 55% w.b.).

P_1 (kPa)	P_2 (kPa)	FAS (average of 4 values)	Standard Deviation of FAS
70	41	39.92	9.27
140	34	34.72	4.66
172	107	37.52	1.43
200	130	36.07	0.64

The sample vessel needed to be easy to open and clean and return to an airtight state. A drainage system was incorporated into the sample vessel to accommodate leaching from wet materials. The vessel material must be able to withstand at least 200kPa of pressure and be airtight at all operating pressures and temperatures. In addition, the vessel material needed to be able to withstand multiple and long-term loading, be corrosion resistant, and be relatively light and cost-effective. Baker *et al.* (1998) used custom-made iron chambers, but this material was thought to be too heavy and cumbersome for this project. Schedule 40 PVC pipe of 0.406m inner diameter and 0.011m thickness was used for the vessel walls and Schedule 80 PVC, 0.022m thick sheets were used for the end caps.

3.3.2. Load Cylinder

Material with an average wet bulk density of 600kgm^{-3} was expected, and at a cross sectional area of approximately 0.130m^2, the mass in 3m depth was approximately 225kg. This translates into a compressive stress of about 18kPa. To apply this load, a 102mm diameter, 1700kPa air cylinder (NCA1 Series, SMC Pneumatics Inc., Indianapolis, IN) was selected. Special options included a dual port and manifold for easy extension and retraction, and a double rod so the piston extension inside the vessel could be determined by measuring the exposed rod length. A larger rod diameter (35mm) was also selected to minimize the chance of fracture at high loads. Subtracting the rod area from the air cylinder area gave the total cross sectional area of the air cylinder as 0.00715m^2. Thus, to simulate the expected compressive stress of 18kPa in the pile, approximately 320kPa needed to be applied to this air cylinder.

3.3.3. Pressure Measurement and Regulation

Oppenheimer *et al.*, (1996) analyzed the performance of their pycnometer and expressed the uncertainty of the FAS reading based on the uncertainty in the volume and pressure readings. Results from the calculations indicated that there was an approximate linear relationship in the uncertainty in FAS due to uncertainty in P_1, V_A or V_B, but the uncertainty in P_1 yielded the greatest uncertainty in FAS. For example, a 1% uncertainty in either V_A or V_B led to approximately 1% error in FAS, but a 1% error in P_1 led to a 3.8% error in FAS. Therefore, it was important to have pressure gauges and pressure regulators that would lead to accurate adjustment and measurement of the pressures in the

pycnometer (Oppenheimer *et al.*, 1996). Error analysis specific to pycnometer designed for this project is presented in Appendix G.

All pressures were measured using pressure transducers (DP15TL, Validyne, Northridge, CA), one for vessel pressure determination and one for air cylinder pressure measurement. The signal was passed through a carrier demodulator (CD15, Validyne, Northridge, CA) and the voltage read with a multimeter (HP 34401A). A variety of replacement diaphragms for the pressure transducers was available to accurately measure the range of expected pressures in the air cylinder. Whenever a diaphragm was replaced, the transducer was calibrated using a dead weight tester (Chandler Engineering, Tulsa, OK). Refer to the "Operators Manual" in Appendix H for detailed calibration procedures. A 1400kPa full scale analog pressure gauge was also installed on the air vessel for rough pressure determinations. Refer to Appendix A for a complete list of the components used and their specifications.

The pressure of chamber 1 needed to be measured independently from the whole system, and the pressure inside the air cylinder used for compressive loading also needed to be measured independently. A schematic drawing of the overall system is presented in Figure 3.2.

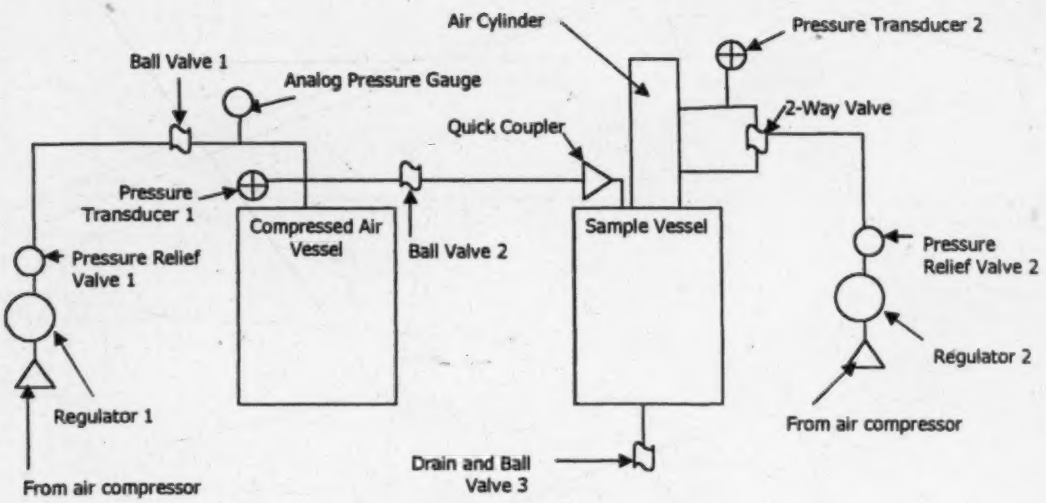

Figure 3.2. Schematic drawing of overall system.

3.4. Pycnometer Construction

Two sections of Schedule 40 PVC pipe were cut to a length of 0.285m and the rims were machined to a smooth finish. Eight circular plates (diameter = 0.508m) were cut out of the Schedule 80 PVC sheet. Each vessel end cap consisted of two of these plates. Two smaller plates were cut for the piston head and drainage floor (diameter = 0.406m). To fit the cylindrical pipe into the end caps to form the vessels, a 0.012m thick groove (inner diameter = 0.406m, depth = 0.0079m) was cut into one side of four of the larger circular plates. Eight equally spaced holes were then drilled around the perimeter of the end caps (centered approximately 0.030m from the edge) to accommodate the 0.012m diameter "ready rod" bolts used to close the vessel. A 0.0095m diameter hole was drilled into the top end cap and was positioned as shown in Figure 3.3. The holes

were then threaded to fit a standard 0.0095m diameter compressed air fitting. Teflon tape was applied to all threaded fittings to ensure an airtight seal.

Custom made polyvinyl gaskets (0.0016m thick) were fitted into each of the four large grooves to ensure the vessel was airtight.

The compressed air vessel was assembled by fitting a grooved plate to each end of one section of the PVC pipe. A small amount of PVC glue was applied to each grooved plate and another plate with holes for the "ready rods" was positioned on the grooved plate. This second end plate was added in order to reach the thickness required to withstand the expected pressures. The "ready rods" were then threaded through the holes and tightened with a washer and nut on each end. The vessel was pressure tested and was airtight up to a pressure of 250kPa.

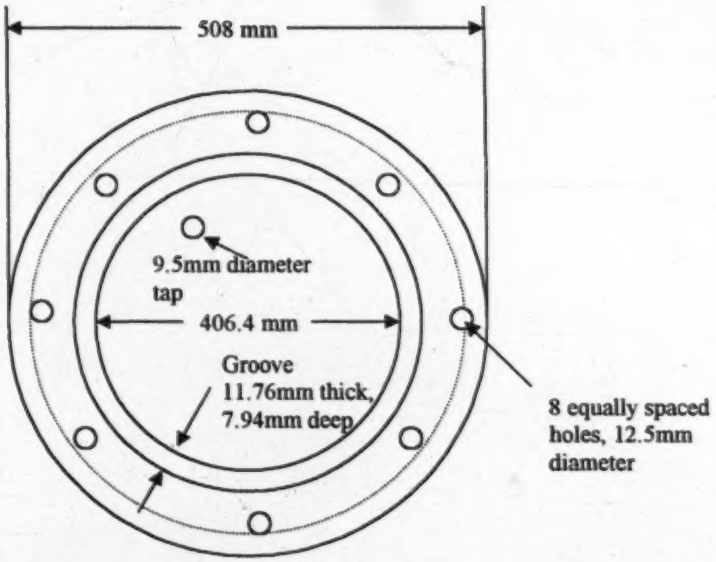

Figure 3.3. Dimensions of end caps (4) and groove. 9.5mm diameter hole tapped for air fittings appeared only on top caps. Sample vessel bottom cap had a similar hole in the center (for the drain) and sample vessel top cap had a large hole (diameter = 0.038m) in the center (for the piston rod).

The sample vessel was assembled similarly, with the following exceptions. A 0.0095m diameter hole was drilled through the center of the bottom cap and was tapped to serve as the drain. A 0.0349m diameter hole was cut and machined into the center of the top cap for the piston rod. The air cylinder was positioned on a steel flange plate and two sections of Schedule 80 PVC (0.203 x 0.101m) with a 0.0349m diameter hole machined in the middle (Figure 3.4). Two oil seals (National Federal-Mogul) were placed in one of the PVC plates between the air cylinder and the top cap to ensure there were no air leaks around the opening for the piston rod. Another 0.203 x 0.101m, 0.0159m thick polyvinyl gasket with a 0.0349m hole cut in the middle was placed between the bottom plastic plate and the top cap to ensure a good seal. Four 0.0095m

diameter, 0.114m long bolts were used to fasten the air cylinder, flange plate and plastic plates to the top cap of the sample vessel. PVC glue was applied to the washers and nuts on the inside of the vessel to eliminate air leaks.

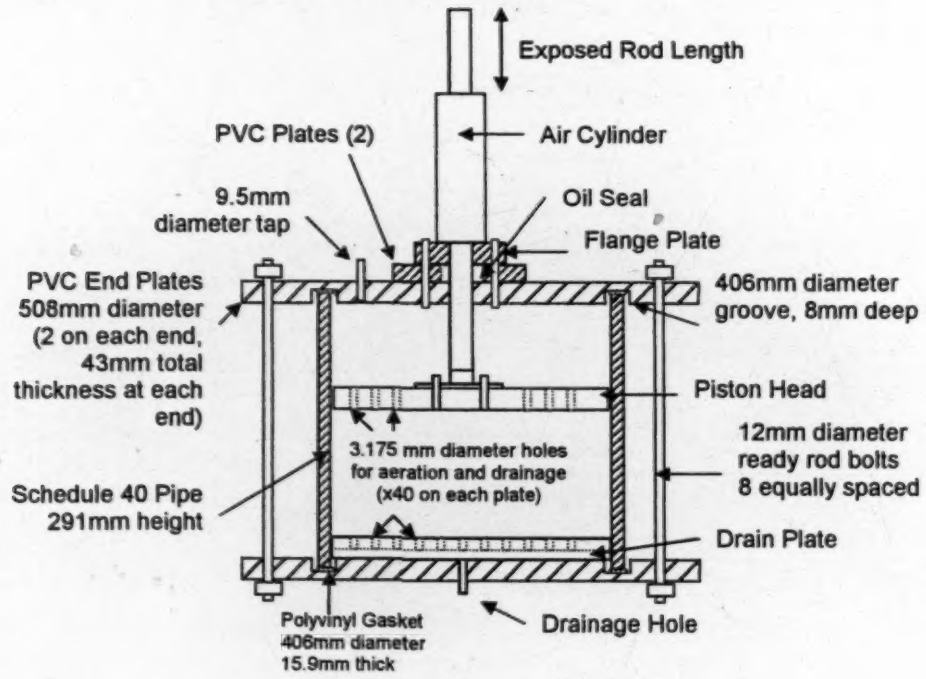
Exposed Rod Length
PVC Plates (2)
Air Cylinder
9.5mm diameter tap
Oil Seal
Flange Plate
PVC End Plates 508mm diameter (2 on each end, 43mm total thickness at each end)
406mm diameter groove, 8mm deep
Piston Head
12mm diameter ready rod bolts 8 equally spaced
3.175 mm diameter holes for aeration and drainage (x40 on each plate)
Schedule 40 Pipe 291mm height
Drain Plate
Polyvinyl Gasket 406mm diameter 15.9mm thick
Drainage Hole

Figure 3.4. Details of sample vessel and piston assembly.
(not drawn to scale)

The piston rod was manufactured with threads at both ends, so a 0.035m nut was welded to a 0.152m diameter, 0.019m thick circular steel plate. The metal plate and nut and a lock nut were then screwed onto one end of the piston rod to form the base of the piston head. The piston head was made out of the same PVC sheet as the end caps. It was cut to a diameter just slightly smaller than the inner diameter of the pipe (0.406m) to allow frictionless extension and retraction but prevent any material from squeezing

around the edge of the piston head. The piston head was perforated with 40 0.003m diameter holes in a circular pattern to allow unrestricted airflow through and around the piston head. The piston head was attached to the metal plate and air cylinder rod with four 0.013m diameter, flat head bolts.

A drain plate was cut out of the Schedule 80 PVC sheet with the same diameter as the piston head (0.406m). Again, 40 0.003m diameter perforations were drilled into the plate, and grooves (0.025m wide and 0.007m deep) were cut between the perforations on the bottom side to ensure the water draining through the perforations flowed to the center and out the drain. These are shown in Figure A.4 in Appendix A.

The sample vessel was assembled in the same manner as the compressed air vessel and the air seal held for all pressures up to 250kPa. The sample vessel was opened by loosening and removing all eight nuts around the perimeter of the top cap. The seal was broken by gently tapping the underside of the top cap with a hammer. The top cap and air cylinder and piston could then be removed, allowing for removal and addition of sample material. Because the sample vessel was repeatedly opened and closed throughout the study, vacuum grease was applied to both grooves after each opening to ensure a good air seal.

3.5. System Calibration

The pycnometer was calibrated for FAS measurements using tap water since water has no free air space. The sample tank was filled in 2L increments with pycnometer readings taken for each addition (Table B.1 in Appendix B).

During the calibration, the theoretical final pressure readings (P_2 in Equation 3.5) were compared with the actual pressure readings. The actual and theoretical final pressure readings were very close, as shown in Figure 3.5. The calibration equation for P_2 was found by plotting the actual P_2 values versus the theoretical P_2 values in Figure 3.5.

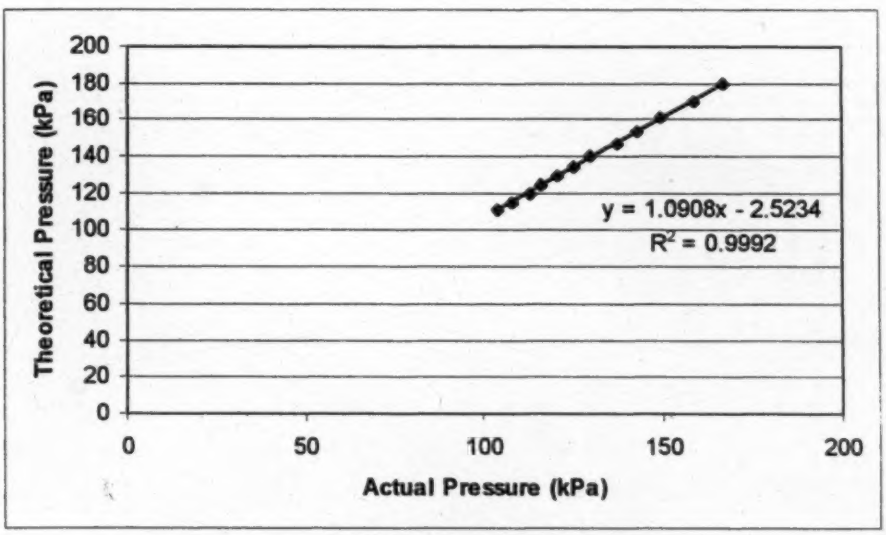

Figure 3.5. Calibration of pycnometer with water

The final, calibrated equation for FAS was

$$FAS = \frac{\frac{P_1 V_A}{1.0908 P_2 - 2.5234} - V_B - V_A + V_S}{V_S} \tag{3.6}$$

The volume of the compressed air vessel (V_A) was 31.005L. V_A would never change and was found both by calculation and with duplicated water addition. V_B would change depending on the stroke of the piston since the piston rod occupied part of the vessel volume. Therefore, the volume of the sample vessel was found at maximum and

minimum piston extensions by duplicated water addition (Appendix B). A linear equation was developed so that the total sample vessel volume could be found at all piston heights and is shown in Equation 3.7.

$$V_B = 0.00094x + 26.8 \ [L] \qquad (3.7)$$

where x is the exposed rod length in mm and the volume is expressed as litres (L).

The volume of the sample would also change with compressive loading. As the sample was compressed, some air and water voids were expelled and the total volume decreased. In fact, the cross sectional area of the sample within the vessel remained constant, but the height of the sample decreased with compressive loading. This was calibrated for by loading the sample vessel with increments of clean gravel. The actual depth of the gravel was measured manually with a tape measure, the lid and piston replaced and the piston extended until it reached the gravel surface. The exposed rod length was then measured and plotted against the actual height of the sample (Figure B.1 in Appendix B). Multiplying the regression equation by the cross sectional area of the sample vessel ($0.130 m^2$), resulted in Equation 3.8 where the sample volume can be calculated at any piston height:

$$V_S = 0.130 (x - 125) \ [L] \qquad (3.8)$$

where x is the exposed rod length in mm and the volume is expressed as litres (L).

3.6. Simulating Compressive Loading

Materials such as compost will compress under their own weight when they are piled. Since the sample must be disturbed to be placed in the pycnometer, these

compressive loads must be simulated inside the vessel in order to predict the FAS values of compressed compost.

The wet bulk density can easily be calculated by dividing the total mass by the sample volume. The mass of compost in the pile at any depth in a pile is found by:

$$Mass = depth * area * bulk\ density \quad (3.9)$$

where mass is in kg, depth is the desired simulated depth in m, area in m^2 and bulk density is in kgm^{-3}.

For this system, the area is simply the cross sectional area of the sample vessel which was $0.130m^2$. Depending on the maximum simulated depth desired, it was convenient to simulate either 0.2m or 0.5m increments of depth. Samples with a lower desired depth (less than 2m) would be loaded with increments of 0.2m. On the other hand, samples with a desired depth of greater than 2m would be loaded with increments of 0.5m to reduce the time required to reach the maximum depth.

Since depth and area are the same for each increment, Equation 3.9 simplifies to:

$$Mass = 0.0648 * \sum \rho_b \text{ for 0.5m increments, and} \quad (3.10a)$$

$$Mass = 0.0259 * \sum \rho_b \text{ for 0.2m increments} \quad (3.10b)$$

where $\sum \rho_b$ is the cumulative sum of the bulk densities at each compressive load.

To convert this mass (kg) to the pressure (kPa) required by the air cylinder, the following equation was used:

$$Pressure = \frac{Mass * 9.81}{0.00715} \quad [kPa] \quad (3.11)$$

where 9.81 is the acceleration due to gravity (ms^{-2}) and 0.00715 is the cross sectional area of the interior of the air cylinder (m^2).

Once the sample was placed in the chamber and the sample vessel was sealed, the piston was slowly extended until it stopped and the exposed rod length indicated the piston had reached the top of the sample. Uncompressed FAS and bulk density readings were taken. To simulate the first depth (0.2 or 0.5m), the calculated pressure (Equation 3.11) was applied to the air cylinder which extended the piston and compressed the sample. The pressure in the cylinder was maintained by the regulator until the piston stopped advancing and the material was compressed. This took anywhere from one hour to three days, depending on the moisture content and rigidity of the material. Once the material was compressed at the desired load, another set of FAS and bulk density readings were taken. The process continued until the material was compressed and FAS and bulk density readings are taken at all desired loads corresponding to the desired simulated depths.

3.7. System Operation

A sample of known mass and moisture content was placed in the sample vessel and the desired pressure was applied to the air cylinder to simulate the required depth. Once the sample was compressed, the vessel volume and sample volume were determined by measuring the exposed rod length and using Equations 3.7 and 3.8 respectively. The compressed air vessel was then pressurized to approximately 200kPa (P_1) and the pressure was recorded. The valve between the vessels was opened and the pressure allowed to equilibrate. The final pressure (P_2) was read and recorded after the system reached equilibrium. The system was then allowed to bleed, returning the vessel pressures to atmospheric. The procedure was repeated until the desired number of

replicates was reached. The bulk density could be calculated easily by dividing the mass by the sample volume. The FAS at the simulated depth could then be calculated by applying the pressures and volumes to Equation 3.6.

Refer to the "Operators Manual" in Appendix H for detailed operation of the pycnometer.

4. Bulk Density and Free Air Space Measurements

4.1. Materials and Methods

4.1.1. Materials

A variety of organic materials were available for analysis. Mature manure compost from a lab-scale trial was one of the materials used. This was made from barley straw and a mixture of manure from the University of Alberta's Edmonton Research Station. Composted municipal solid waste (MSW) was obtained from the City of Edmonton Waste Management Center. The material had been curing for approximately 6 weeks. Pure biosolids were also obtained from the City of Edmonton Waste Management Center and were stored until needed in a sealed plastic container (approximately 2 weeks) at 20°C.

Various amendment materials (leaves, straw and woodchips) were also tested individually and mixed with the biosolids. The biosolids and amendments were mixed to obtain a target moisture content of 55%. Equation 4.1 was used to calculate the ratio of amendment to biosolids material.

$$M_T(MC_T) = M_B(MC_B) + M_A(MC_A) \qquad (4.1)$$

where M_T is the total wet mass required (approximately 20kg), MC_T is the target overall wet basis moisture content (55%), M_B is the mass of pure biosolids, MC_B is the wet basis moisture content of the pure biosolids (70%), M_A is the mass of amendment required and MC_A is the wet basis moisture content of the amendment material. The initial properties of all materials are listed in Table 4.1.

Table 4.1. Initial properties of the materials.

Material	Moisture Content (%, w.b.)	Wet Bulk Density (kgm^{-3})
Manure Compost	25	205
MSW Compost	42	440
Biosolids	70	1000
Straw	0.8	51
Woodchips	9	170
Leaves	30	45

4.1.2. Experimental Methods

Moisture contents throughout this study were measured by gravimetric analysis and oven drying at 104°C for approximately 18 hours, in accordance to standards for the drying of organic materials (ASTM, 1994; ASAE 2000). All moisture contents were an average of duplicate measurements, one taken at the beginning and one at the end of the characterization. Depending on how easily the material compressed, the time between moisture content tests could have been anywhere from one hour to three days, but since the sample vessel was completely sealed during the characterization, the moisture losses to the atmosphere were minimal.

In order to analyze the material at two or three moisture contents, water was added to the dry material and allowed to equilibrate over night before analysis. Equation 4.2 was used to calculate the amount of water addition required to reach the target moisture contents.

$$W = \frac{MC_T M_T - M_w}{1 - MC_T} \tag{4.2}$$

where W is the mass of water added (kg), MC_T is the target wet moisture content (decimal), M_T is the original total mass of the material (kg), and M_W is the mass of the water in the original material (kg). The actual moisture content of the wetted material was also measured by gravimetric analysis and this value was used in all subsequent calculations.

The bulk density and FAS of each material were determined to simulated depths of 3m with the pycnometer as described in Chapter 3 and the "Operators Manual" in Appendix H. The mass of all samples were determined with an electronic platform scale that weighed up to 100kg with a sensitivity of 0.01kg (Accuweigh, Precision Scales, Edmonton, AB) before loading the vessel. All FAS values were averages of three readings. The porosity or total voids were calculated by adding the volumetric moisture content to the FAS. The volumetric moisture content was calculated using Equation 2.3.

4.1.3. Statistical Methods

Since it was difficult to characterize all materials at the same moisture content, the statistical analysis was performed on the materials separately. The manure compost, MSW compost and biosolids material were analyzed with moisture content, depth, and the interaction between moisture content and depth as the sources of variation. The effects of these variables on the FAS, particle density and porosity of the material could then be analyzed with the general linear model procedure in SAS (1998).

In order to determine the effect of material type on the FAS, particle density and porosity, another statistical analysis was performed. This time, the effect of material was tested with moisture content nested within material as the error term.

4.2. Results

4.2.1. Manure Compost and MSW Compost

Each material was characterized to obtain bulk density and FAS profiles (variation with depth) as well as to relate wet bulk density (BD) and FAS. The FAS and bulk density profiles for the manure compost at three moisture contents are shown in Figure 4.1.

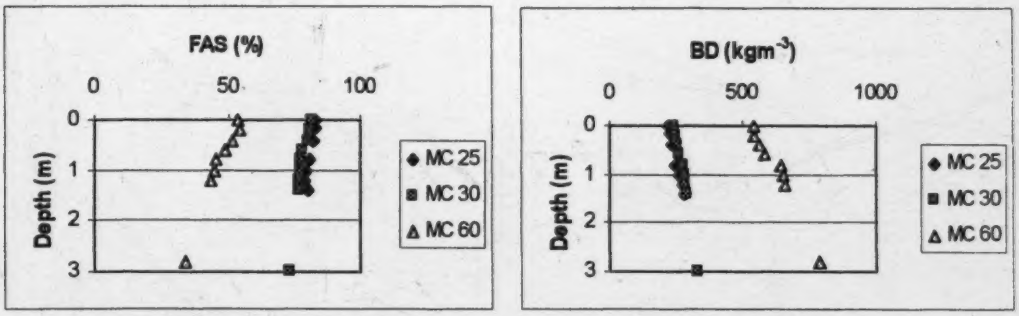

Figure 4.1. Profiles for manure compost a) FAS and b) BD.

As expected, the BD increased with both simulated depth and moisture content. At higher compressive loads, air voids were displaced and the matrix became denser. At higher moisture contents, the water filled the air voids and increased the overall mass of the sample. Figure 4.1 illustrates the reciprocity between FAS and BD and Figure 4.2 illustrates the linear relationship between BD and FAS of the manure compost in this study. These results are in agreement with those of Baker *et al.* (1998) who also observed a linear relationship between dry density and FAS for each moisture content analyzed. The magnitude of the FAS and BD values are within the range of values found in literature (Rynk, 1992).

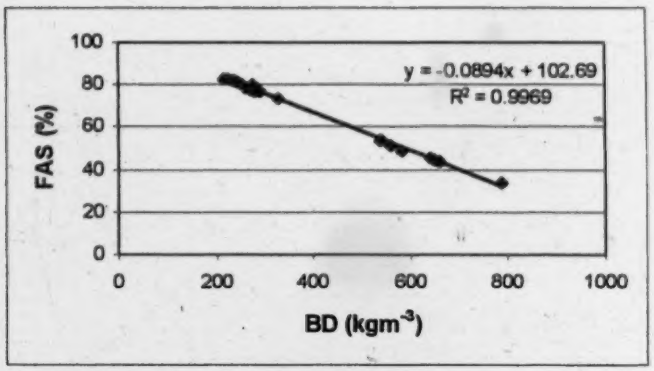

Figure 4.2. FAS vs BD for manure compost.

In this case, since the wet bulk density reflects the moisture content, a single linear relationship exists for this material. It is important to note that the linear relationship in Figure 4.2 is valid only for moisture contents between 25 and 60% (w.b.). The standard errors for the regression parameters are summarized in Table E.1 in Appendix E.

The same kinds of relationships existed for the MSW compost. The profiles for FAS and BD are shown in Figure 4.3. The magnitude of the wet bulk density is slightly higher while the overall FAS is slightly lower than that of the manure compost. The particle size of the MSW was smaller than that of the manure compost, making for a slightly denser and more compact material. As well, the particle sizes were more uniform, eliminating large pore spaces.

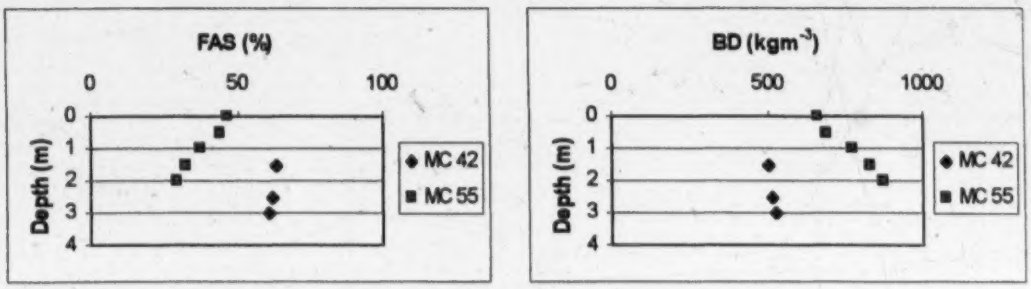

Figure 4.3. Profiles for MSW compost a) FAS and b) BD.

Again, the relationship between the wet bulk density and FAS was linear for the MSW, as seen in Figure 4.4. It is also interesting to note the similarity between the coefficients for the regression equation between the manure compost and the MSW.

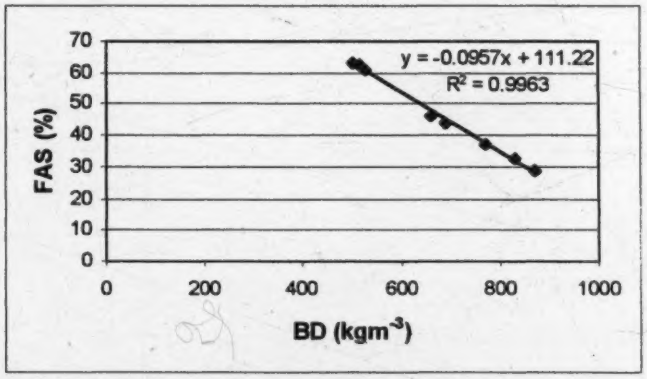

Figure 4.4. FAS vs BD for MSW compost.

4.2.2. Amendment Materials

Similar profiles were found for all the amendment materials tested (leaves, straw and woodchips) (Appendix E). Though the bulk densities were generally lower and FAS was quite high (as high as 90%), the shapes and trends of the FAS and BD profiles followed those of the manure compost and MSW compost. More interesting to note are

the relationships between the wet bulk density and FAS of the leaves, straw and woodchips. Again, they were linear with coefficients very similar to those found earlier, as seen in Figure 4.5.

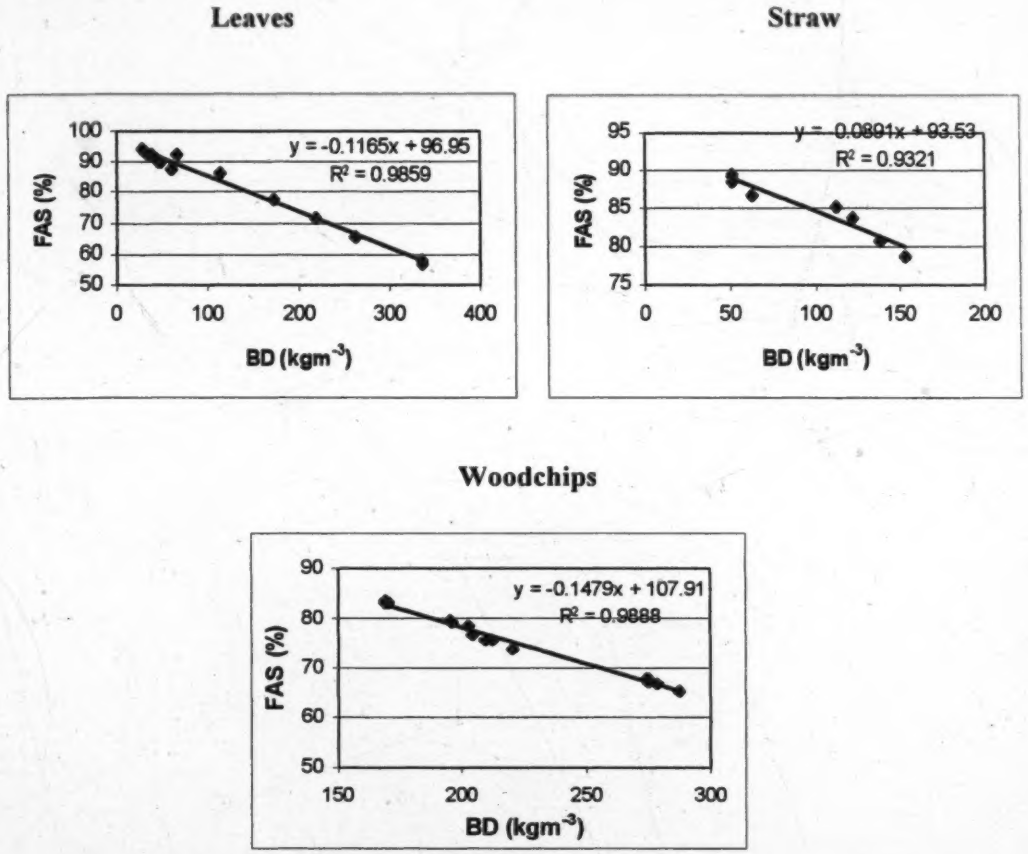

Figure 4.5. Bulk density and FAS relationship for a) leaves (11 to 59% w.b.), (b) straw (0.81 to 50% w.b.), and c) woodchips (9 to 48% w.b.). Standard errors can be found in Table E.1 in Appendix E.

4.2.3. Biosolids

The same trends were found for the pure biosolids and the biosolids mixed with the various amendments (Appendix E). In these cases, the bulk densities were very high, ranging between 500 and 1050kgm^{-3}. At high compressive loads (3m depth) the FAS dropped to 0% for the pure biosolids and biosolids mixed with leaves. Again, the FAS decreased linearly and the BD increased linearly with compressive loading and varied over a much wider range than the other materials, as shown in Figure 4.6 for the biosolids mixed with straw.

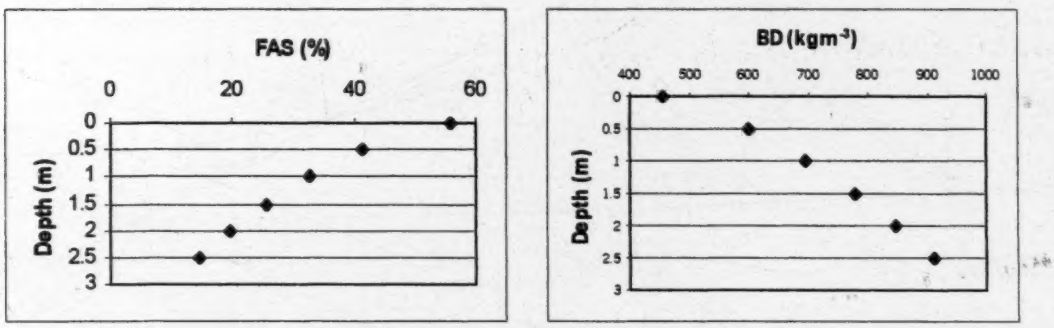

Figure 4.6. Profiles for straw-biosolids, MC = 69% (w.b.) a) FAS and b) bulk density.

The wet bulk density and FAS relationship was again linear, as shown in Figure 4.7 for the biosolids mixed with straw. Again, the coefficients for the regression equation are very similar to those found for the other organic materials in this study.

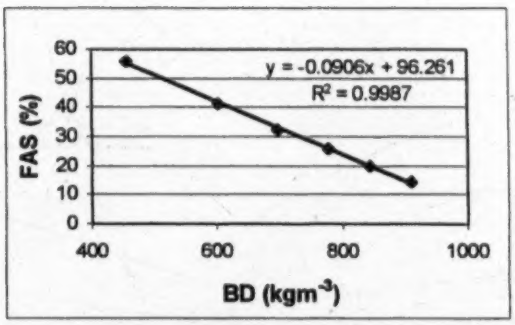

Figure 4.7. FAS vs BD for straw-biosolids.

4.3. Interpretation of Results

4.3.1. Pycnometer Performance

Since there are very few existing methods of measuring the FAS of organic materials, it was impossible to directly compare the results found by the pycnometer to literature values to assess the accuracy of the pycnometer. However, during the water calibration outlined in Section 3.5, the air space volumes found by the pycnometer were very close to the actual air volume found by subtracting the volume of water from the total vessel volume. In addition, the preliminary trial with gravel indicated the accuracy of the pycnometer. The FAS of the gravel was found by water pycnometry and compared to the FAS found by the air pycnometer. The values were accurate within 3% and the air pycnometer values were consistently higher than those found by water pycnometry. Because of the pressures associated with the air pycnometer, all voids, including the micro pores within the particles, are penetrated. These micro volumes are included in the FAS calculated, resulting in a higher FAS value.

The FAS values found by the pycnometer were also precise. The variation among repetitions was very low with the relative error of the FAS reading less than 2.3% and the relative error of the equilibrium pressure reading less than 0.4% (Table G.1 in Appendix G). This indicates that the volume measurements were less precise than the pressure readings. However, the overall FAS values were still accurate and precise.

4.3.2. FAS and Bulk Density

Interpreting the data from Baker *et al.* (1998) and converting their dry bulk densities to wet bulk densities, a graph of wet bulk density versus FAS can be developed for their mixtures of manure, sawdust and cornstalks, and this is shown in Figure 4.8.

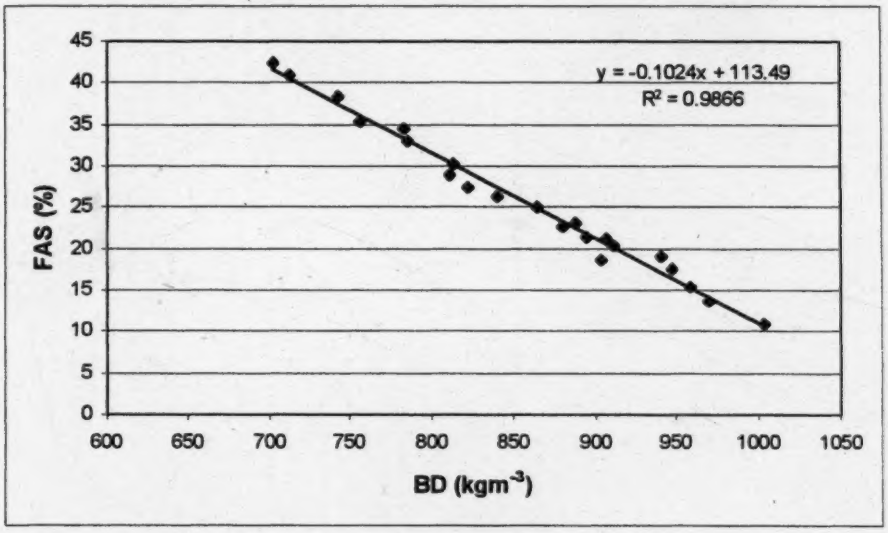

Figure 4.8. FAS vs BD for data from Baker *et al.* (1998) (50 to 70% w.b.).

Again, the coefficients for the regression equation are very similar to those found with the pycnometer and materials used in this study. This suggests that one equation

could describe the FAS and bulk density relationship for all composting materials. It is reasonable to assume that, at a bulk density of 0, there would be 100% FAS. Putting all of the data from this study together with that from Baker *et al.* (1998), and forcing the regression line through the point (0,100), resulted in the graph shown in Figure 4.9. The overall regression equation (FAS = 100 – 0.0889 BD) had an R^2 value of 0.97.

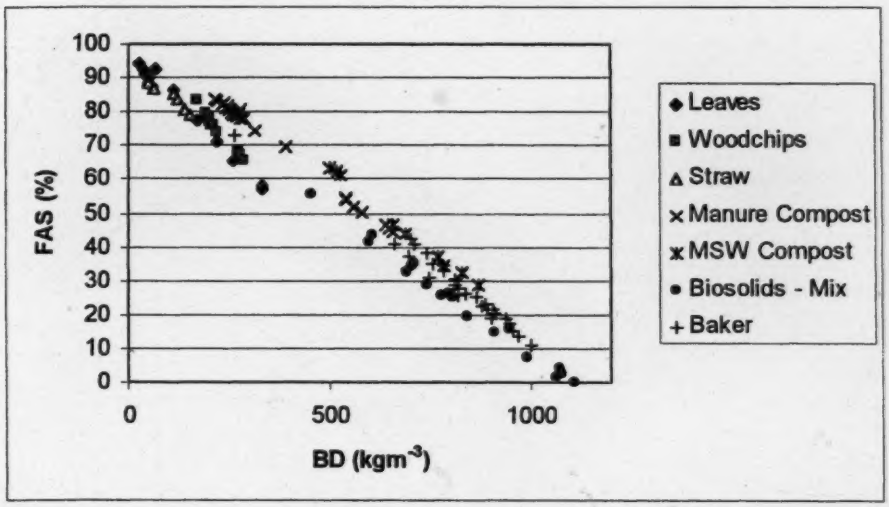

Figure 4.9. FAS vs BD summary of all values from this study, including data from Baker *et al.* (1998).

Thus, it is apparent that, if the BD is known, the FAS can be reliably calculated with the general regression equation:

$$FAS = 100 - 0.09\,BD \qquad (4.3)$$

where FAS is a percentage and BD is the wet bulk density in kgm^{-3}.

Comparing Equations 4.3 with the theoretical relationship (Equation 2.10), it is apparent that the constant 0.09 is equivalent to the term:

$$\frac{MC}{\rho_w} + \frac{100 - MC}{PD} = 0.09 \pm 0.001 \qquad (4.4)$$

where 0.001 is the standard error of the regression parameter (SAS, 1998).

This relationship is valid only for the materials and range of moisture contents analyzed in this study (approximately 10 – 80% w.b.).

4.3.3. Particle Density and Moisture Content

Intuitively, for a given compressive load, the particle density should remain constant at all moisture contents. The mass and volume of solids should be independent of the amount of moisture, assuming that the individual particles do not take up moisture and the water is held only in the empty pores. However, through statistical analysis (SAS, 1998), it was found that the particle density changed slightly with increasing moisture, as represented in Table 4.2. In some cases, this could be explained by the uptake of moisture causing the solid particles to swell, increasing the volume and causing an overall decrease in particle density. In other cases, the uptake of moisture may have weakened the particle structure, causing the particle to collapse, lowering the particle volume and increasing the overall particle density. Whether the particle swelled or collapsed depended on the type of material, the strength of the matrix, and the hydrophobic nature of the material.

In particular, the particle density values for the woodchips appear to be very low, especially at the higher moisture contents. In the material with higher water contents, small pockets of air may have been surrounded by moisture, and the pressurized air may not have penetrated these trapped spaces, resulting in a low FAS reading and a

subsequently low particle density value. The remaining particle densities correspond with published values (Agnew and Leonard, 2002).

Table 4.2. Particle densities and standard errors of compost and amendment materials at various moisture contents.

Material	MCwb (%)	PD (kgm^{-3})	N
Manure Compost	25	1554 ± 94	7
	30	1460 ± 67	9
	60	1695 ± 69	8
MSW Compost	42	1881 ± 34	3
	55	1725 ± 26	5
Straw + Biosolids	69	1147 ± 61	6
Woodchips + Biosolids	55	1171 ± 43	5
Leaves + Biosolids	74	1453 ± 96	4
Pure Biosolids	76	1750 ± 82	4
Woodchips	9	1019 ± 8	3
	34	860 ± 60	7
	47	741 ± 17	5
Leaves	11	454 ± 20	7
	59	633 ± 90	7
Straw	0.81	466 ± 18	4
	50	568 ± 39	6

An analysis of variance (SAS, 1998) was performed on the data from the manure compost, MSW compost and biosolids. For the compost materials the moisture content had a significant effect ($\alpha = 0.05$) on the particle density ($P = 0.0001$ for manure compost and MSW compost). No discernable trend was observed however, likely due to the small number of moisture contents analyzed. For the biosolids material, there was a significant interaction between the moisture content and depth ($P = 0.0443$). This suggests that the behavior of the particle density of the biosolids material was influenced more by the moisture content at one depth than another.

The particle densities were also analyzed for variation with depth. The assumption was made that the particle mass and volume remained constant with compression and the particle density of material at the bottom of the pile was equivalent to the particle density of the same material at the top of a pile, assuming constant moisture content. For the manure compost and MSW compost, the simulated depth had no significant effect ($\alpha = 0.05$) on particle density ($P = 0.1928$ for manure compost and $P = 0.1481$ for MSW compost). Again, since the interaction between moisture content and depth was significant for the biosolids material, the conclusion of constant particle density throughout the pile could not be made for the biosolids material.

Throughout the depth simulation, the moisture content of the manure compost and MSW compost remained approximately constant, even at high compressive loads. Material at higher moisture contents lost some water due to compression, but the overall moisture content changed less than 3% (Tables D.1 to D.6, Appendix D). Since the particle density of the manure compost and MSW compost was not dependent on depth

and if the moisture content was assumed constant, the left hand side in Equation 4.4 remained constant and there was a linear relationship between bulk density and FAS.

Since there was a significant interaction between depth and moisture content for the biosolids material, the assumption of constant moisture content could not be made. Thus, the term in Equation 4.4 was not constant and the relationship between bulk density and FAS was not as linear as the other materials. However, the R^2 values for the regression equations in Figures E.7 to E.9 in Appendix E were still very high, but the number of readings was low and the high R^2 values could be misleading.

While the particle densities varied slightly with moisture content, the values were similar for each of the materials tested. The amendment material (leaves, straw and woodchips) had a lower particle density (500-800kgm^{-3} for leaves, 400-600kgm^{-3} for straw and 700-1000kgm^{-3} for woodchips). The particle densities of the amendment material as found by McCartney and Chen (2000) are shown in Table C.3 in Appendix C. These values are much lower than the particle densities of the same material found in this study. Typical particle densities of compost and compost materials are generally higher (Agnew and Leonard, 2002), in the range of those found in this study. However, McCartney and Chen (2000) used a commercial pycnometer to determine the particle densities and the discrepancy in particle density values could be attributed to the small sample size required for the pycnometer.

The manure compost, MSW compost and biosolids material had roughly similar particle densities (1500-1800kgm^{-3}). These particle densities are also similar to those found for manure and cornstalks compost (1563kgm^{-3}, Baker *et al.*, 1996). The data were also analyzed to test the effect of compost material (manure compost, MSW compost and

biosolids material) on particle density. The material had no significant effect ($\alpha = 0.05$) on the particle density ($P = 0.0554$), suggesting that, like soil, the particle densities of all compost materials are very similar. However, since the P value is less than 0.10, it suggests a trend in the dependence of the particle density on the nature of the material.

4.3.4. Porosity and FAS

Throughout this study, the porosity of the material was calculated using Equation 2.4 based on the FAS from the pycnometer and the volumetric moisture content calculated by Equation 2.3. In addition, the porosity was calculated using Equation 4.5:

$$Porosity = 1 - \frac{BD_{dry}}{PD} \tag{4.5}$$

where BD_{dry} is the dry bulk density and PD is the particle density as calculated by Equation 2.10. Since this PD is calculated using the FAS found by the pycnometer, the porosities found by Equations 4.5 and 2.3 are numerically equivalent (Tables F.1 to F.9 in Appendix F). Since the magnitude of the PD was independent of depth and the moisture content in the pile could be assumed constant for manure compost and MSW compost (Section 4.3.2), the PD in the pile could also be assumed constant. Thus the porosity throughout the pile could be calculated based on the initial PD and the BD at each depth using Equation 4.5. The porosities calculated assuming constant PD were very similar to the porosities calculated using the actual PD at each depth (Tables F.1 to F.9 in Appendix F).

Similarly, the FAS at each depth could be calculated assuming constant PD and Equation 2.10. Again, the FAS calculated assuming constant PD was very similar to the

FAS found by the pycnometer at each depth. This further validates the conclusion of constant PD throughout the pile. In both cases, the FAS of the uncompressed sample was used to calculate the initial PD.

The FAS was dependent on the moisture content of the sample (P = 0.0001 for manure compost and MSW compost, SAS, 1998). At higher moisture contents, air voids were displaced by water and the FAS dropped. Similarly, the FAS dropped with compressive loading, again due to the displacement of air voids (Figures 4.1 and 4.3).

On the other hand, the porosity of the material should be independent of moisture content. The increase in water-filled voids should be proportional to the decrease in air voids. However, the statistical analysis showed that the porosity was dependent (P = 0.0001) on moisture content for all materials (SAS, 1998). This could be attributed to the low number of moisture contents analyzed. Obviously, the porosity was dependent on depth for all materials (P = 0.0001 for all materials, SAS, 1998) as the voids were displaced when the sample settled under loads (Tables F.1 to F.9, Appendix F). There was also a significant interaction between the material and depth on the porosity of the material. This suggests that the porosity decreased with depth at different rates for various materials.

4.3.5. Wet Bulk Density Profiles and Dry Bulk Density

Depending on the particle size and rigidity of the material, Schaub (1997) found that the dry bulk density changed with increasing moisture content. The dry bulk density of compost increased with moisture while the dry bulk density of peat decreased with moisture (Section 2.6). In this study, the dry bulk density of all materials increased with

moisture (Tables F.1 to F.5 in Appendix F). This could be explained by the "settling" effect of the material as it was wetted. The decrease in total volume would increase the dry bulk density. Similarly, the dry bulk density of the materials increased with compressive loading, as seen in Tables F.1 to F.9 in Appendix F. Again, the mass of solids remained constant, but the total volume decreased with compressive loading, increasing the overall dry bulk density.

The wet bulk density profiles found for manure compost compare well with those found by Schaub-Szabo and Leonard (1999). A plot of the wet bulk density versus depth (Figure 4.10) yielded a best-fit regression equation of the form $BD = Az^B$, as found by Schaub-Szabo and Leonard (1999) in Equation 2.1. The coefficients of the regression equations are summarized in Table 4.3, along with those found in Schaub-Szabo and Leonard (1999).

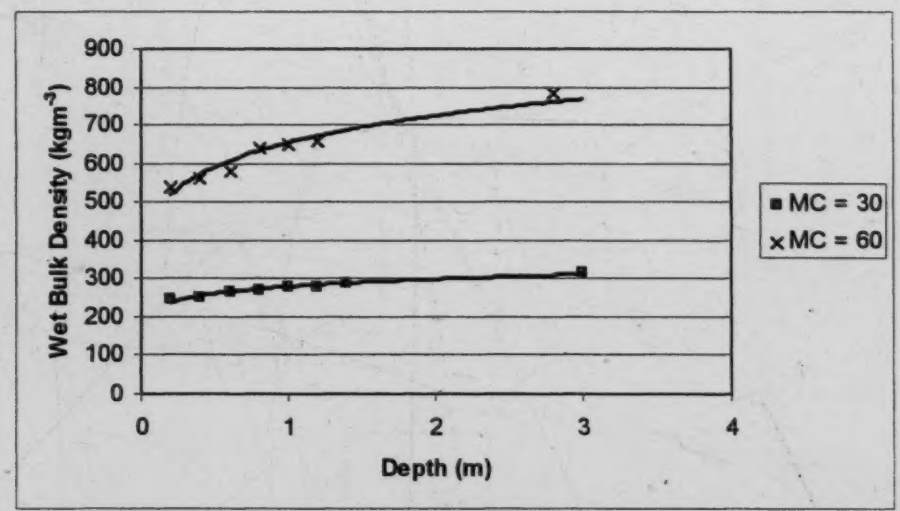

Figure 4.10. Regression equation curves of bulk density at any depth for manure compost at two moisture contents.

Table 4.3. Summary of bulk density and depth regression coefficients ($BD = A(depth)^B$) for manure compost.

MC_{wb} (%)	A	B	R^2
30	279.12	0.0971	0.96
47*	495.17	0.1040	0.92 - 0.99
60	654.36	0.1457	0.94

* 47% moisture content data from Schaub-Szabo and Leonard (1999).

Since manure compost at 47% moisture content was not analyzed in this study, a direct comparison cannot be made. However, both the constant (A) and exponent (B) values for manure compost at 30% moisture content are lower than those at 47%, and both regression values for manure compost at 60% moisture content are higher than those at 47%. These data validate the conclusions made by Schaub-Szabo and Leonard (1999).

4.3.6. Compressibility and the Soil Compression Equation

It is well documented that increasing the moisture content of a material will increase its compressibility, or the ease with which the material decreases in volume when subjected to a mechanical load (Stone and Ekwue, 1996; Schaub, 1997). Dry materials tend to be rigid and withstand compressive forces, while wet materials collapse when loaded. This is further confirmed by the behavior of the amendment material used in this study. The dry woodchips (MC = 8.56% w.b.) did not compress, even at high loads. The volume of the sample at no load was 18.02L while the sample volume at maximum load (approximately 100kPa or 3m depth) was 17.91L. The sample volume decreased by only 0.11L. Increasing the moisture content to 33.6% (w.b.) increased its

compressibility considerably, as the sample volume reduction increased to 2.15L. This trend was also observed with the data for straw. The decrease in volume of the dry straw (MC = 0.81% w.b.) was only 0.11L while the sample volume reduction of the wet straw (MC = 50% w.b.) was 9.35L. Refer to Tables D.1 to D.6 in Appendix D for data.

Using the approach of McCartney and Chen (2000), these data also show that compost materials behave like soil under compression. Using the initial FAS and the volume changes found with the pycnometer, and putting these values into the soil compression equation (Equation 2.5), the subsequent FAS can be found for each depth. Again, the soil compression equation assumes the moisture content and particle density does not change with compressive loading. Even though small amounts of water leached from the wet materials at high compressive loads, the moisture contents remained almost constant (less than 3% difference) and the particle density for all materials was unchanged with compressive loading (SAS, 1998). Therefore, the soil compression equation (Equation 2.5) was valid for these data.

The values found with the soil compression equation were comparable to every FAS result found by the pycnometer, as shown in Figure 4.11 for manure compost. At higher compressive loads, the FAS found by the pycnometer deviated slightly from the FAS calculated by the soil compression equation, as indicated by the negative intercept. However, the relationship was still highly linear.

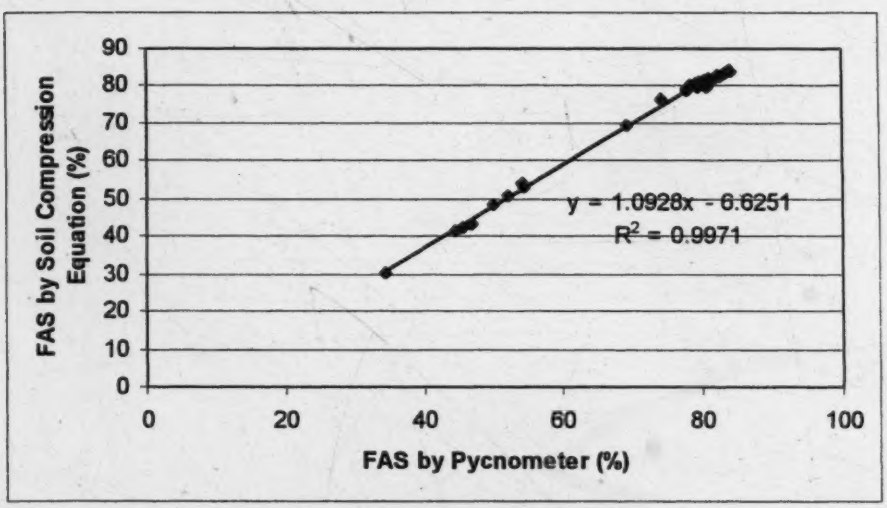

Figure 4.11. Comparison of FAS values of manure compost from pycnometer and soil compression equations.

Again, this conclusion is supported by the statistical analysis. An analysis of variance was performed in SAS and no significant difference ($\alpha = 0.05$) was found between the pycnometer readings and the FAS values calculated by the soil compression equation ($P = 0.9664$ for manure compost, $P = 0.9724$ for MSW compost, $P = 0.9979$ for the biosolids material and $P = 0.6015$ for the amendment materials).

Despite the slight deviation at high loads, the soil compression equation accurately predicts the FAS of compost under compression. However, given the initial FAS, the volume reduction at each depth must still be known. Volume measurements of compost *in situ* are impractical, and the assumption of constant moisture content is often invalid for wet materials, so another method of determining the FAS of compressed compost is needed. The correlation with wet bulk density looks promising.

4.4. Limitations and Recommendations

The modified air pycnometer is a useful tool in the characterization of compost, but it has some limitations. The device requires about 20L of material for accurate results and gives individual FAS results in about 10 minutes. However, a complete characterization with compressive loading takes about one week as the material requires about 24 hours to completely compress at each load.

In addition, the pycnometer measures the micro FAS within the material whereas other methods like the specific gravity bottle and water pycnometry generally give macro FAS values. With the air pycnometer and the associated pressures used, all micropores within the matrix and particles are penetrated whereas only the pores between particles are accounted for in other methods. This leads to the problem of measuring "available airspace". Relating the FAS to the amount of oxygen available for aerobic microorganisms is the key. Haug (1995) noted that 95% of maximum oxygen consumption rate was maintained when macro FAS was between 20 and 35%. Sufficient oxygen was available to the microorganisms when the air spaces occupied 35% of the solid volume. This oxygen consumption rate may require the maintenance of a higher value when the micro FAS is considered. Future work is needed to determine the actual relationship between micro and macro FAS.

The bulk density and FAS values found with the pycnometer matched those for manure compost published by Baker *et al.* (1998) within 5%. However, the FAS results for the amendment material (leaves, straw and woodchips) were much higher than those published by McCartney and Chen (2000), and the generalized equation relating FAS and bulk density does not hold true for their data. This could be related to the problem of

measuring macro FAS versus micro FAS. However, the general behavior of FAS and bulk density with compression found in this study matched that of McCartney and Chen (2000).

While the bulk density of the compressed samples followed a trend similar to that found in another study (Schaub-Szabo and Leonard, 1999), the simulation may not have been representative of the conditions found in a pile. In both this study and the work done by Schaub-Szabo and Leonard (1999), the samples were compressed in cylindrical vessels (diameter ≈ 500mm). Thus, the sample was restricted as it was compressed since the material was not allowed to move laterally. Conditions found in a pile are more open, allowing the material near the bottom to spread out as it is compressed. In other words, the bulk density profiles found by simulation may overestimate the bulk density values at the bottom of the pile. Larger diameter vessels would minimize this error, but larger vessels require loads which may be impractical to simulate in the laboratory.

The linear relationship between FAS and wet bulk density is valid only for material with moisture contents in the range quantified by this study (approximately 10 to 80% w.b.). The regression equations found between bulk density and FAS can make it extremely easy to predict the FAS at the bottom of the pile, given the bulk density profile. However, literature shows that the bulk density itself changes significantly from the feedstock to the finished material (Larney *et al.*, 2000). But what about the shape of the bulk density profile? Will the profile change significantly throughout the process? Future work needs to be done to investigate this.

Since each material was analyzed at different moisture contents and, in some cases, different depths, it was difficult to make direct comparisons among the materials.

Thus, the conclusion of constant particle density among composting materials is not as strong as it could be with proper experimental design. Characterizing each material at 3 or 4 moisture contents and the same loading pattern would make it easier to analyze and make the resulting conclusions stronger. This work showed the presence of trends among materials, but the conclusions need to be verified by future trials.

5. Conclusions

The ability to reliably determine the FAS and bulk density of compost at any time and under any condition will make compost process management more effective. Composting times will shorten and the quality of the end product will improve.

The modified air pycnometer designed and built for this project provided accurate measurements of FAS and bulk density for a variety of compost and feedstock materials. The variation among repetitions was very low, indicating that the results were also precise. The air cylinder and piston provided for easy and accurate compression, allowing the development of bulk density and FAS profiles, which were previously very cumbersome to determine.

The FAS and bulk density profiles of the compost material followed the trends established by McCartney and Chen (2000) and Baker *et al.* (1998). The FAS decreased with loading and increasing moisture content while the wet bulk density increased with loading and increasing moisture content. The dry bulk density of all materials increased with both increasing moisture and compressive loading.

The relationship between FAS and bulk density was linear and was the same for all the materials tested under loads. The linear relationship, however, is valid only for wet moisture contents between 10 and 80%. The linearity of the relationship is explained by the reciprocal relationship between moisture content and particle density. The particle density changed slightly with increasing moisture, likely due to the swelling or collapse of organic particles, but the moisture content of the samples stayed approximately constant with loading. In addition, the magnitude of the particle densities of the compost

material studied was roughly similar, between 1500-1800kgm^{-3} while the amendment material (woodchips, straw, leaves) had lower particle densities (450-650kgm^{-3}).

The compost material followed soil compression laws, as shown in McCartney and Chen (2000) and by the results from this study. Knowing the initial FAS and the volume reduction due to compression, the compressed FAS can be calculated based on soil compression equations. However, one FAS measurement is still required and accurate volume reduction predictions are very difficult on a full-scale level.

While the pycnometer provided accurate, quick and reliable FAS and bulk density readings, in its current form it would be impractical and cumbersome to use in the field. However, the development of bulk density and depth relationships and the correlation between FAS and bulk density will make full-scale process management easier and more effective.

6. References

Agnew, J.M., and J.J. Leonard, 2002. The physical properties of compost: a review. Compost Science and Utilization, *in press (accepted December, 2001).*

ASAE. 2000. Moisture measurement—forages. ASAE S358.2. ASAE Standards 2000. American Society of Agricultural Engineers. St Joseph, MI.

ASTM. 1994. Standard test methods for bulk density of peat and peat products. D 4531-86. Annual Book of ASTM Standards. Section 4. Construction; Volume 04.08 Soil and Rock. ASTM, Philadelphia, PA.

Baker, S.M., T.L. Richard, Z. Zhang and S. Monteiro da Rocha. 1998. Determining the free air space inside compost mixtures using a gas pycnometer. Paper no. 984094, American Society of Agricultural Engineering, Orlando, FL.

Fogiel, A.C., R.D. von Bernuth, F.C. Michel Jr., and T.L. Louden. 1999. Experimental verification of the natural convective transfer of air through a dairy manure compost media. Paper no. 99-4053. American Society of Agricultural Engineering, Toronto, ON.

Geddis, A.M., Guzman, A.G. and Basset, R.L., 1996. NUREG/GR – 6457. Rapid estimation of solid volume in large tuff cores using a gas pycnometer. Office of Nuclear Regulatory Research, U.S. Nuclear Regulatory Commission, Washington, DC.

van Ginkle, G.T., P.A.C. Raats and I.A. van Haneghem. 1999. Bulk density and porosity distributions in a compost pile. *Netherlands Journal of Agricultural Science,* 47:105-121.

Glancey, J.L. and S.C. Hoffman. 1994. Physical properties of solid waste materials. Paper no. 94-1592. American Society of Agricultural Engineering, Atlanta, GA.

Hamelers, H.V.M. 1992. A theoretical model of compost kinetics. *In:* Hoitink, H.A.J. and H. Keener (eds.) *Proceedings of the International Composting Research Symposium,* 36-58.

Haug, R.T. 1995. The Practical Handbook of Compost Engineering. Lewis Publishers, Boca Raton, FL.

He, X.T., T.J. Logan and S.J. Traina. 1995. Physical and chemical characteristics of selected U.S. municipal solid waste composts. *Journal of Environmental Quality*, 24:543-552.

Jeris J.S., and R.W.Regan. 1973. Controlling environmental parameters for optimum composting. II. Moisture, free air space and recycle. *Compost Science*, 14:8-15.

Larney, F.J., A.F. Olson, A.A. Carcamo and C. Chang. 2000. Physical changes during active and passive composting of beef feedlot manure in winter and summer. *Bioresource Technology*, 75:139-148.

Leege, P.B. and W.H. Thompson. (Eds.) 1997.Test methods for the physical examination of compost and composting. *In:* Test Methods for the Examination of Composting and Compost, U.S. Composting Council.

McCartney, D. and H. Chen. 2000. Physical modelling of the composting environment: determining the free air space (FAS) and bulk density (BD) profiles of composting feedstock materials. *Proceedings of the 10th Annual Composting Council Conference*, Edmonton, AB.

Miller, F.C. 1991. Biodegradation of solid wastes by composting. *In:* Martin A.M. (ed.). *Biological degradation of Wastes*, Elsevier Applied Science, London, 2-29.

Mohsenin, N.N. 1986. Physical Properties of Plant and Animal Materials. 2nd Ed. Gordon and Breach Science Publishers, New York, NY.

Oppenheimer, J., Martin, A.G., and Walker, L.P. 1996. Measurements of air-filled porosity in unsaturated organic matrices using a pycnometer. *Bioresource Technology*, 59:241-247.

Mu, R. and J.J. Leonard. 1999. Measurement of air flow through MSW-sewage sludge compost. *Canadian Agricultural Engineering*, 41(2):93-97.

Raviv, M., S.Tarre, Z.Geler and G. Shelef. 1987. Changes in some physical and chemical properties of fibrous solids from cow manure and digested cow manure during composting. *Biological Wastes*, 19(4):309-318.

Rynk, R. 1992. On-Farm Composting Handbook. Northeast Regional Agricultural Engineering Service, Cooperative Extension. Ithaca, NY.

SAS 1998. SAS system for elementary statistical analysis. SAS Institute Inc. Cary, NC.

Schaub, S.M. 1997. A method for characterizing the bulk density of compost and other compressible materials. MSc Thesis, Department of Agriculture, Food and Nutritional Science, University of Alberta.

Schaub-Szabo, S.M. and J.J. Leonard. 1999. Characterizing the bulk density of compost. *Compost Science and Utilization*, 7(4):15-24.

Stone, R.J. and E. I. Ekwue. 1996. Soil compressibility as influenced by sewage sludge incorporation. *J. agric. Engng Res.* 64: 227-236.

Shell, B.J. 1955. The mechanism of oxygen transfer through a compost material. PhD Thesis, Department of Civil and Sanitary Engineering, Michigan State University.

Tseng, D.Y., J.J. Chalmers, O.H. Tuovinen and H.A.J. Hoitink. 1995. Characterization of a bench-scale system for studying the biodegradation of organic solid wastes. *Biotechnol. Progr.* 11:443-451.

Waller, P.L. and A.M. Harrison. 1991. Estimation of pore space and the calculation of air volume in horticultural substrates. *Acta Horticulturae*, 294:29-37.

APPENDIX A

Pycnometer Pictures

Equipment Specifications

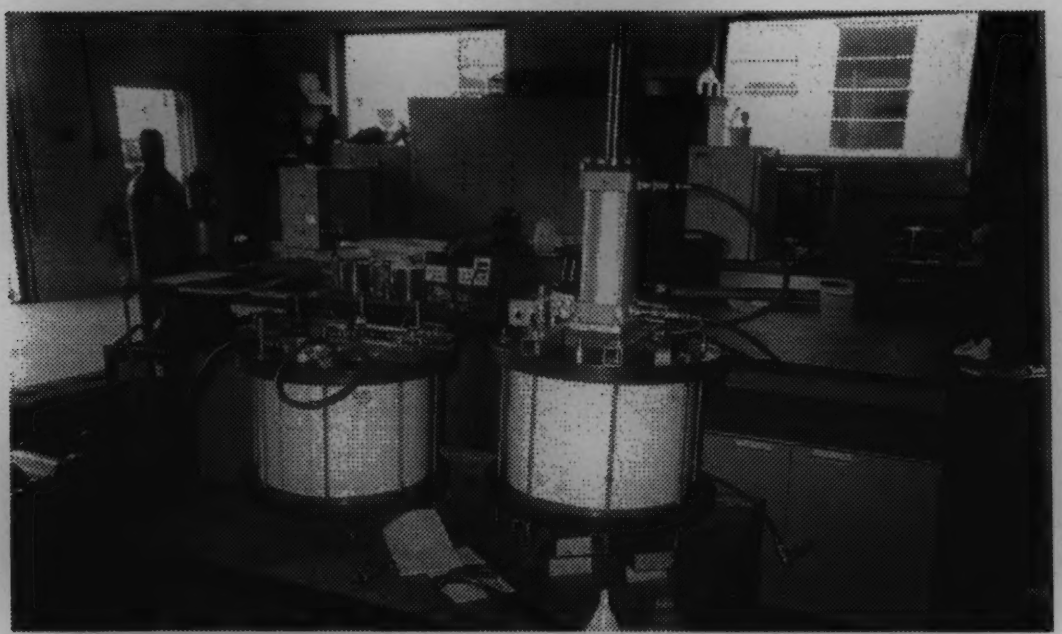

Figure A.1. Overall pycnometer setup. Compressed air vessel is on the left, the sample vessel is on the right.

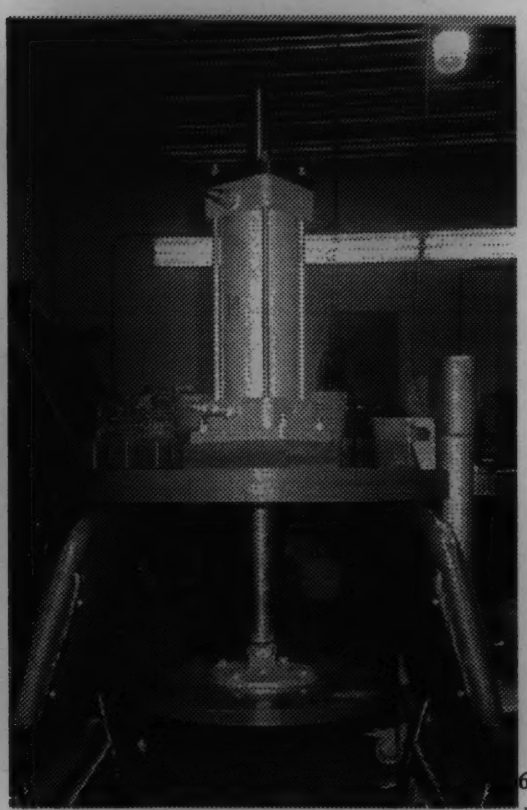

Figure A.2. Air cylinder and piston assembly.

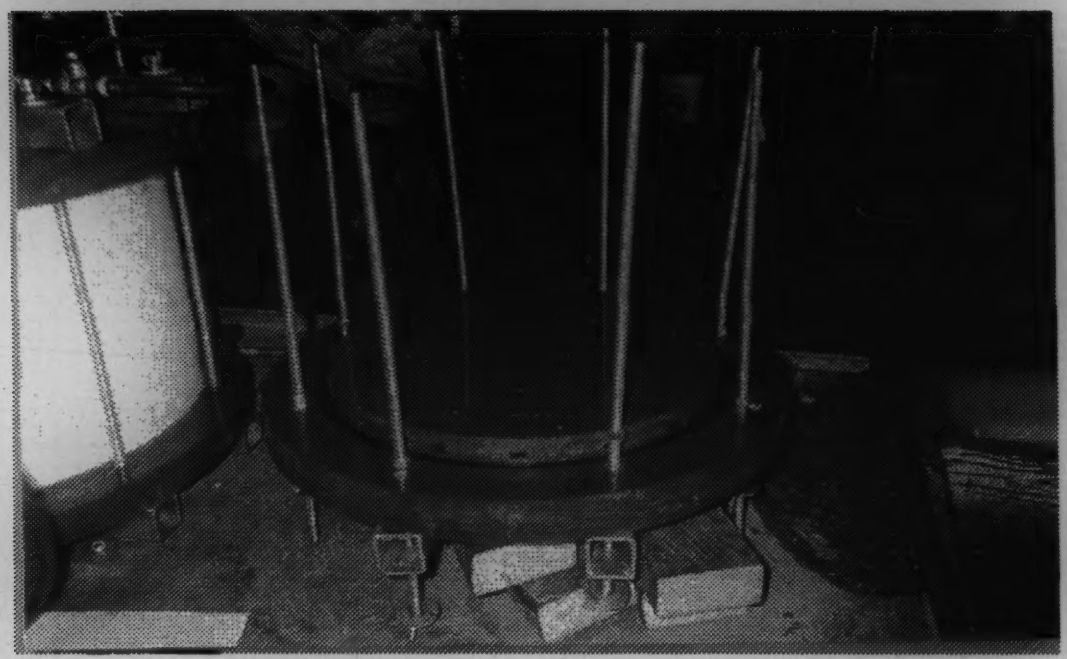

Figure A.3. Sample vessel drainage floor. Cap, piston and vessel walls are removed.

Figure A.4. Drainage tile. Grooves on bottom of the tile run along the perforations to the middle, ensuring all water drains out the hole in the middle of the bottom cap.

Equipment Specifications

Air Cylinder—NCA1WF400-0800-XB5E16-98011CDN, SMC Pneumatics Inc, Indianapolis, IN.

Regulators (x2)—NAR4000-NO3, SMC Pneumatics Inc, Indianapolis, IN.

Pressure Relief Valves—NAP100, SMC Pneumatics Inc, Indianapolis, IN.

2-Way Valve—VH302-N03, SMC Pneumatics Inc, Indianapolis, IN.

Pressure Transducers—DP15TL, Validyne Engineering Corp., Northridge CA.

Carrier Demodulator—CD15, Validyne Engineering Corp., Northridge CA.

Multimeter—34401A, Hewlett Packard Multimeter.

Dead Weight Tester—Cat. No. 23-145, Chandler Engineering Co., Tulsa OK.

Air Compressor—4.85kW, 94.6L Coleman Powermate Professional.

Quick Couplers—19mm diameter, standard thread.

Air Hoses—12.7mm diameter, standard.

Nipples, T's, Connectors, Bushings—19 or 12.7mm diameter, brass, standard thread.

Ball Valves (x3)—B + K, 12.7mm diameter ball valves.

APPENDIX B

Calibration of Pycnometer

Vessel Volume Determination

Pycnometer Calibration and Volume Determination

Volume of compressed air vessel

The inner diameter of the PVC pipe was measured at seven points around the perimeter and an average inner diameter was calculated as 0.4064m. To determine the height of the inside of the vessel when closed, the top cap was removed and the height of the wall from the vessel floor to the top lip was measured at seven points around the perimeter. The average height was 0.245m. Since the depth of the groove (including the polyvinyl gasket) was 0.00630m, the total height when the vessel was closed was 0.245m – 0.00630m, or 0.239m. The volume (not including volumes of fittings) was then $\pi D^2 h/4$ or 30.990L.

The volume of the tap was estimated to be 0.00498L. The volume of the transducer (from the specifications in the casing) was 0.00107L and the total volume of all fittings and hoses was estimated to be 0.00863L. Thus, the total volume of the compressed air vessel was 31.005L.

Volume of sample and sample vessel

Since the volume of the sample vessel would be impossible to calculate because of the drainage floor and piston head, the volume was determined by duplicated water addition. The vessel was closed and the piston was fully extended (exposed rod length = 127mm). Water was added to the vessel through the hole for the tap until the water level reached the top of the hole. The total volume of water (max piston extension) was recorded as 26.90L. The piston was then fully retracted (exposed rod length = 318mm), creating more space in the vessel as the shaft was no longer taking up as much space. More water was added until the vessel was full once again, and the total volume (min piston extension) was 27.08L. The equation of the straight line between these points allowed the sample vessel volume to be calculated at any piston extension and is expressed as:

$$V_B = 0.0009424\,x + 26.78 \qquad (B.1)$$

where V_B is the sample vessel volume in litres [L] and x is the exposed rod length in mm.

The sample volume was calibrated by using increments of gravel. The cap and piston assembly was removed and approximately 6L of gravel was added to the vessel. The height of the gravel sample was calculated by subtracting the remaining head space from the total height of the vessel. The cap and piston was replaced and the vessel was sealed. The piston was then extended until the piston head reached the gravel and the exposed rod length was measured. The actual gravel height was plotted against the exposed rod length reading at 6 points (Figure B.1). The regression equation allowed the actual height of the sample to be calculated by measuring the exposed rod length.

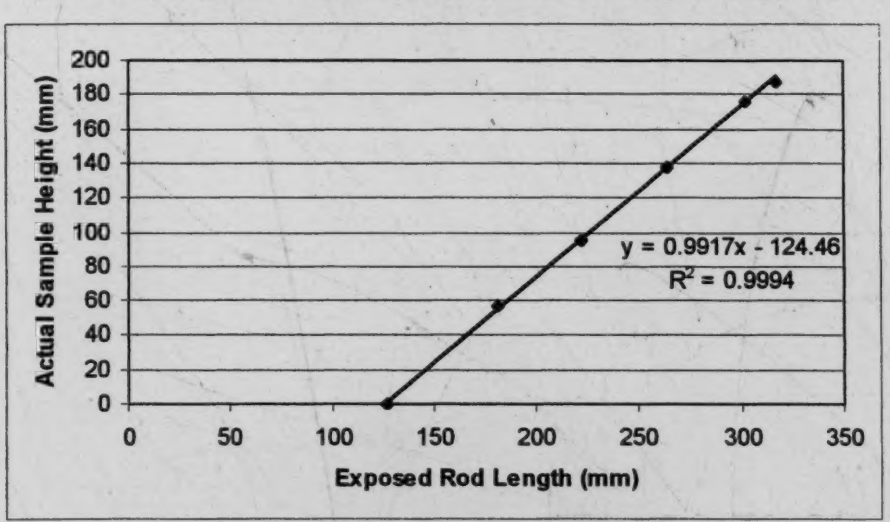

Figure B.1. Calibration curve for determining sample volume.

The actual volume of the sample was then calculated by multiplying the height by the cross sectional area of the vessel ($0.130m^2$). The sample volume can be calculated at all piston extensions using the following equation:

$$V_s = 0.130(x - 125) \qquad (B.2)$$

where Vs is the sample volume in litres [L] and x is the exposed rod length in mm.

The pycnometer was calibrated for FAS measurements using tap water since water has no free air space. The sample tank was filled in 2L increments through the tap in the sample vessel with FAS readings taken for each addition (Table B.1).

Table B.1. Calibration of pycnometer with water data.

P_1 (V)	P_1 (kPa)	Vs (L)	P_2 actual (V)	P_2 actual (kPa)	P_2 theoretical (kPa)
10.05	207.85	0	5.035	104	111
10.05	207.85	2	5.222	108	115
10.05	207.85	4	5.463	113	120
10.05	207.85	6	5.617	116	124
10.05	207.85	8	5.832	121	129
10.05	207.85	10	6.063	125	135
10.05	207.85	12	6.294	130	140
10.05	207.85	14	6.642	137	147
10.05	207.85	16	6.911	143	154
10.05	207.85	18	7.235	150	162
10.05	207.85	20	7.691	159	170
10.05	207.85	22	8.07	167	180

The theoretical final pressure (P_2) was calculated from Equation 3.5, the initial pressure (P_1), the compressed air vessel volume (31.005L) and the volume of the sample vessel (26.9L). The volume of the sample vessel was constant throughout the calibration as the piston position was not changed. The actual pressure was plotted against the theoretical pressure (Figure 3.5) and the resulting regression equation was used in the final, calibrated equation (Equation 3.6).

APPENDIX C

Comparable Data

Table C.1. Initial properties of feedstock material (prior to mixing and loading). (McCartney and Chen 2000)

Feedstock Mixture	Moisture Content (%, w.b.)	Wet Bulk Density kgm^{-3}
Biosolids	74.33	1017.2
Straw	8.91	47.0
Woodchips	12.56	139.0
Leaves	24.34	72.3

Table C.2. Initial properties of the materials used in this study.

Material	Moisture Content (%, w.b.)	Wet Bulk Density (kgm^{-3})
Biosolids	70.23	1000
Straw	0.81	51
Woodchips	8.56	170
Leaves	30.05	45

Table C.3. Free air space (FAS) and wet bulk density (BD) of loaded amendments, MC = 55% (w.b.) (McCartney and Chen 2000)

	Woodchips				Leaves				Straw			
Load (kPa)	Depth (m)	FAS (%)	BD (kgm^{-3})	PD* (kgm^{-3})	Depth (m)	FAS (%)	BD (kgm^{-3})	PD* (kgm^{-3})	Depth (m)	FAS (%)	BD (kgm^{-3})	PD* (kgm^{-3})
0	0.1	37	360	257.09	0.1	34	280	190.85	0.1	47	170	144.28
4.3	1.1	26	420	255.35	1.3	10	380	189.95	2.1	22	250	144.18
8.6	2.2	24	430	254.55	2.5	8	380	185.81	3.8	15	270	142.89
12.8	3.1	22	450	259.56	3.6	5	400	189.42	5.4	12	280	143.13

* PD = particle density as calculated by Equation 2.10.

APPENDIX D

Raw Data

Table D.1. Raw data for manure compost (MC = 25%).

Depth (m)	Mass H_2O Drained (kg)	Total Sample Mass (kg)	MCwb (%)	Cylinder Pressure (kPa)	Compression Time (min/day)	Outside Rod Length (mm)	Vb (L)	Vs (L)	BD (kgm^{-3})	P1 (V)	P2 (V)	FAS (%)	FAS average	FAS std dev
0.00	0.00	4.50	25.0	0.0	-	308	27.07	20.62	218.23	10.00*	5.317	83.0	84.0	1.060
											5.279	85.1		
											5.305	83.8		
0.20	0.00	4.50	25.0	6.0	12 min	304	27.07	20.18	222.99	10.00	5.289	84.3	83.4	0.751
											5.314	83.0		
											5.314	83.0		
0.40	0.00	4.50	25.0	15.9	12 min	296	27.06	19.26	233.64	10.00	5.302	82.9	82.3	0.493
											5.318	82.0		
											5.316	82.1		
0.80	0.00	4.50	25.0	33.2	50 min	286	27.05	18.14	248.07	10.00	5.294	82.3	81.6	0.643
											5.312	81.3		
											5.316	81.1		
1.00	0.00	4.50	25.0	44.1	90 min	280	27.04	17.45	257.88	10.00	5.329	79.5	79.6	0.231
											5.329	79.5		
											5.323	79.9		
1.20	0.00	4.50	25.0	54.5	1100 min	271	27.04	16.44	274.39	10.00	5.315	79.2	79.5	0.462
											5.303	80.0		
											5.315	79.2		
1.40	0.00	4.50	25.0	68.3	390 min	269	27.04	16.21	277.61	10.00	5.287	80.7	80.6	0.141
											5.291	80.5		

* All pressure readings are in volts (V). Multiply voltage by 20.685 to convert to pressure (kPa).

Table D.1 (con't). Raw data for manure compost (MC = 30%)

Depth (m)	Mass H_20 Drained (kg)	Total Sample Mass (kg)	MCwb (%)	Cylinder Pressure (kPa)	Compression Time (min/day)	Outside Rod Length (mm)	Vb (L)	Vs (L)	BD (kgm^{-3})	P1 (V)	P2 (V)	FAS (%)	FAS average	FAS std dev
0.00	0.00	4.00	30.0	0.0	-	275	27.04	16.87	237.11	10.00	5.255	83.52	82.5	0.895
											5.279	82.00		
											5.280	81.94		
0.20	0.00	4.00	30.0	8.4	10 min	270	27.04	16.33	244.95	10.00	5.282	81.21	81.1	0.405
											5.291	80.63		
											5.279	*81.41*		
0.40	0.00	4.00	30.0	17.2	10 min	266	27.03	15.87	252.05	10.00	5.281	80.80	80.4	0.344
											5.288	80.33		
											5.291	80.13		
0.60	0.00	4.00	30.0	26.1	150 min	260	27.03	15.21	262.98	10.00	5.279	80.11	79.4	1.061
											5.306	78.22		
											5.288	80.00		
0.80	0.00	4.00	30.0	35.5	258 min	256	27.02	14.75	271.18	10.00	5.287	78.98	78.4	0.762
											5.307	77.54		
											5.291	78.69		
1.00	0.00	4.00	30.0	45.1	900 min	253	27.02	14.41	277.59	10.00	5.276	79.29	78.6	1.075
											5.291	79.19		
											5.302	77.38		
1.20	0.00	4.00	30.0	55.0	205 min	252	27.02	14.29	279.91	10.00	5.288	78.23	77.8	1.011
											5.285	78.45		
											5.310	76.60		
1.40	0.00	4.00	30.0	64.9	300 min	248	27.02	13.83	289.22	10.00	5.277	78.35	77.9	0.623
											5.279	78.19		
											5.292	77.20		
3.00	0.00	4.00	30.0	147.0	5 days	234	27.00	12.25	326.53	10.00	5.292	74.24	74.2	0.057
											5.295	74.16		

Table D.1 (con't). Raw data for manure compost (MC ≈ 60%)

Depth (m)	Mass H_2O Drained (kg)	Total Sample Mass (kg)	MCwb (%)	Cylinder Pressure (kPa)	Compression Time (min/day)	Outside Rod Length (mm)	Vb (L)	Vs (L)	BD (kgm^{-3})	P1 (V)	P2 (V)	FAS (%)	FAS average	FAS std dev
0.00	0.00	10.15	63.0	0.0	-	292	27.06	18.83	539.03	10.00	5.865	54.02	54.2	0.156
											5.862	54.15		
											5.858	54.33		
0.20	0.23	9.92	62.1	19.2	20 min	288	27.05	18.37	540.01	10.00	5.832	54.47	54.4	0.235
											5.840	54.09		
											5.831	54.52		
0.40	0.06	9.86	61.9	38.4	20 min	281	27.05	17.56	561.5	10.00	5.823	52.82	52.1	0.695
											5.850	51.45		
											5.841	51.93		
0.60	0.10	9.76	61.5	58.3	85 min	274	27.04	16.79	581.3	10.00	5.854	49.11	50.0	0.824
											5.830	50.35		
											5.832	50.67		
0.80	0.01	9.75	61.5	79.0	1180 min	260	27.03	15.21	641.03	10.00	5.798	47.10	46.8	0.987
											5.789	47.62		
											5.822	45.71		
1.00	0.00	9.75	61.5	102.0	30 min	258	27.03	14.98	650.87	10.00	5.789	46.81	45.6	1.047
											5.821	44.94		
											5.819	45.06		
1.20	0.02	9.73	61.4	124.9	180 min	256	27.02	14.75	659.66	10.00	5.813	44.62	44.6	0.771
											5.801	45.33		
											5.827	43.79		
2.80	0.01	9.72	61.4	319.5	1140 min	234	27.00	12.36	786.4	10.00	5.802	34.86	34.3	0.506
											5.811	34.22		
											5.816	33.86		

Table D.2. Raw data for MSW compost.

Depth (m)	Mass H_2O Drained (kg)	Total Sample Mass (kg)	MCwb (%)	Cylinder Pressure (kPa)	Compression Time (min/day)	Outside Rod Length (mm)	Vb (L)	Vs (L)	BD (kgm^{-3})	P1 (V)	P2 (V)	FAS (%)	FAS average	FAS std dev
1.0*	0	8.5	42.3	50.0*	-	276	27.04	17.02	499.41	10.0	5.581	64.32	63.83	0.574
											5.587	63.98		
											5.601	63.20		
1.5	0	8.5	42.3	89.3	1440 min	275	27.04	16.90	502.96	10.0	5.586	63.78	63.50	0.254
											5.592	63.45		
											5.595	63.28		
2.5	0	8.5	42.3	133.9	1440 min	271	27.04	16.44	517.03	10.0	5.594	62.31	62.38	0.464
											5.600	61.96		
											5.584	62.88		
3.0	0	8.5	42.3	135.1	3 days	268	27.03	16.10	527.95	10.0	5.589	61.87	61.13	0.667
											5.605	60.93		
											5.611	60.58		
0.0	0	11.75	55.5	0.0	-	283	27.05	17.79	660.48	10.0	5.958	46.97	46.50	0.418
											5.975	46.17		
											5.971	46.36		
0.5	0	11.75	55.5	58.7	1440 min	276	27.04	17.02	690.36	10.0	5.958	44.62	44.20	0.465
											5.977	43.70		
											5.965	44.28		
1.0	0	11.75	55.5	120.1	2800 min	260	27.03	15.21	772.52	10.0	5.982	36.79	37.12	0.304
											5.975	37.17		
											5.971	37.39		
1.5	0	11.75	55.5	188.8	1440 min	251	27.02	14.18	828.63	10.0	5.970	32.97	32.49	0.604
											5.975	32.68		
											5.990	31.81		
2.0	0	11.75	55.5	262.6	1440 min	245	27.01	13.52	869.08	10.0	5.982	29.62	28.89	0.992
											5.978	29.29		
											6.003	27.76		

Table D.3. Raw data for biosolids material.

Material	Depth (m)	Mass H_20 Drained (kg)	Total Sample Mass (kg)	MCwb (%)	Cylinder Pressure (kPa)	Compression Time (min/day)	Outside Rod Length (mm)	Vb (L)	Vs (L)	BD (kgm^{-3})	P1 (V)	P2 (V)	FAS (%)	FAS average	FAS std dev
Pure Biosolids	0.0	0.000	16.30	76.0	0.0	-	278	27.04	17.21	947.12	10.0	6.638	15.80	15.75	0.161
												6.636	15.88		
												6.644	15.57		
	0.5	0.000	16.30	76.0	84.2	40 min	259	27.03	15.09	1080.19	10.0	6.682	2.10	2.67	0.620
												6.654	3.33		
												6.671	2.58		
	1.0	0.000	16.30	76.0	180.3	120 min	259	27.03	15.09	1080.19	10.0	6.662	2.98	2.38	0.663
												6.673	2.50		
												6.692	1.67		
	1.5	0.000	16.30	76.0	276.4	1300 min	260	27.03	15.21	1071.66	10.0	6.644	4.53	4.08	0.859
												6.677	3.09		
												6.642	4.62		
Woodchips-Biosolids	0.0	0.000	9.70	63.0	0.0	-	266	27.03	15.87	611.21	10.0	5.922	42.57	43.28	0.618
												5.902	43.64		
												5.902	43.64		
	0.5	0.000	9.70	63.0	54.3	1180 min	247	27.01	13.72	707.00	10.0	5.904	34.84	34.40	0.382
												5.914	34.21		
												5.915	34.15		
	1.0	0.000	9.70	63.0	117.2	380 min	241	27.01	13.06	742.73	10.0	5.940	29.21	28.61	0.866
												5.942	29.01		
												5.956	27.62		
	1.5	0.000	9.70	63.0	183.3	996 min	233	27.00	12.14	799.01	10.0	5.906	26.29	26.03	0.225
												5.911	25.94		
												5.912	25.87		
	2.0	0.000	9.70	63.0	254.3	45 min	232	27.00	12.02	806.99	10.0	5.907	25.48	24.87	0.768
												5.928	24.01		
												5.912	25.13		
	2.5	0.000	9.70	63.0	326.1	1360 min	225	26.99	11.25	862.22	10.0	5.911	20.17	20.05	0.644
												5.922	19.35		
												5.905	20.62		

Table D.3 (con't). Raw data for biosolids material.

Material	Depth (m)	Mass H_20 Drained (kg)	Total Sample Mass (kg)	MCwb (%)	Cylinder Pressure (kPa)	Compression Time (min/day)	Outside Rod Length (mm)	Vb (L)	Vs (L)	BD (kgm^{-3})	P1 (V)	P2 (V)	FAS (%)	FAS average	FAS std dev
Leaves-Biosolids	0.0	0.000	11.75	73.9	0.0	-	271	27.04	16.44	716.46	10.0	6.111	35.13	34.94	0.335
												6.111	35.13		
												6.123	34.55		
	0.5	0.010	11.74	73.9	63.7	1400 min	230	27.00	11.82	993.23	10.0	6.145	7.85	7.30	1.125
												6.173	6.01		
												6.142	8.05		
	1.0	0.240	11.50	73.3	152.0	1560 min	221	26.99	10.79	1065.80	10.0	6.113	1.48	1.62	0.598
												6.102	2.28		
												6.118	1.11		
	1.5*	0.400	11.10	72.3	246.8	2760 min	214	26.98	10.01	1137.30	10.0	6.064	0.00	0.00	0.001
												6.069	0.00		
												6.058	0.00		
Straw-Biosolids	0.0	0.000	6.55	69.0	0.0	-	253	27.02	14.41	454.54	10.0	5.602	56.61	55.72	0.825
												5.627	54.98		
												5.618	55.57		
	0.5	0.000	6.55	69.0	40.4	1440 min	222	26.99	10.9	600.92	10.0	5.620	41.36	41.42	0.265
												5.616	41.71		
												5.622	41.19		
	1.0	0.000	6.55	69.0	93.8	1440 min	209	26.98	9.41	696.07	10.0	5.614	32.78	32.58	0.523
												5.612	32.98		
												5.622	31.99		
	1.5	0.000	6.55	69.0	155.8	1440 min	200	26.97	8.41	778.83	10.0	5.601	26.36	25.51	0.892
												5.617	24.58		
												5.608	25.58		
	2.0	0.000	6.55	69.0	225.0	1440 min	194	26.96	7.75	845.16	10.0	5.600	20.34	19.61	0.641
												5.608	19.37		
												5.611	19.13		
	2.5	0.020	6.53	69.0	300.2	1440 min	189	26.96	7.17	910.74	10.0	5.594	14.69	14.43	0.697
												5.592	14.96		
												5.602	13.64		

Table D.4. Raw data for straw.

Depth (m)	Mass H_20 Drained (kg)	Total Sample Mass (kg)	MCwb (%)	Cylinder Pressure (kPa)	Compression Time (min/day)	Outside Rod Length (mm)	Vb (L)	Vs (L)	BD (kgm^{-3})	P1 (V)	P2 (V)	FAS (%)	FAS average	FAS std dev
0.00	0.00	0.75	0.81	0.00	-	256.00	27.02	14.75	50.85	10.00	5.146	89.41	89.53	0.286
											5.147	89.33		
											5.140	89.86		
2*	0.00	0.75	0.81	8.07	10 min	256.00	27.02	14.75	50.85	10.00	5.154	88.80	89.18	0.380
											5.149	89.18		
											5.144	89.56		
3.00	0.00	0.75	0.81	27.17	20 min	255.00	27.02	14.64	51.23	10.00	5.158	88.41	88.44	0.421
											5.152	88.87		
											5.163	88.03		
10.2 **	0.00	0.75	0.81	103.42	150 min	231.00	27.00	11.91	62.97	10.00	5.138	87.80	86.70	1.040
											5.160	85.73		
											5.151	86.58		
0.00	0.25	1.75	50.80	0.00	-	308.00	27.07	20.60	84.95	10.00	5.223	88.04	88.43	0.400
											5.216	88.41		
											5.208	88.84		
1.50*	0.03	1.72	50.00	22.68	10 min	261.00	27.03	15.32	112.27	10.00	5.200	85.82	85.20	0.605
											5.217	84.61		
											5.209	85.18		
2.00	0.00	1.72	50.00	32.68	20 min	251.00	27.02	14.06	122.33	10.00	5.202	84.47	83.69	0.743
											5.221	82.99		
											5.213	83.61		
2.50	0.00	1.72	50.00	43.51	120 min	236.00	27.00	12.48	137.82	10.00	5.218	81.26	80.66	0.541
											5.234	80.51		
											5.230	80.21		
3.00	0.00	1.72	50.00	55.78	1200 min	225.00	26.99	11.25	152.89	10.00	5.221	79.01	78.82	0.424
											5.220	79.11		
											5.228	78.33		
3.50	0.00	1.72	50.00	69.36	350 min	217.00	26.99	10.33	166.51	10.00	5.232	75.98	75.08	0.942
											5.240	75.15		
											5.250	74.10		

*Depths less than 2m at 0.81% MC and 1.5m at 50% MC could not be simulated because pressure required in air cylinder was too low to be reliably measured by the pressure transducer.

Table D.5. Raw data for woodchips.

Depth (m)	Mass H_2O Drained (kg)	Total Sample Mass (kg)	MCwb (%)	Cylinder Pressure (kPa)	Compression Time (min/day)	Outside Rod Length (mm)	Vb (L)	Vs (L)	BD (kgm^{-3})	P1 (V)	P2 (V)	FAS (%)	FAS average	FAS std dev
0.00	0.00	3.05	8.56	0.00	-	285.00	27.05	18.02	169.26	10.00	5.277	83.22	83.22	0.00
											5.277	83.22		
											5.277	83.22		
0.50	0.00	3.05	8.56	15.03	10 min	285.00	27.05	18.02	169.26	10.00	5.291	82.39	83.41	0.91
											5.264	83.74		
											5.262	84.11		
3.44*	0.00	3.05	8.56	103.40	10 min	284.00	27.05	17.91	170.30	10.00	5.274	83.29	83.35	0.08
											5.272	83.41		
0.00	0.00	3.65	33.60	0.00	-	291.00	27.06	18.71	195.08	10.00	5.333	80.62	79.65	1.02
											5.349	79.74		
											5.370	78.58		
0.50	0.00	3.65	33.60	17.35	10 min	290.00	27.06	18.60	196.24	10.00	5.336	80.35	79.12	1.07
											5.370	78.45		
											5.368	78.56		
1.00	0.00	3.65	33.60	34.75	150 min	285.00	27.05	18.02	202.55	10.00	5.336	79.77	78.47	1.20
											5.363	78.21		
											5.377	77.42		
1.50	0.00	3.65	33.60	52.81	15 min	284.00	27.05	17.91	203.80	10.00	5.368	77.79	76.95	0.73
											5.388	76.65		
											5.392	76.42		
2.00	0.00	3.65	33.60	70.95	80 min	280.00	27.05	17.45	209.17	10.00	5.398	75.44	75.78	0.48
											5.383	76.33		
											5.396	75.57		
2.50	0.00	3.65	33.60	89.56	20 min	278.00	27.04	17.22	211.96	10.00	5.384	76.01	75.75	0.27
											5.393	75.47		
											5.388	75.77		
3.00	0.00	3.65	33.60	108.39	1091 min	272.00	27.04	16.56	220.41	10.00	5.401	74.01	74.07	0.40
											5.406	73.70		
											5.393	74.50		

*Material was did not compress at depths between 0.5 and 3.44m so no FAS readings were taken.

Table D.5 (con't). Raw data for woodchips.

Depth (m)	Mass H_20 Drained (kg)	Total Sample Mass (kg)	MCwb (%)	Cylinder Pressure (kPa)	Compression Time (min/day)	Outside Rod Length (mm)	Vb (L)	Vs (L)	BD (kgm^{-3})	P1 (V)	P2 (V)	FAS (%)	FAS average	FAS std dev
0.00	0.18	4.22	48	0.00	-	261.00	27.03	15.32	275.46	10.00	5.472	67.38	67.71	0.28
											5.464	67.84		
											5.463	67.90		
0.50	0.02	4.20	47	24.48	10 min	261.00	27.03	15.32	274.15	10.00	5.459	68.16	68.03	0.34
											5.467	67.64		
											5.457	68.29		
1.00	0.01	4.19	47	48.88	15 min	260.00	27.03	15.21	275.48	10.00	5.479	66.63	67.11	0.46
											5.471	67.15		
											5.465	67.54		
1.50	0.01	4.18	47	73.36	120 min	258.00	27.03	14.98	279.04	10.00	5.460	67.37	66.95	0.40
											5.467	66.91		
											5.472	66.58		
2.00	0.00	4.18	47	98.18	90 min	254.00	27.02	14.52	287.88	10.00	5.496	63.96	65.23	1.70
											5.487	64.57		
											5.449	67.16		

Table D.6. Raw data for leaves.

Depth (m)	Mass H_20 Drained (kg)	Total Sample Mass (kg)	MCwb (%)	Cylinder Pressure (kPa)	Compression Time (min/day)	Outside Rod Length (mm)	Vb (L)	Vs (L)	BD (kgm^{-3})	P1 (V)	P2 (V)	FAS (%)	FAS average	FAS std dev
0.00	0.00	0.48	11.35	0.00	-	275	27.04	16.87	28.45	10.0	5.077	95.27	94.48	0.708
											5.092	94.25		
											5.097	93.91		
0.50	0.00	0.48	11.35	2.53	10 min	250	27.02	14.06	34.14	10.0	5.096	92.92	92.79	1.345
											5.115	91.38		
											5.082	94.06		
1.00	0.00	0.48	11.35	5.56	10 min	240	27.01	12.94	37.09	10.0	5.089	93.00	92.76	0.996
											5.104	91.67		
											5.082	93.62		
1.50	0.00	0.48	11.35	8.89	180 min	226	26.99	11.36	42.25	10.0	5.087	92.40	91.06	1.178
											5.109	90.19		
											5.105	90.59		
2.00	0.00	0.48	11.35	12.62	15 min	220	26.99	10.67	44.99	10.0	5.107	89.77	90.41	0.597
											5.100	90.52		
											5.096	90.95		
2.50	0.00	0.48	11.35	166.16	20 min	215	26.98	10.09	47.57	10.0	5.091	91.09	90.00	1.196
											5.099	90.18		
											5.112	88.72		
3.00	0.00	0.48	11.35	208.22	1095 min	197	26.97	8.09	59.33	10.0	5.085	89.86	87.37	2.214
											5.115	85.63		
											5.108	86.61		

Table D.6 (con't). Raw data for leaves.

Depth (m)	Mass $H^2 0$ Drained (kg)	Total Sample Mass (kg)	MCwb (%)	Cylinder Pressure (kPa)	Compression Time (min/day)	Outside Rod Length (mm)	Vb (L)	Vs (L)	BD (kgm^{-3})	P1 (V)	P2 (V)	FAS (%)	FAS average	FAS std dev
0.00	0.00	1.35	58.78	0.00	-	305	27.07	20.29	66.54	10.0	5.136	92.61	92.76	0.168
											5.134	92.72		
											5.130	92.94		
0.50	0.00	1.35	58.78	5.92	25 min	231	27.00	11.91	113.35	10.0	5.141	87.52	86.21	1.268
											5.168	84.99		
											5.156	86.11		
1.00	0.00	1.35	58.78	16.00	85 min	195	26.96	7.83	172.41	10.0	5.144	81.10	77.68	3.077
											5.186	75.13		
											5.174	76.82		
1.50	0.00	1.35	58.78	31.30	60 min	180	26.95	6.17	218.80	10.0	5.155	74.18	71.35	2.528
											5.175	70.57		
											5.182	69.31		
2.00	0.00	1.35	58.78	50.81	30 min	171	26.94	5.13	263.16	10.0	5.160	68.06	65.60	2.302
											5.173	65.23		
											5.181	63.50		
2.50	0.00	1.35	58.78	74.19	1200 min	161	26.93	4.02	335.82	10.0	5.168	57.26	57.08	2.490
											5.160	59.47		
											5.178	54.50		
3.00	0.00	1.35	58.78	104.04	140 min	161	26.93	4.02	335.82	10.0	5.151	61.94	58.18	3.721
											5.165	58.10		
											5.178	54.50		

APPENDIX E

Remaining Profiles and BD vs FAS Graphs

Summary of Slopes and Intercepts of BD vs FAS Graphs

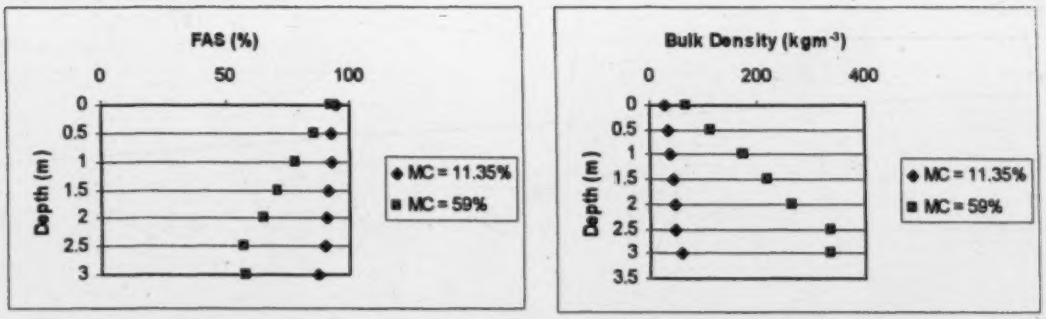

Figure E.1. Profiles for leaves at two moisture contents a) FAS and b) BD.

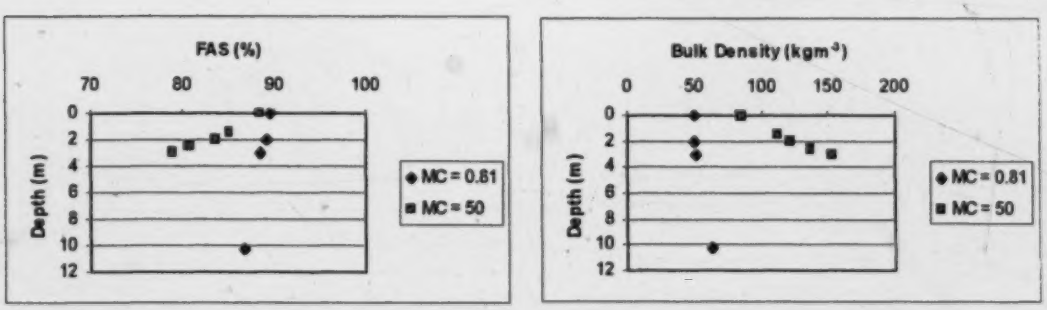

Figure E.2. Profiles for straw at two moisture contents a) FAS and b) BD.

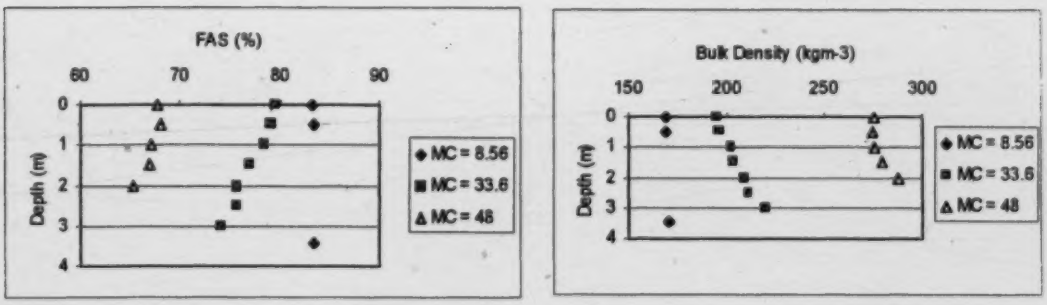

Figure E.3. Profiles for woodchips at three moisture contents a) FAS and b) BD.

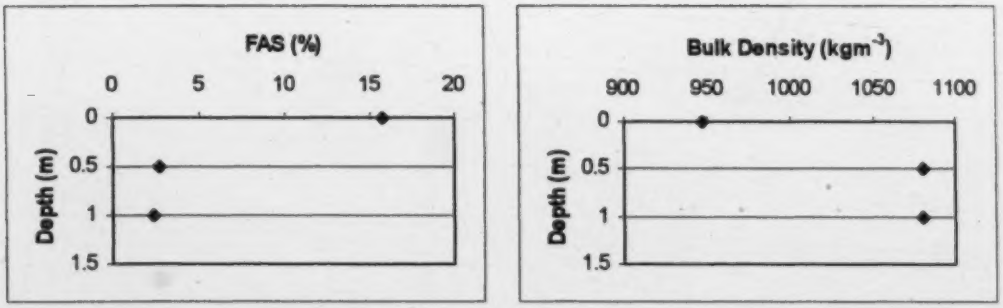

Figure E.4. Profiles for pure biosolids (MCwb = 76%) a) FAS and b) BD.

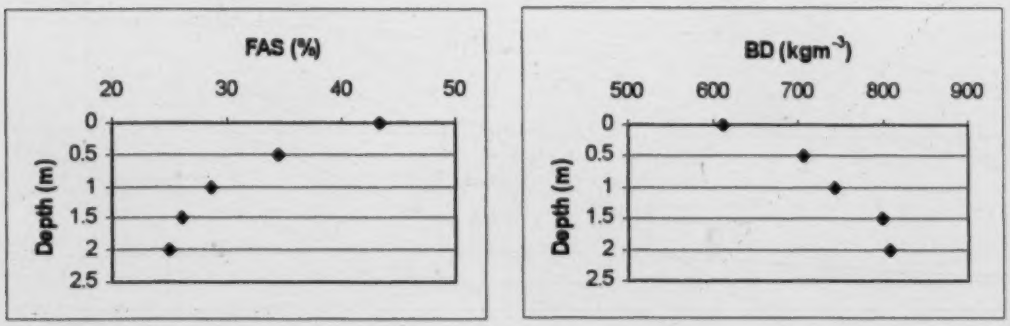

Figure E.5. Profiles for woodchips-biosolids (MCwb = 55%) a) FAS and b) BD.

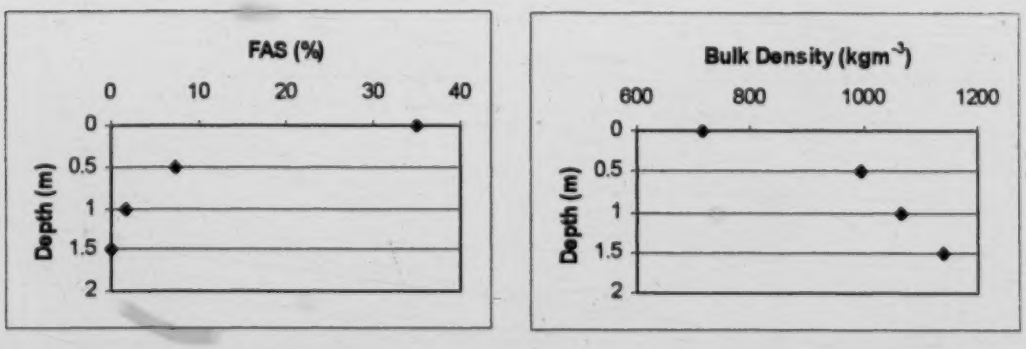

Figure E.6. Profiles for leaves-biosolids (MCwb = 74%) a) FAS and b) BD.

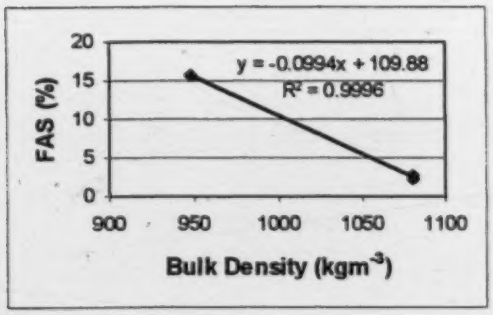

Figure E.7. FAS vs BD for pure biosolids.

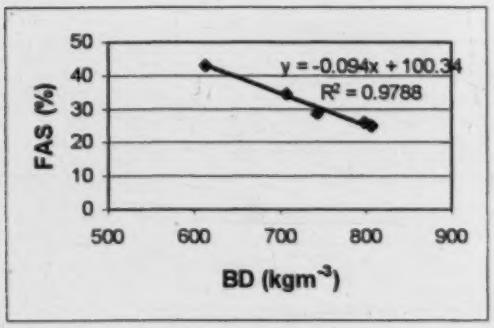

Figure E.8. FAS vs BD for woodchips-biosolids.

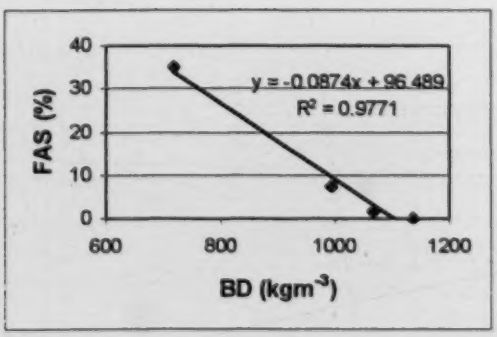

Figure E.9. FAS vs BD for leaves-biosolids.

Table E.1. Summary of slope, intercept and standard error values from BD vs FAS regression equations.

Material	Slope ($\%kg^{-1}m^{3}$)	Standard Error for Slope	Intercept (%)	Standard Error for Intercept
Manure compost	0.0957	0.00096	111.22	0.40
MSW compost	0.0894	0.0024	102.69	1.63
Woodchips	0.1479	0.0040	107.91	0.99
Leaves	0.1165	0.0040	96.95	0.68
Straw	0.0891	0.010	93.53	0.99
Pure biosolids	0.0994	0.0039	109.88	4.083
Woodchips-biosolids	0.094	0.008	100.34	5.88
Leaves-biosolids	0.0906	0.0057	96.26	5.60
Straw-biosolids	0.0874	0.0016	96.49	1.18
*Cornstalks-manure	0.1024	0.0030	113.49	2.50
**Overall	0.084	0.001	96.30	0.76

* Data from Baker *et al.* (1998)

** Includes all data (from this study and Baker *et al.*, 1998) in one regression equation

APPENDIX F

Summary of Calculations

Tables F.1 to F.9 were generated using the depth, wet bulk density (BD_{wet}), wet basis moisture content (MC_{wet}) and the FAS found by the pycnometer to calculate the volumetric moisture content (MC_{vol}), dry bulk density (BD_{dry}), particle density (PD) and porosity of each material. The following equations were used.

The volumetric moisture content was calculated using a variation of Equation 2.3:

$$MC_{vol} = \frac{MC_{wet} BD_{wet}}{\rho_w} \qquad (F.1)$$

where ρ_w is the density of water ($1000 kgm^{-3}$).

The dry bulk density was calculated using Equation F.2.

$$BD_{dry} = BD_{wet}(1-MC_{wet}) \qquad (F.2)$$

where MC_{wet} is expressed as a decimal and BD_{dry} and BD_{wet} have units of kgm^{-3}.

FAS_1 is the FAS found by the pycnometer and is an average of 3 readings.

FAS_2 is the FAS found by the soil compression equation (Equation 2.5). The first reading from the pycnometer is used as the initial FAS.

PD is the particle density calculated using Equation 4.8 and FAS_1 (FAS found by pycnometer).

The total porosity was calculated using Equation F.3.

$$Porosity_1 = FAS + MC_{vol} \qquad (F.3)$$

The total porosity was also calculated using Equation 4.5 ($Porosity_2$). Since the particle density required for Equation 4.5 is calculated using the same FAS used in Equation F.3, $Porosity_1$ and $Porosity_2$ are numerically equivalent calculations.

FAS_3 is the FAS assuming constant particle density. Calculated using Equation 2.10 and the initial PD found for each level of moisture content. Numerically equivalent to the FAS_2 calculation (same assumptions made – FAS dependent on volume changes only) except at higher moisture contents the values deviate slightly due to the small errors in volume determination.

$Porosity_3$ is the total porosity assuming constant PD. Uses equation for $Porosity_2$, but PD assumed constant.

Table F.1. Summary of calculations for manure compost.

Depth (m)	BDwet (kgm^{-3})	MCwet (%)	MCvol (%)	BDdry (kgm^{-3})	FAS_1 (%)	FAS_2 (%)	PD kgm^{-3}	$Porosity_1$ (%)	$Porosity_2$ (%)	FAS_3 (%)	$Porosity_3$ (%)
0	218.08	25	5.45	163.56	84.03	84.03	1554.64	89.48	89.48	84.03	89.48
0.2	223.04	25	5.58	167.28	83.39	83.67	1515.72	88.97	88.96	83.67	89.24
0.4	233.68	25	5.84	175.26	82.31	82.89	1479.01	88.15	88.15	82.89	88.73
0.8	248.11	25	6.20	186.08	81.56	81.83	1520.38	87.76	87.76	81.83	88.03
1	257.9	25	6.45	193.43	79.66	81.11	1392.19	86.11	86.11	81.11	87.56
1.2	273.66	25	6.84	205.25	79.49	79.95	1501.93	86.33	86.33	79.95	86.80
1.4	277.53	25	6.94	208.15	80.65	79.67	1677.48	87.59	87.59	79.67	86.61
0	237.11	30	7.11	165.98	82.51	82.51	1599.49	89.62	89.62	82.51	89.62
0.2	244.95	30	7.35	171.46	81.1	81.93	1484.33	88.45	88.45	81.93	89.28
0.4	252.05	30	7.56	176.43	80.38	81.41	1463.14	87.94	87.94	81.41	88.97
0.6	262.98	30	7.89	184.09	79.29	80.60	1435.90	87.18	87.18	80.60	88.49
0.8	271.19	30	8.14	189.83	78.38	80.00	1407.78	86.52	86.52	80.00	88.13
1	277.59	30	8.33	194.31	78.25	79.52	1447.65	86.58	86.58	79.52	87.85
1.2	279.92	30	8.40	195.94	77.79	79.35	1418.58	86.19	86.19	79.35	87.75
1.4	289.23	30	8.68	202.46	77.92	78.67	1510.52	86.60	86.60	78.67	87.34
3	317.46	30	9.52	222.22	74.24	76.58	1368.68	83.76	83.76	76.58	86.11
0	539.32	63	33.98	199.55	54.17	54.17	1683.55	88.15	88.15	54.17	88.15
0.2	540.01	62.1	33.53	204.66	54.36	53.05	1690.70	87.89	87.89	54.31	87.84
0.4	561.50	61.9	34.76	213.93	52.08	50.88	1625.27	86.84	86.84	52.54	87.29
0.6	581.30	61.5	35.75	223.80	50.04	48.63	1574.93	85.79	85.79	50.96	86.71
0.8	641.03	61.5	39.42	246.79	46.81	43.29	1792.67	86.23	86.23	45.92	85.34
1	650.87	61.5	40.03	250.58	45.6	42.42	1743.60	85.63	85.63	45.09	85.12
1.2	659.66	61.4	40.50	254.63	44.58	41.52	1706.99	85.08	85.08	44.37	84.88
2.8	785.77	61.4	48.25	303.31	34.31	30.27	1738.79	82.56	82.56	33.74	81.98

Table F.2. Summary of calculations for MSW compost.

Depth (m)	BDwet (kgm^{-3})	MCwet (%)	MCvol (%)	BDdry (kgm^{-3})	FAS_1 (%)	FAS_2 (%)	PD kgm^{-3}	$Porosity_1$ (%)	$Porosity_2$ (%)	FAS_3 (%)	$Porosity_3$ (%)
1.5	502.96	42.3	21.28	290.21	63.5	63.5	1906.14	84.78	84.78	63.50	84.78
2.5	517.03	42.3	21.87	298.33	62.38	62.48	1894.19	84.25	84.25	62.48	84.35
3	527.95	42.3	22.33	304.63	61.13	61.69	1842.02	83.46	83.46	61.69	84.02
0	660.48	55.5	36.66	293.92	46.5	46.5	1745.01	83.16	83.16	46.50	83.16
0.5	690.36	55.5	38.32	307.21	44.2	44.08	1757.03	82.52	82.52	44.08	82.39
1	772.52	55.5	42.87	343.77	37.12	37.43	1718.40	79.99	79.99	37.43	80.30
1.5	828.63	55.5	45.99	368.74	32.49	32.88	1713.41	78.48	78.48	32.88	78.87
2	869.08	55.5	48.23	386.74	28.89	29.60	1690.61	77.12	77.12	29.60	77.84

Table F.3. Summary of calculations for leaves.

Depth (m)	BDwet (kgm^{-3})	MCwet (%)	MCvol (%)	BDdry (kgm^{-3})	FAS_1 (%)	FAS_2 (%)	PD (%)	$Porosity_1$ (%)	$Porosity_2$ (%)	FAS_3 (%)	$Porosity_3$ (%)
0	28.45	11.35	0.32	25.22	94.48	94.48	485.34	94.80	94.80	94.48	94.80
0.5	34.14	11.35	0.39	30.27	92.79	93.38	443.60	93.18	93.18	93.38	93.76
1	37.09	11.35	0.42	32.88	92.76	92.80	482.24	93.18	93.18	92.80	93.23
1.5	42.25	11.35	0.48	37.45	91.06	91.80	442.74	91.54	91.54	91.80	92.28
2	44.99	11.35	0.51	39.88	90.41	91.27	439.24	90.92	90.92	91.27	91.78
2.5	47.57	11.35	0.54	42.17	89.98	90.77	444.85	90.52	90.52	90.77	91.31
3	59.33	11.35	0.67	52.60	87.37	88.49	439.91	88.04	88.04	88.49	89.16
0	66.53	58.78	3.91	27.42	92.76	92.76	823.76	96.67	96.67	92.76	96.67
0.5	113.35	58.78	6.66	46.72	86.2	87.67	654.63	92.86	92.86	87.67	94.33
1	172.41	58.78	10.13	71.07	77.68	81.24	583.21	87.81	87.81	81.24	91.37
1.5	218.80	58.78	12.86	90.19	71.35	76.19	571.22	84.21	84.21	76.19	89.05
2	263.16	58.78	15.47	108.47	65.59	71.36	572.68	81.06	81.06	71.36	86.83
2.5	335.82	58.78	19.74	138.43	57.08	63.46	597.16	76.82	76.82	63.46	83.20
3	335.82	58.78	19.74	138.43	58.19	63.46	627.20	77.93	77.93	63.46	83.20

Table F.4. Summary of calculations for straw.

Depth (m)	BDwet (kgm^{-3})	MCwet (%)	MCvol (%)	BDdry (kgm^{-3})	FAS_1 (%)	FAS_2 (%)	PD (%)	$Porosity_1$ (%)	$Porosity_2$ (%)	FAS_3 (%)	$Porosity_3$ (%)
0	50.85	0.81	0.04	50.44	89.53	89.53	483.62	89.57	89.57	89.53	89.57
2	50.85	0.81	0.04	50.44	89.18	89.53	467.91	89.22	89.22	89.53	89.57
3	51.23	0.81	0.04	50.82	88.44	89.45	441.16	88.48	88.48	89.45	89.49
10.2	62.97	0.81	0.05	62.46	86.7	87.03	471.45	86.75	86.75	87.03	87.08
0	84.95	50.8	4.32	41.80	88.43	88.43	576.14	92.75	92.75	88.43	92.75
1.5	112.27	50	5.61	56.14	85.2	84.44	611.07	90.81	90.81	84.64	90.26
2	122.33	50	6.12	61.17	83.69	83.05	600.05	89.81	89.81	83.27	89.38
2.5	137.82	50	6.89	68.91	80.66	80.90	553.54	87.55	87.55	81.15	88.04
3	152.89	50	7.64	76.45	78.82	78.81	564.77	86.46	86.46	79.09	86.73
3.5	166.51	50	8.33	83.26	75.08	76.93	501.69	83.41	83.41	77.22	85.55

Table F.5. Summary of calculations for woodchips.

Depth (m)	BDwet (kgm^{-3})	MCwet (%)	MCvol (%)	BDdry (kgm^{-3})	FAS_1 (%)	FAS_2 (%)	PD (%)	$Porosity_1$ (%)	$Porosity_2$ (%)	FAS_3 (%)	$Porosity_3$ (%)
0	169.26	8.56	1.45	154.77	83.22	83.22	1009.50	84.67	84.67	83.22	84.67
0.5	169.26	8.56	1.45	154.77	83.41	83.22	1022.17	84.86	84.86	83.22	84.67
3.44	170.30	8.56	1.46	155.72	83.35	83.12	1024.99	84.81	84.81	83.12	84.57
0	195.08	33.6	6.55	129.53	79.65	79.65	938.98	86.20	86.20	79.65	86.20
0.5	196.24	33.6	6.59	130.30	79.12	79.53	912.07	85.71	85.71	79.53	86.12
1	202.55	33.6	6.81	134.49	78.47	78.87	913.42	85.28	85.28	78.87	85.68
1.5	203.8	33.6	6.85	135.32	76.95	78.74	835.20	83.80	83.80	78.74	85.59
2	209.17	33.6	7.03	138.89	75.78	78.18	807.87	82.81	82.81	78.18	85.21
2.5	211.96	33.6	7.12	140.74	75.75	77.89	821.71	82.87	82.87	77.89	85.01
3	220.41	33.6	7.41	146.35	74.07	77.01	790.06	81.48	81.48	77.01	84.41
0	275.46	48	13.22	143.24	67.71	67.71	751.20	80.93	80.93	67.71	80.93
0.5	274.15	47	12.89	145.30	68.03	67.71	761.33	80.92	80.92	67.77	80.66
1	275.48	47	12.95	146.00	67.11	67.48	732.12	80.06	80.06	67.62	80.56
1.5	279.04	47	13.11	147.89	66.95	66.98	741.86	80.06	80.06	67.20	80.31
2	287.88	47	13.53	152.58	65.23	65.93	718.35	78.76	78.76	66.16	79.69

Table F.6. Summary of calculations for pure biosolids.

Depth (m)	BDwet (kgm^{-3})	MCwet (%)	MCvol (%)	BDdry (kgm^{-3})	FAS_1 (%)	FAS_2 (%)	PD (%)	$Porosity_1$ (%)	$Porosity_2$ (%)	FAS_3 (%)	$Porosity_3$ (%)
0	947.12	76	71.98	227.31	15.75	15.75	1852.73	87.73	87.73	15.75	87.73
0.5	1080.19	76	82.09	259.25	2.67	3.91	1701.58	84.76	84.76	3.91	86.01
1	1080.19	76	82.09	259.25	2.38	3.91	1669.79	84.47	84.47	3.91	86.01
1.5	1071.66	76	81.45	257.20	4.08	4.67	1776.99	85.53	85.53	4.67	86.12

Table F.7. Summary of calculations for woodchips-biosolids.

Depth (m)	BDwet (kgm^{-3})	MCwet (%)	MCvol (%)	BDdry (kgm^{-3})	FAS_1 (%)	FAS_2 (%)	PD (%)	$Porosity_1$ (%)	$Porosity_2$ (%)	FAS_3 (%)	$Porosity_3$ (%)
0	611.21	55	33.62	275.04	43.28	43.28	1190.50	76.90	76.90	43.28	76.90
0.5	707	55	38.89	318.15	34.4	34.39	1190.90	73.29	73.28	34.39	73.28
1	742.73	55	40.85	334.23	28.61	31.08	1094.40	69.46	69.46	31.08	71.93
1.5	799.01	55	43.95	359.55	26.03	25.85	1197.54	69.98	69.98	25.85	69.80
2	806.99	55	44.38	363.15	24.87	25.11	1181.13	69.25	69.25	25.11	69.50

Table F.8. Summary of calculations for leaves-biosolids.

Depth (m)	BDwet (kgm^{-3})	MCwet (%)	MCvol (%)	BDdry (kgm^{-3})	FAS_1 (%)	FAS_2 (%)	PD (%)	$Porosity_1$ (%)	$Porosity_2$ (%)	FAS_3 (%)	$Porosity_3$ (%)
0	714.72	74	52.89	185.83	34.94	34.94	1526.84	87.83	87.83	34.94	87.83
0.5	993.232	74	73.50	258.24	7.3	9.51	1344.94	80.80	80.80	9.59	83.09
1	1065.8	73	77.80	287.77	1.62	0.87	1398.52	79.42	79.42	3.35	81.15
1.5	1108.89	72	79.84	310.49	0	0.00	1540.14	79.84	79.84	0.00	79.66

Table F.9. Summary of calculations for straw-biosolids.

Depth (m)	BDwet (kgm^{-3})	MCwet (%)	MCvol (%)	BDdry (kgm^{-3})	FAS_1 (%)	FAS_2 (%)	PD (%)	$Porosity_1$ (%)	$Porosity_2$ (%)	FAS_3 (%)	$Porosity_3$ (%)
0	454.545	69	31.36	140.91	55.72	55.72	1090.93	87.08	87.08	55.72	87.08
0.5	600.917	69	41.46	186.28	41.42	41.46	1088.32	82.88	82.88	41.46	82.92
1	696.068	69	48.03	215.78	32.58	32.19	1112.77	80.61	80.61	32.19	80.22
1.5	778.835	69	53.74	241.44	25.51	24.13	1163.54	79.25	79.25	24.13	77.87
2	845.161	69	58.32	262.00	19.61	17.67	1186.92	77.93	77.93	17.67	75.98
2.5	910.739	69	62.84	282.33	14.43	11.01	1242.15	77.27	77.27	11.28	74.12

APPENDIX G

Table G.1. Relative errors for FAS and P_2 readings for manure compost.

Depth (m)	MCwb (%)	BD (kgm^{-3})	P2 (V)	FAS (%)	FAS average	FAS Std dev	FAS rel error (%)	P2 rel error (%)
0.00	25.0	218.23	5.317	83.0	84.0	1.060	1.26	0.366
			5.279	85.1				
			5.305	83.8				
0.20	25.0	222.99	5.289	84.3	83.4	0.751	0.90	0.272
			5.314	83.0				
			5.314	83.0				
0.40	25.0	233.64	5.302	82.9	82.3	0.493	0.60	0.164
			5.318	82.0				
			5.316	82.1				
0.80	25.0	248.07	5.294	82.3	81.6	0.643	0.79	0.221
			5.312	81.3				
			5.316	81.1				
1.00	25.0	257.88	5.329	79.5	79.6	0.231	0.29	0.065
			5.329	79.5				
			5.323	79.9				
1.20	25.0	274.39	5.315	79.2	79.5	0.462	0.58	0.130
			5.303	80.0				
			5.315	79.2				
1.40	25.0	277.61	5.287	80.7	80.6	0.141	0.18	0.053
			5.291	80.5				
0.00	30.0	237.11	5.255	83.52	82.5	0.895	1.09	0.269
			5.279	82.00				
			5.280	81.94				
0.20	30.0	244.95	5.282	81.21	81.1	0.405	0.50	0.118
			5.291	80.63				
			5.279	81.41				
0.40	30.0	252.05	5.281	80.80	80.4	0.344	0.43	0.097
			5.288	80.33				
			5.291	80.13				
0.60	30.0	262.98	5.279	80.11	79.4	1.061	1.34	0.260
			5.306	78.22				
			5.288	80.00				
0.80	30.0	271.18	5.287	78.98	78.4	0.762	0.97	0.200
			5.307	77.54				
			5.291	78.69				
1.00	30.0	277.59	5.276	79.29	78.6	1.075	1.37	0.247
			5.291	79.19				
			5.302	77.38				
1.20	30.0	279.91	5.288	78.23	77.8	1.011	1.30	0.258
			5.285	78.45				
			5.310	76.60				
1.40	30.0	289.22	5.277	78.35	77.9	0.623	0.80	0.154
			5.279	78.19				
			5.292	77.20				
3.00	30.0	326.53	5.292	74.24	74.2	0.057	0.08	0.040
			5.295	74.16				

Table G.1 (con't). Relative errors for FAS and P_2 readings for manure compost.

Depth (m)	MCwb (%)	BD (kgm^{-3})	P2 (V)	FAS (%)	FAS average	FAS std dev	FAS rel error (%)	P2 rel error (%)
0.00	63.0	539.03	5.865	54.02	54.2	0.156	0.29	0.060
			5.862	54.15				
			5.858	54.33				
0.20	62.1	540.01	5.832	54.47	54.4	0.235	0.43	0.085
			5.840	54.09				
			5.831	54.52				
0.40	61.9	561.5	5.823	52.82	52.1	0.695	1.34	0.235
			5.850	51.45				
			5.841	51.93				
0.60	61.5	581.3	5.854	49.11	50.0	0.824	1.65	0.228
			5.830	50.35				
			5.832	50.67				
0.80	61.5	641.03	5.798	47.10	46.8	0.987	2.11	0.294
			5.789	47.62				
			5.822	45.71				
1.00	61.5	650.87	5.789	46.81	45.6	1.047	2.30	0.309
			5.821	44.94				
			5.819	45.06				
1.20	61.4	659.66	5.813	44.62	44.6	0.771	1.73	0.224
			5.801	45.33				
			5.827	43.79				
2.80	61.4	786.4	5.802	34.86	34.3	0.506	1.48	0.122
			5.811	34.22				
			5.816	33.86				

Error Analysis of Equation 2.10

Partial derivatives were obtained with respect to each of the three parameters:

$$\frac{\partial FAS}{\partial MC} = BD\left(\frac{\rho_w - PD}{\rho_w PD}\right) \tag{G.1}$$

$$\frac{\partial FAS}{\partial BD} = \left(\frac{MC}{\rho_w} + \frac{100 - MC}{PD}\right) \tag{G.2}$$

$$\frac{\partial FAS}{\partial PD} = \frac{BD(100 - MC)}{PD^2} \tag{G.3}$$

Percentage error was calculated by:

$$\%\,\text{Error in FAS} = \frac{\sqrt{\left(\frac{\partial FAS}{\partial MC}\partial MC\right)^2 + \left(\frac{\partial FAS}{\partial BD}\partial BD\right)^2 + \left(\frac{\partial FAS}{\partial PD}\partial PD\right)^2}}{FAS} \tag{G.4}$$

where ∂MC, ∂BD and ∂PD varied between 0 and 30% of the absolute value. Absolute parameter values were taken as MC = 50%, BD = 400kgm^{-3} and PD = 1500kgm^{-3}.

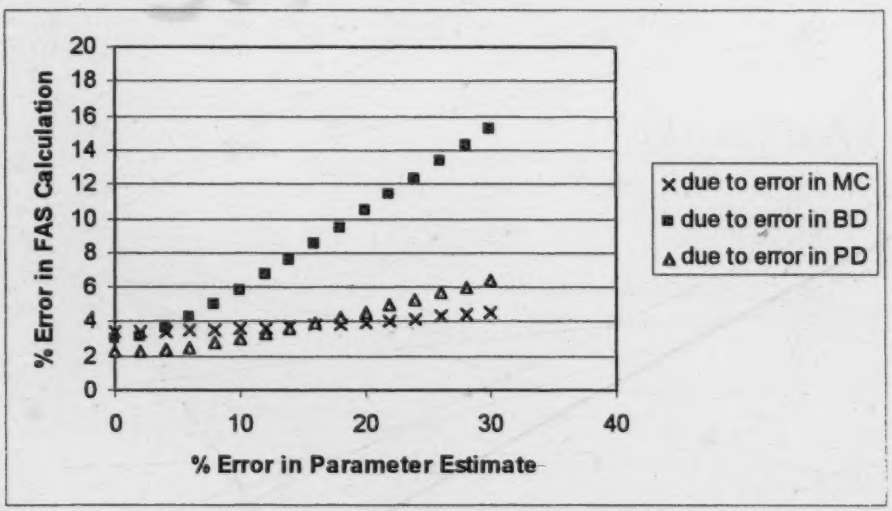

Figure G.1. Error analysis of Equation 2.10.

Note: for individual parameters, the error in the other parameters were assumed constant (5% for bulk density, 10% for moisture content and 15% for particle density).

Error Analysis of Equation 3.6

Partial derivatives were taken with respect to P_1, P_2, V_A, V_B, and V_S in order to assess the cumulative error associated with each of the pressure and volume measurements. The error associated with the regression parameters (1.0908 and 2.5234) were negligible and omitted from this analysis.

$$\frac{\partial FAS}{\partial P_1} = \frac{V_A}{V_S(kP_2 - w)} \tag{G.5}$$

$$\frac{\partial FAS}{\partial P_2} = \frac{-kP_1V_A}{V_S(kP_2 - w)^2} \tag{G.6}$$

$$\frac{\partial FAS}{\partial V_A} = \frac{P_1}{V_S(kP_2 - w)} - \frac{1}{V_S} \tag{G.7}$$

$$\frac{\partial FAS}{\partial V_B} = \frac{-1}{V_S} \tag{G.8}$$

$$\frac{\partial FAS}{\partial V_S} = \frac{-P_1V_A}{(kP_2 - w)V_S^2} + \frac{V_A - V_B}{V_S^2} \tag{G.9}$$

where k and w are the regression parameters 1.0908 and 2.5234 respectively. Typical values and the absolute errors associated with the parameters are summarized below:

$P_1 = 207\text{kPa} \pm 0.2\text{kPa}$

$P_2 = 110\text{kPa} \pm 0.2\text{kPa}$

$V_A = 31.01\text{L} \pm 0.01\text{L}$

$V_B = 27.04\text{L} \pm 0.01\text{L}$

$V_S = 16.00\text{L} \pm 0.01\text{L}$

The percentage error in the FAS calculating using the pycnometer equation was found using an equation similar to G.4. With the values and errors shown above, the percentage error in the FAS calculation was 0.99%. Even if the error associated with the sample volume measurement (V_S) increases to 0.1L, the percentage error in FAS is less than 3%.

APPENDIX H

Operator's Manual for Pycnometer

Operating Manual for

Modified Air Pycnometer

University of Alberta
Date Last Revised: March, 2002

Contact: Joy Agnew
Phone: 492 4616
Email: jagnew@ualberta.ca

1.0 INTRODUCTION

This air pycnometer was designed and built at the University of Alberta as a part of a Masters of Science project on the physical properties of compost. A pycnometer uses Boyles' Gas Law (the Ideal Gas Law) to measure the volume of air voids in a sample of any type of material. The air cylinder and piston assembly were added to the sample chamber to simulate compressive loading. This allows the user to obtain air volume values that can be found at the bottom of a pile of the given material as well as at any depth. This way, the researcher can develop air volume profiles for any desired material.

In addition to measuring air voids, the pycnometer also gives accurate bulk density values if the mass of the material in the sample chamber is known. If the moisture content of the material is known, the porosity can also be calculated. Therefore, bulk density and porosity profiles can be obtained as well as air volume profiles.

Individual free air space (FAS) and bulk density readings can be obtained in about 10 minutes while complete profiles require approximately one week. This is due to the amount of time required to achieve complete settlement at each compressive load. Generally, each load increment requires 24 hours to settle.

2.0 OVERVIEW OF APPARATUS

The pycnometer consists of two vessels, a compressed air vessel and a sample vessel. The compressed air vessel is permanently closed and is never opened while the sample vessel needs to be opened and resealed for every sample. The vessels are joined by an air hose and a quick coupler on the sample vessel.

An air compressor is connected to the compressed air vessel through a series of air hoses, a pressure regulator, a pressure relief valve and a pressure gauge and transducer. The air compressor can also be connected to the air cylinder on the sample vessel to simulate

compressive loading. The air cylinder is also connected to a regulator, pressure relief valve and pressure transducer.

A drainage system is also built into the sample vessel to accommodate for leachate draining from excessively wet material. A hole in the bottom of the vessel leads to a hose and valve for easy draining.

Refer to Figures 2.1 and 2.2 for schematic drawing and overview of actual apparatus, showing the placement of the valves, regulators and transducers.

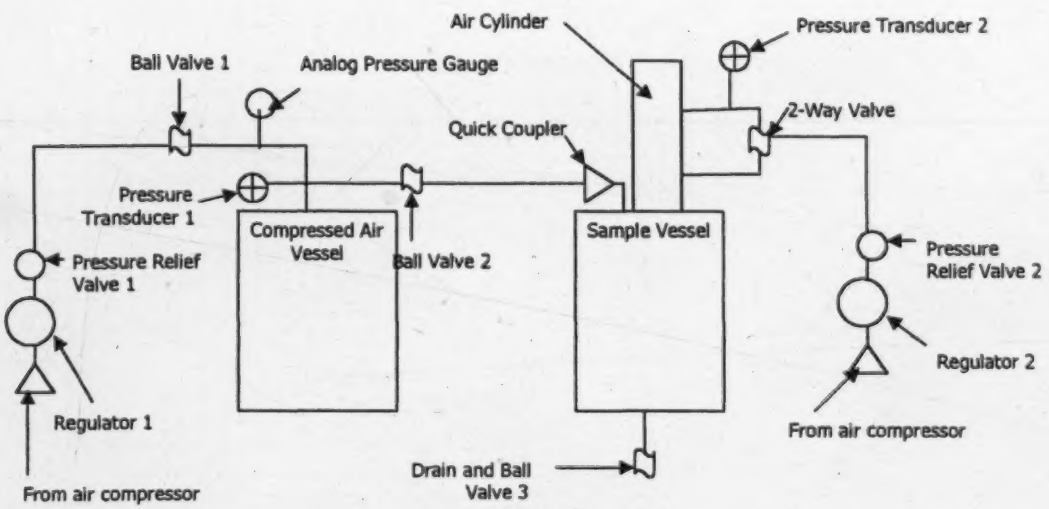

Figure 2.1. Schematic Drawing of Air Pycnometer Setup

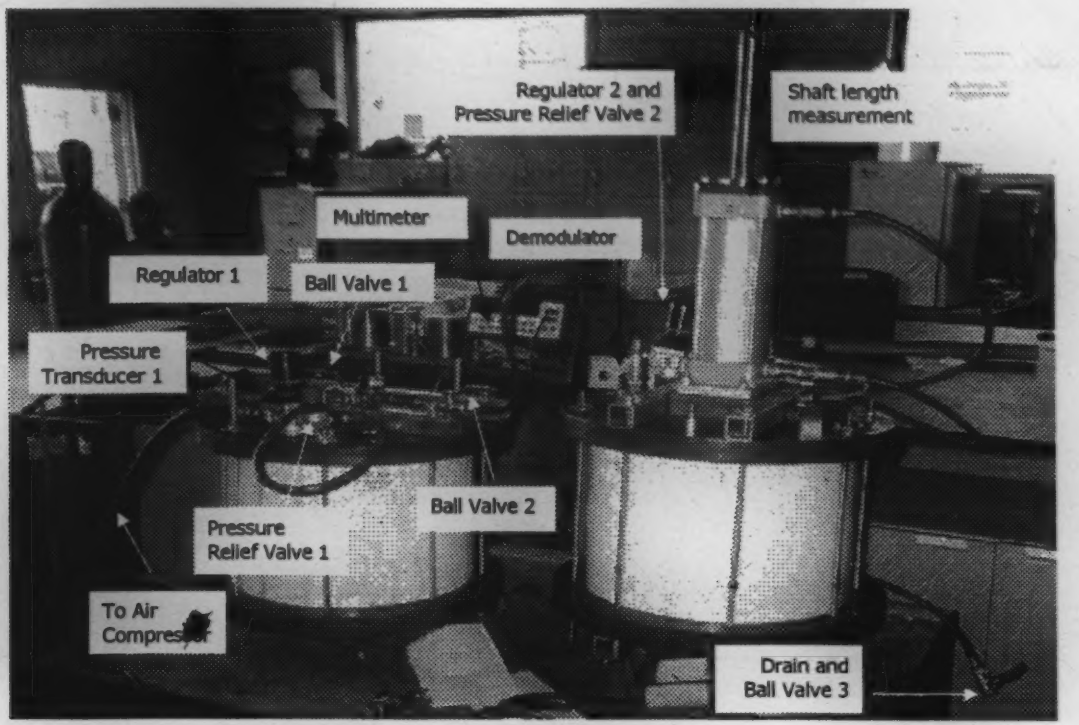

Figure 2.2. Orientation of Actual Apparatus

3.0 OPERATION OF APPARATUS

NOTE: Please read all of the instructions before the first operation. After at least one run, use the flowchart at the end of this section for quick reference.

NOTE: Do not alter the settings on the pressure relief valves. They are set to exhaust when the pressure in the air vessel exceeds 240kPa (35psi) and when the pressure in the air cylinder exceeds 345kPa (50psi). This is for the safety of the user and equipment.

3.1 Step by Step Outline for FAS Readings

A. Obtain sample and record mass

Obtain approximately 20L of the material to be tested (a 5 gallon pail full). Record the weight of the material and container with a large industrial scale.

B. Open the sample vessel

Open the sample vessel by removing all 8 nuts around the perimeter of the lid. Remove the two cross bars and set aside. The rods should slip down so they are flush with the holes in the lip (this will make the removal of the cap and cylinder easier).

Gently tap the underside of the lip with a hammer while pulling upwards until you can feel the seal break. Rock the lid back and forth until it becomes loose enough to pull off. Gently lift it off and place on its side on the table.

C. Replace screen on drain plate and add sample

Remove any material remaining in the sample vessel. Ensure that the mesh screen is covering the drain plate and pour the new material into the vessel. Make sure it pours in evenly and fills the vessel to the black mark on the inside. Smooth out the top of the material. Weigh the container and any remaining material and record. You can use any of the remaining material for moisture content analysis.

D. Retract piston and clean rim and groove

If the piston attached to the lid and air cylinder is extended, push it back so the piston head is less than 50mm from the underside of the lid. This will eliminate any extra compaction while tightening the lid.

Wipe the rim of the vessel and the groove in the lid to remove any debris that might compromise the seal. If the gasket in the groove of the lid is loose apply a *small* amount of vacuum grease around the groove to hold it in place.

E Replace lid and piston

Line up the numbered rods with the numbered holes in the lid and gently replace the lid and cylinder assembly onto the sample vessel. Wriggle each of the rods into their respective holes until the lid falls into place (it may not fall completely into the groove but it will later during tightening). Make sure the rods are vertical by lining one of the rods up with the writing on the side of the vessel. The lid can still be turned a little if they are not completely vertical.

Replace the two crossbars, again lining up the numbers. Push the rods up through the holes and replace the washers and nuts and hand tighten.

F. Tighten nuts in a star pattern

Use the 9/16" flat wrench and pliers to tighten the nuts in a star pattern. This is important to ensure a good air seal. Tighten nuts in order: 3, 7, 5, 1, 2, 6, 4, 8.

G. Move piston to top of sample

Make sure the piston moved down to just touch the top of the sample. If it hasn't (the black mark on the piston rod is still visible about 10mm above the lip of the rod opening), attach the regulator/valve apparatus to the air cylinder. The air hose with the pressure transducer is attached to the top quick coupler and the other hose attaches to the bottom coupler. Close the regulator (loosen counter clockwise until it stops turning) and turn the two way valve to "extend" (clockwise). Attach the air compressor to the quick coupler

on the regulator. Slowly open the regulator (turning clockwise) and keep an eye on the piston shaft. Once the pressure is high enough to slowly move the shaft down and it stops, open the regulator and return the air compressor hose to the regulator/valve setup on the compressed air vessel (regulator 1).

H. Take shaft measurement

The volume of the sample can now be determined by measuring the length of the exposed rod outside of the cylinder. Take the measurement from the bottom of the lip to the very top of the rod. The measurement can be taken in either inches or millimetres, but be sure to use the correct calibration equation. The calculated volume then has the units of litres (L) (Equations 2a and 2b, next section).

I. Check for drainage

If the material is excessively wet, check to see if any leachate has drained from the material. Open the drain valve into a graduated cylinder and shake the hose. Record the amount of liquid drained, if any, and close the drain valve.

J. Check for airleaks

Check to see if the sample vessel is airtight. First, make sure the demodulator and multimeter are attached to pressure transducer 1 and the demodulator is calibrated for this transducer (zero = 716 and span = 527). (If the transducer hasn't been calibrated for over a week, it should be recalibrated and the new zero and span readings should be used. Refer to Section 3.4 for calibration procedures). This gives a 10V output at 207kPa of pressure.

Attach the air hose between the vessels, setting aside the extra quick coupler. Close valve 2 (between the two vessels) and open valve 1 to pressurize the air vessel. You should hear air rushing into the vessel and the analog pressure gauge should slowly increase along with the voltage reading. When the voltage reading is approximately 10V (the magnitude is not important when checking to see if the sample vessel is airtight), close valve 1 and open valve 2. Again, you should be able to hear air rushing into the

sample vessel and the voltage reading should quickly drop. Once the voltage reaches a minimum, it should slowly rise as the pressure equilibrates. Once it reaches a maximum voltage (the equilibrium pressure) it should stay steady for about 5-10 seconds then slowly decline (small air leaks are unavoidable). However, if it reaches a maximum then *quickly* declines, there is an air leak in the sample vessel. Bleed the system, retighten the nuts and repeat the process to check for air leaks.

K. Begin taking FAS readings, bleed the system

If the sample vessel is airtight, the system is ready to take readings. Bleed the system by removing the hose from the sample vessel and return the extra quick coupler to the hose to bleed the compressed air vessel. The system is completely bled when the voltage reading is approximately -0.040V. If, when valve 2 is closed, the voltage output quickly rises, open valve 2 again and allow to bleed some more. A complete bleed requires approximately 2 minutes.

L. Pressurize air vessel and take equilibrium reading

Follow the same procedure as before to pressurize the air vessel to 207kPa. This time, record the voltage output (P_1) after the reading settles before opening valve 2. After opening valve 2, allow to settle again and record equilibrium pressure (P_2). Use the spreadsheet provided for easy record keeping. Once P_2 is recorded, bleed the system and repeat until the required number of repetitions is achieved.

3.2 Crunching the Numbers

Note: A spreadsheet can be found at the end of this documentation. It should be helpful in keeping the numbers straight throughout the process.

While waiting for pressure to equilibrate or the vessels to completely bleed, the volume of the sample vessel and sample can be calculated. (Since the volume of the piston shaft inside the sample vessel varies with sample volume, the volume of the sample vessel is

also variable and must be calculated for each compressive load.) The equations to calculate V_B (sample vessel) and V_s (sample) are as follows:

$$V_B = 26.9 + 0.0243207*(x-5) \quad [L] \qquad \textbf{(Equation 1a)}$$

where x is the exposed rod length in inches and V_B is the vessel volume in litres.

$$V_B = 0.0009424\,x + 26.78\ [L] \qquad \textbf{(Equation 1b)}$$

where x is the exposed rod length in millimeters and V_B is the vessel volume in litres

$$V_s = 3.294(0.9917\,x - 4.9001) \quad \textbf{(Equation 2a)}$$

where x is the exposed rod length in inches and V_s is the vessel volume in litres.

$$V_s = 0.12965(0.9917\,x - 124.46) \quad \textbf{(Equation 2b)}$$

where x is the exposed rod length in millimeters and V_s is the sample volume in litres

** Remember to measure the entire shaft length to the bottom of the lip of the shaft opening.

The FAS can now be calculated based on the pressure readings and the volume calculations using the following equation

$$FAS = \frac{\frac{P_1 V_a}{1.0908P_2 - 0.366} - V_a - V_B + V_s}{V_s} \qquad \textbf{(Equation 3a)}$$

where P_1 and P_2 are pressures in psi,

V_a is the volume of the compressed air vessel (31.005L),

V_B is the volume of the sample vessel (L),

V_s is the volume of the sample (L),

and $1.0908P_2 - 0.366$ is the calibration equation found by testing materials of known FAS (water and gravel).

Note: The calibration for pressure transducer 1 is 10V = 30psi so simply multiply the voltage reading by 3 to obtain the units of psi.

If you are working with pressure units of kPa instead of psi, Equation 3 becomes:

$$FAS = \frac{\frac{P_1 V_a}{1.0908 P_2 - 2.5234} - V_a - V_B + V_s}{V_s} \quad \textbf{(Equation 3b)}$$

where P_1 and P_2 are pressures in kPa and the remaining variables are the same as in Equation 3a.

Note: The calibration for pressure transducer 1 is 10V = 207kPa, so multiply the voltage reading by 20.7 to obtain the units of kPa.

3.3 Simulating Compressive Loading

The wet bulk density can easily be calculated by dividing the total mass by Vs. The pressure required for the next increment of compressive loading can also be calculated. The mass of compost at any depth in a pile is found by:

Mass = depth * area * bulk density (Equation 4)

where mass is in kg, depth in m, area in m^2 and bulk density is in kgm^{-3}. For this system, the area is simply the cross sectional area of the sample vessel which is $0.12965m^2$. Depending on the maximum depth desired, it is convenient to simulate either 0.2m or 0.5m increments of depth. Material with an initial bulk density of $600kgm^{-3}$ or greater should be loaded at 0.5m increments while less bulky materials loaded at 0.2m increments.

Since the depth and area are the same for each increment, the above equation simplifies to:

Mass = 0.064825 * $\sum\rho_b$ for 0.5m increments, and (Equation 5a)

Mass = 0.025932 * $\sum\rho_b$ for 0.2m increments (Equation 5b)

Where $\sum\rho_b$ is the cumulative sum of the bulk densities at each compressive load and mass is in kg.

To convert this mass to the pressure required by the air cylinder,

Pressure = Mass(2.20462/11.07586), or (Equation 6a)

Pressure = Mass(0.199047) (Equation 6b)

where 2.20462 is the conversion ratio for kg to lb and 11.07568 is the cross sectional area of the interior of the air cylinder [in^2]. This yields a pressure in psi.

To work with pressure units of kPa,

Pressure = Mass(9.81/0.0071457), or (Equation 7a)

Pressure = Mass(1.373) (Equation 7b)

where 9.81 is the acceleration due to gravity (ms^{-2}) and 0.0071457 is the cross sectional area of the interior of the air cylinder [m^2]. This yields a pressure in kPa.

This pressure can then be converted to voltage depending on the calibration of the second pressure transducer. (Refer to Section 3.4 for pressure transducer selection and calibration.)

Once the FAS readings are obtained and you are ready to simulate the next compressive load increment, bleed the system and attach the air compressor hose to the regulator setup for the air cylinder. Attach the demodulator cable to pressure transducer 2 and set the zero and span dials to the appropriate values for this transducer (Refer to Section 3.4).

Turn the regulator dial clockwise until the desired voltage output appears on the monitor. Take an initial shaft length reading and adjust the regulator dial to maintain a steady cylinder pressure (it takes about 3-4 minutes to settle to a constant pressure). After an appropriate amount of settling time (up to 24 hours) remove the air compressor hose and take a final shaft length reading. (For some dry, rigid materials the piston retracts slightly after the pressure is removed so take the shaft length reading AFTER removing the air compressor hose). This shaft length is then used to calculate V_B and V_s.

If the material is excessively wet or the compressive load is very high, check for drainage after settlement but before taking a FAS reading. Again, open the drain valve into a graduated cylinder and shake the hose until all liquid is drained. Record the amount of liquid drained. Don't forget to close the drain valve before pressurizing the vessel.

Continue taking FAS readings and simulating compressive loading until your sample is characterized. Often, the first FAS reading after compressive loading is invalid or is an outlier. This may be due to the fact that the pressure transducer needs to "warm up" or the vessel material is "cold" and needs to expand slightly. The first pressure cycle can be used to make sure the system is still airtight.

3.4 Calibrating the Pressure Transducer

The pressure transducers used in this system have the capability of measuring a wide range of pressures with the replacement diaphragms. The diaphragm in pressure transducer 1 should never need to be replaced or recalibrated since the pressure in the air vessel is usually the same (30 psi or 207kPa) If the system has not been used for a long period of time, pressure transducer should be recalibrated to ensure proper operation. However, depending on the initial bulk density of the material, the pressure needed to simulate compressive loading can range from 10psi to 50psi (68.9 kPa to 344.7 kPa). To obtain accurate loading, the diaphragm rated to the required pressure should be used. This may require the user to change and calibrate the diaphragm in pressure transducer 2.

Note: Do not exceed a pressure of 50psi (344.7 kPa) in the air cylinder. Even though the air cylinder is rated to 250psi (1724 kPa), the mounting bolts onto the plate can handle only 50psi (344.7 kPa).

Table 3.4.1. Expected maximum pressure based on initial bulk density (estimate).

Initial Bulk Density (kgm^{-3})	Maximum Air Cylinder Pressure Needed (psi) to Simulate approximately 3 m depth	Maximum Air Cylinder Pressure Needed (kPa) to Simulate approximately 3m in depth
30	3	20.7
100	10	68.9
200	20	137.9
500	40	275.8

Once you have selected the proper diaphragm (using the conversion table on the lid of the diaphragm kit), remove pressure transducer 2 from the regulator apparatus (keep the short pressure line attached to the transducer) using the 9/16" flat wrench. Using the Allan wrench supplied in the transducer kit, remove the 4 screws from the transducer and CAREFULLY pull the transducer apart. (The connections in the transducer are rather old and brittle and detach very easily. If this happens, you will need to resolder the connections before replacing the diaphragm.) The old diaphragm can be pulled out and replaced with the new one, ensuring the o-rings fit into the grooves on either side of the diaphragm. Replace the screws and tighten.

Each time a diaphragm is replaced, it needs to be recalibrated using the dead weight tester. To prime the dead weight tester, open both valves and turn the crank clockwise until it is all the way down. Close valve 1 and turn the crank counterclockwise until it is fully open again. This fills the lines with oil that is needed to build the pressure in the system. Close valve 2 and open valve 1 and the dead weight tester is ready for use.

Attach the pressure line on the transducer to the dead weight tester and tighten (Teflon tape helps make a good seal). Attach the demodulator to the transducer with the

transducer cable and set both the span and zero dials to 500. The voltage output should be approximately zero. If it isn't adjust the zero dial until the voltage output reads zero. Use the provided weights to simulate the maximum pressure that will be experienced by the system. Place them on the gray platform. Slowly begin turning the crank clockwise while spinning the gray platform to reduce static friction effects. Once the oil pressure in the system equals the weight on the scale, it will rise out of the cylinder. Once the platform has risen high enough to clear the screw below the platform, stop turning the crank, and adjust the span dial so the voltage output reads the desired voltage (it is a good idea to calibrate it so the maximum pressure reads 10V). Lock the dials and unscrew the crank so the system returns to zero pressure. Readjust the zero dial so the output again reads zero.

Repeat this process three or four times until you no longer need to readjust the dials to read the desired voltage (0V at no pressure and 10V at maximum pressure). Record the span and zero dial settings so you can reset it later when simulating compressive loading. Reattach pressure transducer 2 to the regulator setup on the air cylinder.

STEP BY STEP INSTRUCTIONS

Steps for Air Pycnometer Operation

A. Obtain sample and record mass
B. Open sample vessel
C. Replace screen on drain plate and add sample to sample vessel
D. Retract piston, clean rim and groove
E. Replace lid and piston
F. Tighten nuts in star pattern (3,7,5,1,2,6,4,8)
G. Move piston to top of sample
H. Take shaft measurement (x)
I. Check for drainage
J. Check for airleaks
    a. Yes → retighten bolts and take shaft measurement
    b. No → begin taking readings
K. Begin taking readings, bleed system
L. Pressurize air vessel and take equilibrium reading
M. Repeat from K until desired number of repetitions is obtained

Steps for Compressive Loading Simulation

A. Obtain proper diaphragm and calibrate if necessary
B. Calculate required pressure for next increment (Equations 5 and 6)
C. Attach air compressor and demodulator to air cylinder, adjust zero and span dials
D. Turn 2-way valve to "extend"
E. Open regulator until voltage output reads the required pressure
F. Take shaft length measurement
G. Adjust regulator until pressure stabilizes
H. Allow to settle (up to 24 hours)
I. Remove air compressor hose and take final shaft length measurement
J. Check for drainage
K. Take FAS readings

RECORDING DATA

MC_{vol} = (BD*MCwet)/1000 * 100%

(rod length in inches, pressure in psi)

Porosity (%) = FAS (%) + MCvol (%)

Depth (m)	Pressure (kPa/V)	t (min)	x (in)	Total Mass (kg)	MCwb (%)	Mass H_2O Drained (kg)	V_B (L)	V_s (L)	BD (kgm^{-3})	P_1 (V)	P_2 (V)	FAS (%)	FAS avg (%)	Porosity (%)
									Σ					
									Σ					
									Σ					
									Σ					
									Σ					

V_B = 26.9 + 0.0243207(x-5)

V_s = 3.294(0.9917x-4.9001)

Mass = 0.064825 * $\sum \rho_b$ for 0.5m increments, and

Mass = 0.025932 * $\sum \rho_b$ for 0.2m increments

Pressure = Mass*0.199047

Pressure Transducer 1 Calibration: 10V = 30psi, Va = 31.005L

$$FAS = \frac{\frac{P_1 * Va}{1.0908 * P_2 - 0.366} - Va - V_B + Vs}{Vs}$$

RECORDING DATA

MC_{vol} = (BD*MCwet)/1000 * 100%

(rod length in mm, pressure in kPa)

Porosity (%) = FAS (%) + MCvol (%)

Depth (m)	Pressure (kPa/V)	t (min)	x (in)	Total Mass (kg)	MCwb (%)	Mass H_2O Drained (kg)	V_B (L)	V_s (L)	BD (kgm^{-3})	P_1 (V)	P_2 (V)	FAS (%)	FAS avg (%)	Porosity (%)
									Σ					
									Σ					
									Σ					
									Σ					
									Σ					

V_B = 0.0009424x + 26.78

V_s = 0.12965(0.9917x-124.46)

Pressure Transducer 1 Calibration: 10V = 207kPa, Va = 31.005L

Mass = 0.064825 * $\sum \rho_b$ for 0.5m increments, and

Mass = 0.025932 * $\sum \rho_b$ for 0.2m increments

Pressure = Mass*1.373

$$FAS = \frac{P_1 * Va}{1.0908 * P_2 - 2.5234} - Va - V_B + Vs$$

$$Vs$$

APPENDIX I

Detailed Drawings

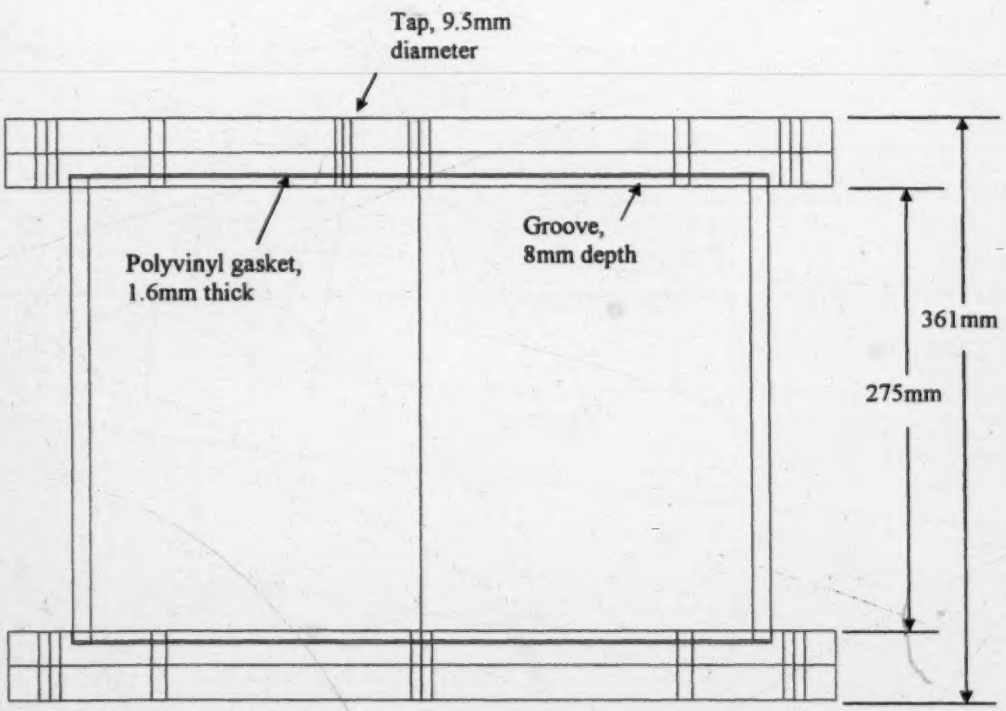

Air Vessel, Front View		End caps = Schedule 80 PVC, Walls = Schedule 40 PVC	
04-01-2002	Drawn by: Penny Howells	Designed by: Joy Agnew	Plate 1 of 7

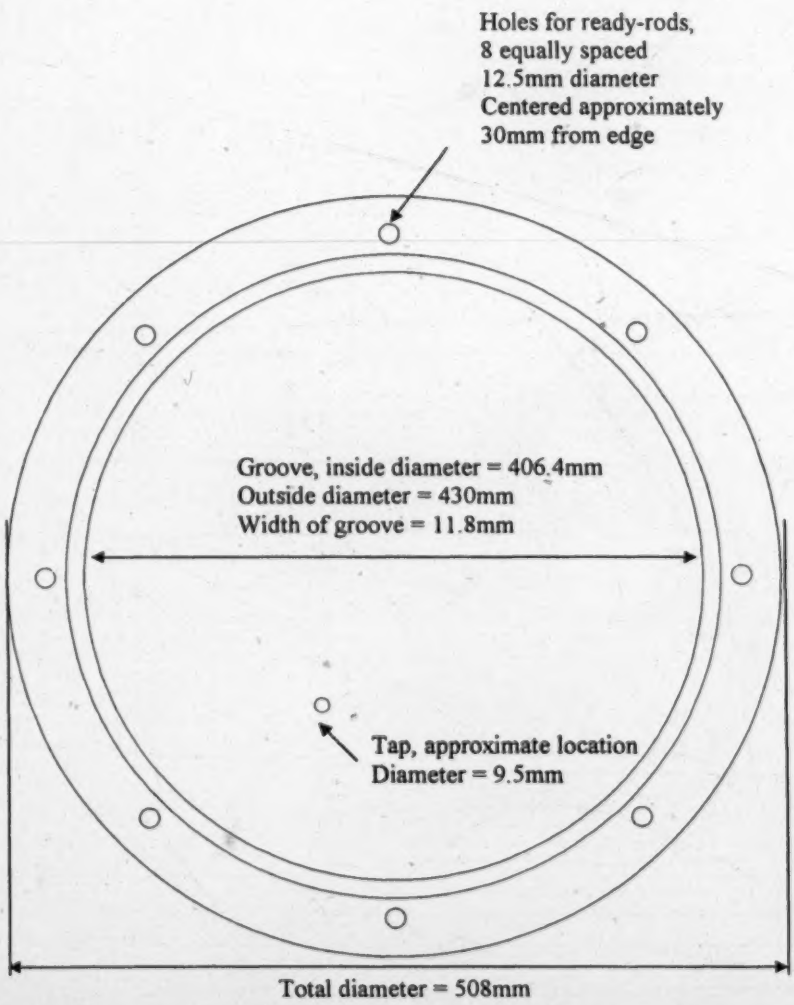

NOTE: Inside Bottom Cap is identical except there is no tap. Outside Top and Bottom Caps are also identical except there are no grooves on either and no tap in the Outside Bottom Cap.

Air Vessel, Inside Top Cap		Schedule 80 PVC	
04-01-2002	Drawn by: Penny Howells	Designed by: Joy Agnew	Plate 2 of 7

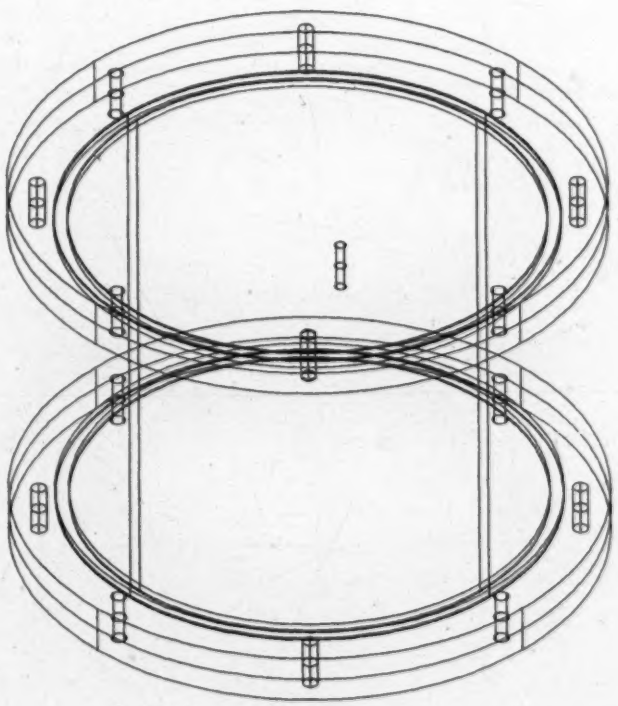

Air Vessel, Assembly		End Caps = Schedule 80 PVC, Walls = Schedule 40 PVC	
04-01-2002	Drawn by: Penny Howells	Designed by: Joy Agnew	Plate 3 of 7

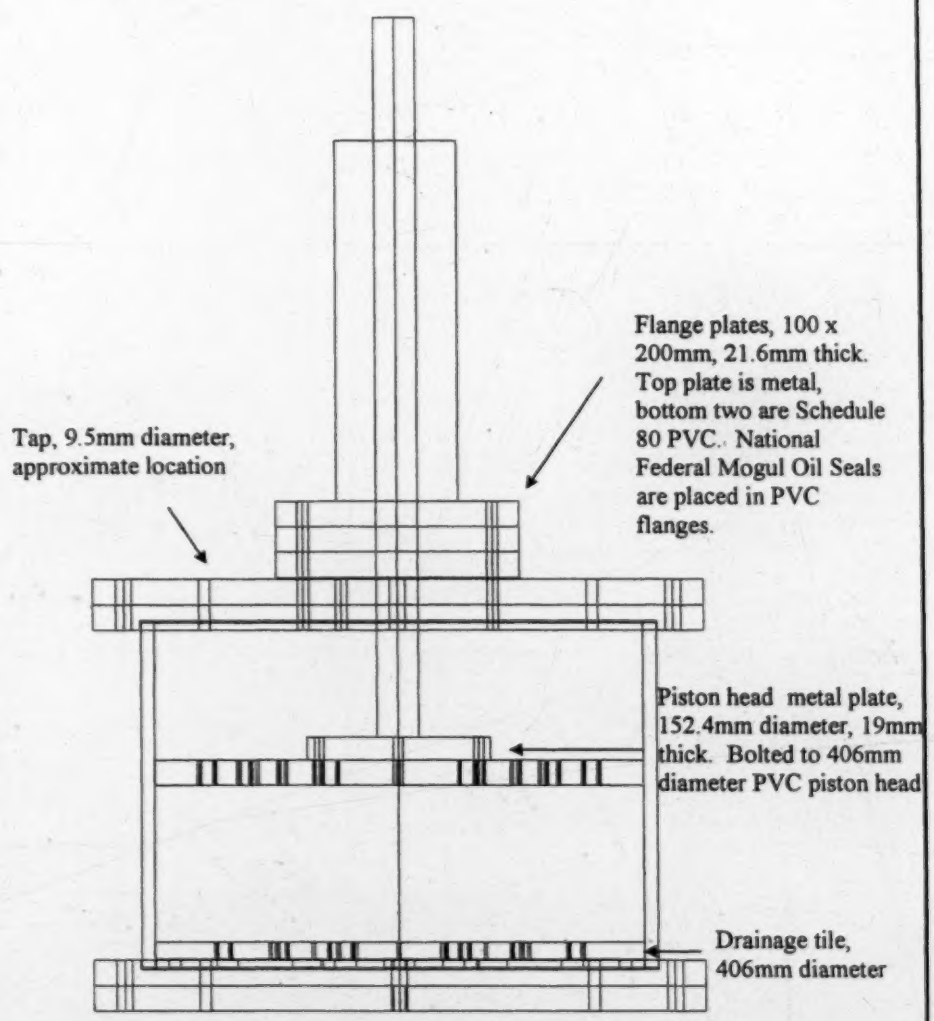
Flange plates, 100 x 200mm, 21.6mm thick. Top plate is metal, bottom two are Schedule 80 PVC. National Federal Mogul Oil Seals are placed in PVC flanges.
Tap, 9.5mm diameter, approximate location
Piston head metal plate, 152.4mm diameter, 19mm thick. Bolted to 406mm diameter PVC piston head
Drainage tile, 406mm diameter

Note: Height of vessel and thickness of end caps identical to air vessel (Plate 1).

Sample Vessel, Front View		End caps = Schedule 80 PVC Walls = Schedule 40 PVC Piston Head and Drainage Plate = Schedule 80 PVC	
04-01-2002	Drawn by: Penny Howells	Designed by: Joy Agnew	Plate 4 of 7

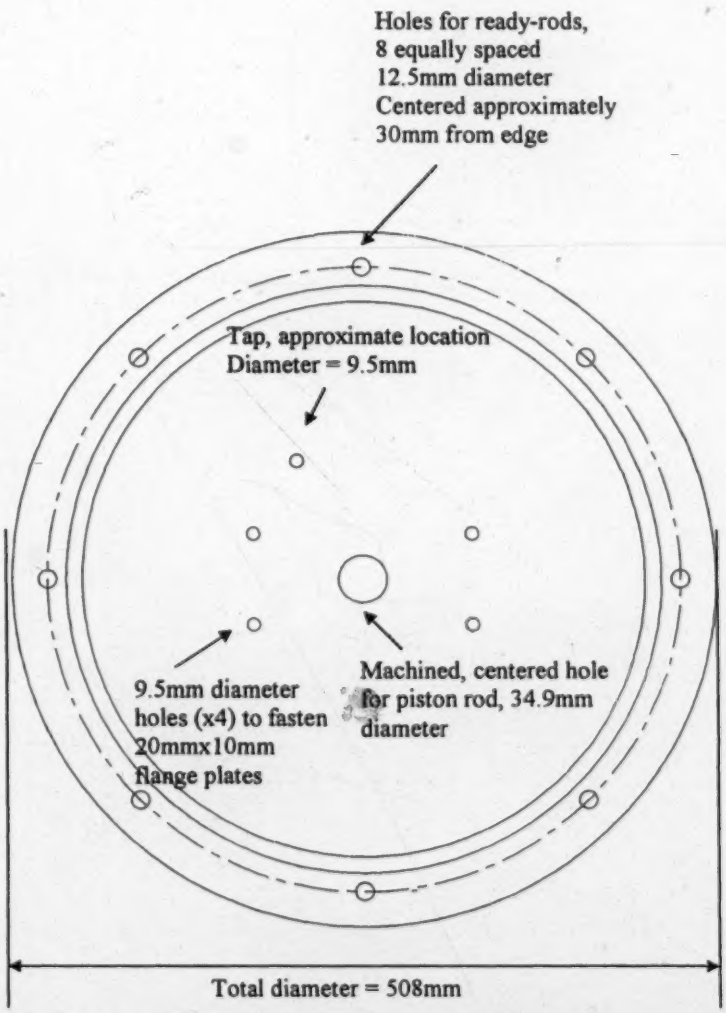

NOTE: Groove dimensions identical to groove dimensions in Air Vessel. Outside Top Cap for Sample Vessel is identical to Inside Top Cap for Sample Vessel except there is no groove on outside cap.

Sample Vessel, Inside Top Cap		Schedule 80 PVC	
04-01-2002	Drawn by: Penny Howells	Designed by: Joy Agnew	Plate 5 of 7

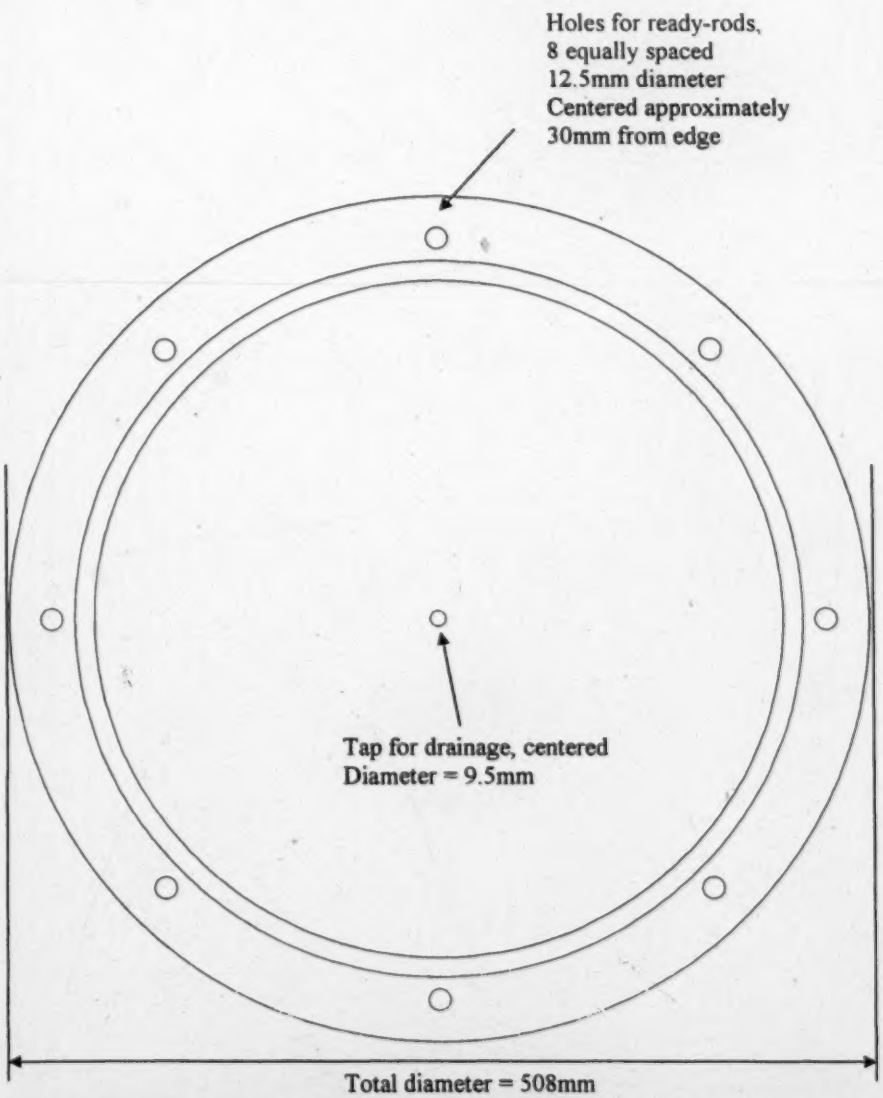

NOTE: Groove dimensions identical to groove dimensions in Air Vessel. Outside Bottom Cap for Sample Vessel is identical to Inside Bottom Cap for Sample Vessel except there is no groove on outside cap.

Sample Vessel, Inside Bottom Cap		Schedule 80 PVC	
04-01-2002	Drawn by: Penny Howells	Designed by: Joy Agnew	Plate 6 of 7

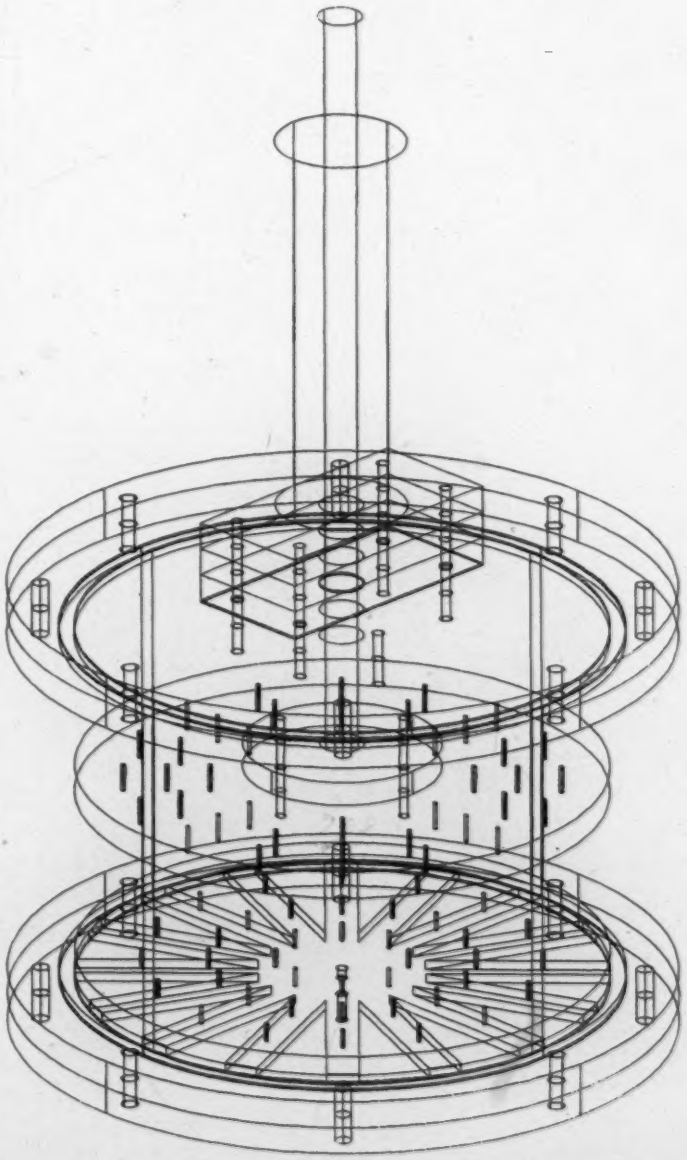

Sample Vessel, Assembly		End Caps = Schedule 80 PVC, Walls = Schedule 40 PVC Piston Head and Drainage Plate = Schedule 80 PVC	
04-01-2002	Drawn by: Penny Howells	Designed by: Joy Agnew	Plate 7 of 7